AD NUMBER
ADB010481
LIMITATION CHANGES
TO: **Approved for public release; distribution is unlimited.**
FROM: **Distribution authorized to U.S. Gov't. agencies only; Test and Evaluation; 26 MAR 1976. Other requests shall be referred to Pacific Missile Test Center, Point Mugu, CA 93042.**
AUTHORITY
PMTC notice, 23 Jun 1980

Technical Publication TP-76-7

ANALYSIS OF THE POWER SPECTRAL DENSITY OF TAPE RECORDER FLUTTER

(AIRTASK A5355352 054D 5W47410030, Work Unit A535210000002)

By

E. L. LAW
Instrumentation Development Division

26 March 1976

DISTRIBUTION LIMITED TO U.S. GOVERNMENT AGENCIES ONLY; TEST AND EVALUATION INFORMATION; 26 MARCH 1976. OTHER REQUESTS FOR THIS DOCUMENT MUST BE REFERRED TO THE COMMANDER (CODE 4250), PACIFIC MISSILE TEST CENTER, POINT MUGU, CALIFORNIA 93042.

PACIFIC MISSILE TEST CENTER

Point Mugu, California

PACIFIC MISSILE TEST CENTER

AN ACTIVITY OF THE NAVAL AIR SYSTEMS COMMAND

IRA N. SCHWARZ, CAPT USN
Commander

W. L. MILLER
Technical Director

This report describes work performed under AIRTASK 5355352 054D 5W47410030, Missile Flight Evaluation Systems, work unit A535210000002, Range Telemetry Support.

Mr. B. E. Bishop, Head, Instrumentation Technology Branch, and Mr. K. L. Berns, Head, Instrumentation Development Division, have reviewed this report for publication.

Released by:
M. H. CAIN
Telemetry Project Manager

Technical Publication TP-76-7

Published by . . . . Technical Publications Division
Photography and Technical Information Department
Security classification . . . . UNCLASSIFIED
First printing . . . . 200 copies

UNCLASSIFIED

SECURITY CLASSIFICATION OF THIS PAGE (When Data Entered)

REPORT DOCUMENTATION PAGE		READ INSTRUCTIONS BEFORE COMPLETING FORM
1. REPORT NUMBER TP-76-7	2. GOVT ACCESSION NO.	3. RECIPIENT'S CATALOG NUMBER
4. TITLE (and Subtitle) ANALYSIS OF THE POWER SPECTRAL DENSITY OF TAPE RECORDER FLUTTER		5. TYPE OF REPORT & PERIOD COVERED
		6. PERFORMING ORG. REPORT NUMBER
7. AUTHOR(s) E. L. Law		8. CONTRACT OR GRANT NUMBER(s)
9. PERFORMING ORGANIZATION NAME AND ADDRESS Pacific Missile Test Center Point Mugu, California 93042		10. PROGRAM ELEMENT, PROJECT, TASK AREA & WORK UNIT NUMBERS AIRTASK A5355352 054D 5W47410030, Work Unit A535210000002
11. CONTROLLING OFFICE NAME AND ADDRESS Naval Air Systems Command Washington, DC 20361		12. REPORT DATE 26 Mar[redacted]76
		13. NUMBER OF PAGES 83
14. MONITORING AGENCY NAME & ADDRESS (if different from Controlling Office)		15. SECURITY CLASS. (of this report) UNCLASSIFIED
		15a. DECLASSIFICATION/DOWNGRADING SCHEDULE

16. DISTRIBUTION STATEMENT (of this Report)

Distribution limited to U.S. Government agencies only; test and evaluation information; 26 March 1976. Other requests for this document must be referred to the Commander (Code 4250), Pacific Missile Test Center, Point Mugu, California 93042.

17. DISTRIBUTION STATEMENT (of the abstract entered in Block 20, if different from Report)

18. SUPPLEMENTARY NOTES

19. KEY WORDS (Continue on reverse side if necessary and identify by block number)

Analog tape recorders
Flutter
Interchannel time displacement error
Tape recorder servo response system
Time base error

20. ABSTRACT (Continue on reverse side if necessary and identify by block number)

This report presents the results of a study on the flutter, servo, and interchannel time displacement error characteristics of analog magnetic tape recorders. The main conclusions are that the flutter spectrum of a crossplay between two tape recorders can be predicted if the flutter characteristics of each tape recorder are known and that many tape recorders have underdamped servo systems that cause some flutter components to be amplified in the tape servo mode.

DD FORM 1 JAN 73 1473 EDITION OF 1 NOV 65 IS OBSOLETE

UNCLASSIFIED

SECURITY CLASSIFICATION OF THIS PAGE (When Data Entered)

ACKNOWLEDGMENT

The author wishes to express his gratitude to the following people: **N. R. Dragoo** and **D. L. Laubaucher** for their devoted and accurate performance of laboratory tests; **W. T. Norton** and **D. H. Barthuli** for their cooperation in the use of tape recorders; **F. R. Hartzler** for his coordination and guidance; **R. L. Cole** for his excellent art work; and **Dr. W. R. Hedeman** of Aerospace Corporation for his technical guidance.

CONTENTS

CONTENTS (Concluded)

DEFINITIONS

Flutter: A dimensionless factor describing an effect due to the difference between the instantaneous tape speed during recording and the instantaneous tape speed during playback.

Interchannel time displacement error (ITDE): Relative time error between two tracks of a multitrack magnetic tape recorder.

Differentiated interchannel time displacement error (DITDE): Derivative of ITDE with respect to time. Gives difference frequency between same signal on two tracks of a multitrack magnetic tape recorder.

Time base error: In analog instrumentation magnetic tape recording, the total time error of a playback signal with respect to a relatively error-free reference.

TP-76-7
26 March 1976

PACIFIC MISSILE TEST CENTER
Point Mugu, California

ANALYSIS OF THE POWER SPECTRAL DENSITY OF TAPE RECORDER FLUTTER

(AIRTASK A5355352 054D 5W47410030,
Work Unit 535210000002)

By
E. L. LAW

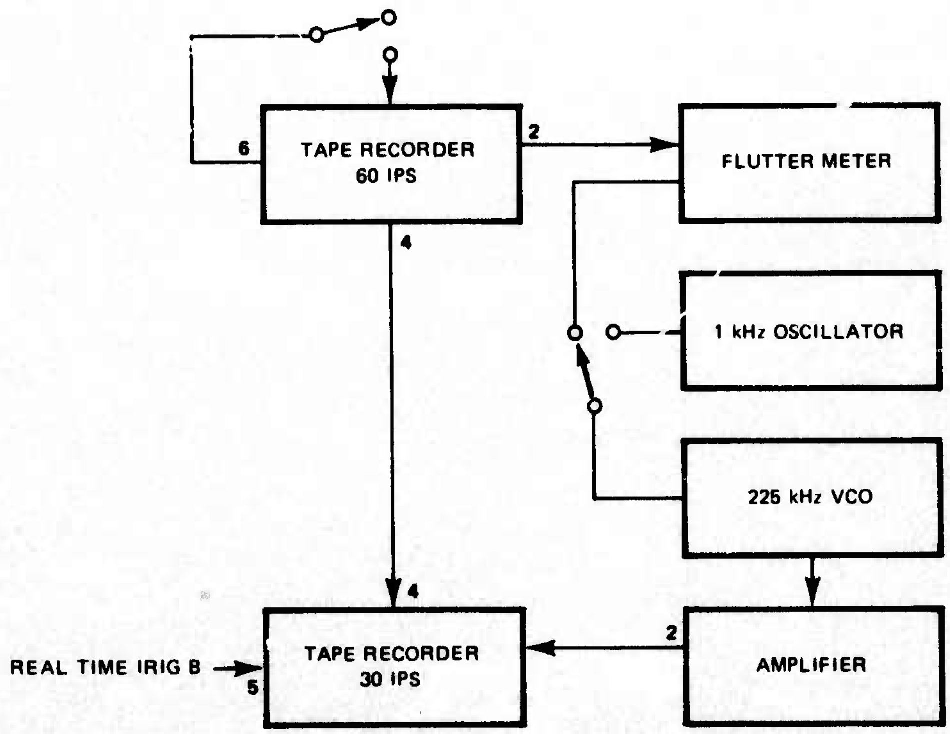

SUMMARY

This report presents the results of a study on the flutter, servo, and interchannel time displacement error characteristics of analog magnetic tape recorders. The main conclusions are that the flutter spectrum of a crossplay between two tape recorders can be predicted if the flutter characteristics of each tape recorder are known, and that many tape recorders have underdamped servo systems that cause some flutter components to be amplified in the tape servo mode.

Publication UNCLASSIFIED.

PRECEDING PAGE BLANK-NOT FILMED

INTRODUCTION

The work reported herein was conducted under AIRTASK A5355352 054D 5W47410030, Missile Flight Evaluation Systems, and work unit A535210000002, Range Telemetry Support, which was established to provide technical support to the Telemetry Group of the Range Commanders Council.

The primary purposes of this study were to determine the power spectral density of flutter in an analog instrumentation magnetic tape recorder and to try to predict the resultant flutter spectrum when a tape is recorded on one tape recorder and reproduced on another tape recorder. The tape recorder flutter experiment consisted of recording tapes on each of six tape recorders (designated A, B, C, D, E, and F) and reproducing each of these tapes on each of the six tape recorders. Each of the tape recorders was a different model and three different manufacturers were represented in the sample. The flutter output of each of these playbacks was recorded for later analysis. Plots were then made of the power spectral density of the flutter. Samples of these plots and the results of their analysis are presented.

The tapes were played back in both tachometer and tape servo mode on the four tape recorders which had tape servo capability (recorders A and D did not have tape servo capability). The servo responses of these four tape recorders were measured and are presented. The interchannel time displacement error (ITDE) was measured and differentiated (DITDE) with respect to frequency for these four recorders. DITDE is proportional to the instantaneous difference frequency between the outputs of the two tracks on which the same signal has been recorded.

FLUTTER TEST PROCEDURES

First, the following information was recorded on 9,200-foot reels of 1/2 inch degaussed virgin tape at 60 ips (inches per second) for each of the six tape recorders (see figure 1):

Track 2 – 108 kHz sine wave from a MICOM 8300W flutter meter at 13 decibels (dB) above normal record level (for best noise performance*). The MICOM 8300W includes a stable oscillator; a high-quality, phase-lock discriminator; a statistical volmeter; and a wave analyzer.

Track 4 – IRIG B timing.

*Secretariat, Range Commanders Council, White Sands Missile Range. Test Methods for Telemetry Systems and Subsystems by the Telemetry Group Inter-Range Instrumentation Group. White Sands, NM, Revised July 1975. (Document 118-73) UNCLASSIFIED.

Track 6 – 100 kHz reference signal (for only the four machines having tape servo systems).

Tracks 1, 3, 5, 7 – No signal recorded.

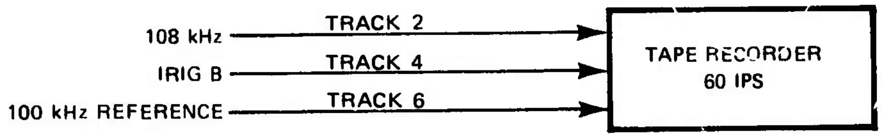

Figure 1. Setup for Recording Flutter Tapes.

Each of these six test tapes was then reproduced on all of the six tape recorders, using the set-up shown in figure 2. Sections of approximately 2 minutes duration at the 10, 50, and 90 percent locations of each of the reels of tape were recorded on a second tape recorder and will be referred to as the data tapes. The four tapes with the recorded 100-kHz reference signals were also played back in the tape servo mode on the four recorders equipped with this feature. This gave 108 two-minute segments in the tachometer mode, and 48 two-minute segments in tape servo mode. The test tapes were processed as follows. The flutter meter sensitivity was set at 0.03 percent and the low-pass filter was set at 20 kHz. The voltage-controlled oscillator (VCO) was set to a center frequency of 225 kHz and the deviation sensitivity was set at approximately 84 kHz/volt. Both a DC and an AC calibration of the VCO were recorded on the data tape. The DC calibration levels were -0.8V, 0V, and +0.8V, which set the VCO to 157.5 kHz, 225 kHz, and 292.5 kHz, respectively. The AC calibration consisted of a 118 mV (millivolt) rms (root mean square) (or 333 mV peak-to-peak) sine wave at a frequency of 1 kHz. This is equivalent to a 0.035 percent rms (or 0.1 percent peak-to-peak) flutter reading, because the flutter meter delivers a 100-mV, peak-to-peak signal when the peak-to-peak flutter equals the selected sensitivity.

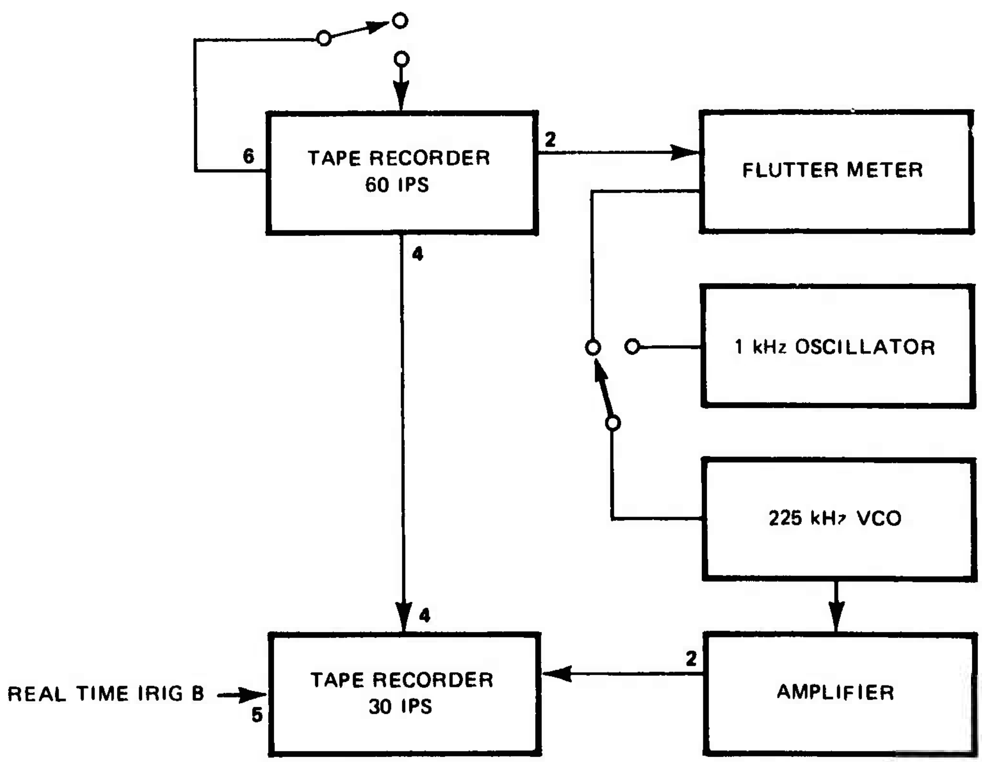

Figure 2. Setup for Recording Flutter Test Tapes.

FLUTTER ANALYSIS PROCEDURES

The data tapes were plotted for analysis as shown in figure 3. The EMR 410 discriminator was set to a center frequency of 225 kHz, with peak deviation set to 90 kHz and the low-pass filter set at 40 kHz.

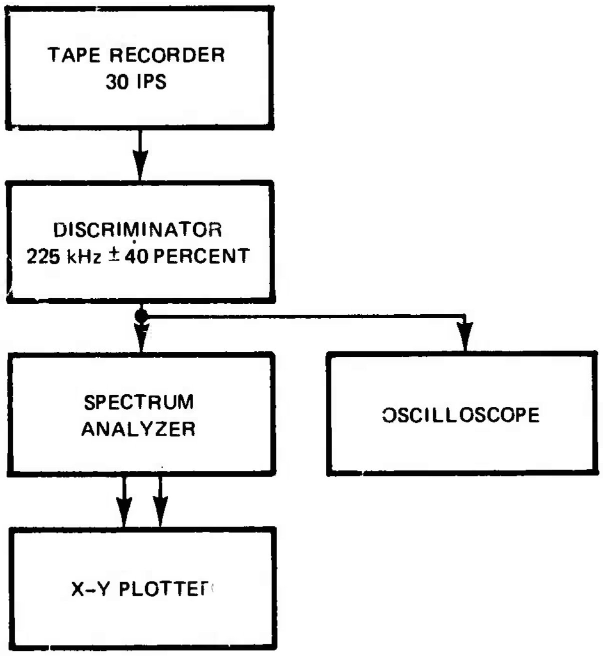

Figure 3. Setup for Recording Power Spectral Densities.

The EMR 1510 spectrum analyzer samples the input signal and calculates a 256-point power spectrum using a 1,024-point discrete Fourier transform. The analysis bandwidth, full-scale amplitude, number of spectra averaged, and windowing function (either rectangular or Hanning) are all selectable. Four analysis bandwidths (25.6 Hz, 256 Hz, 2.56 kHz, and 25.6 kHz) were used in this study (see table 1) and the Hanning window was always selected. The Hanning window weights the X_nth data point as follows:

$$X_n \text{ (out)} = \left[0.5 - 0.5 \cos\left(\frac{2\pi (n-1/2)}{1{,}024}\right)\right] X_n \text{ (in)}; \; 1 < n < 1{,}024$$

Table 1. Spectral Analysis Parameters

Analysis Bandwidth	Filter Equivalent Noise Power Bandwidth (Hertz)	Number of Spectra Averaged	95 Percent Confidence Limits of Spectral Accuracy (Random Data) (Decibels)	Full-Scale Amplitude (Volts)
25.6 Hz	0.15	4	+3.4, −5.7	3.16
256 Hz	1.5	32	+1.4, −1.7	3.16
2.56 kHz	15	128	+0.72, −0.76	10.0
25.6 kHz	150	128	+0.72, −0.76	10.0

The X-Y plotter was calibrated using the spectra of the AC calibration signals. The vertical calibration was 10 dB/inch, while the horizontal calibration was the analysis bandwidth equals 10 inches. The plots were calibrated so that full scale equaled 0.08 percent rms flutter for the 25.6 Hz and 256 Hz spectra and 0.25 percent rms flutter for the 2.56 kHz and 25.6 kHz spectra. Figures 4 and 5 show the typical spectrum of the AC calibration signals in a 2.56 kHz and a 25.6 kHz bandwidth. All spurious spectral components are more than 70 dB below 1 percent rms flutter, which verifies the fact that no significant error was added by recording on the second tape recorder. The flutter spectra are analyzed in appendix A.

RECORDER TRANSPORT SERVO RESPONSE PROCEDURE

The tape transport servo response was measured using a method proposed in an informal memorandum by Dr. M. H. Nichols.* Figure 6 shows a block diagram of the measurement method. The 100-kHz reference signal was frequency modulated by a sinusoid and recorded on a tape. This tape was then reproduced in the tape servo mode. The reference output was applied to a discriminator and then to a spectrum analyzer. The ratio of the output in tape servo mode to the output in tachometer mode was the measure of how well the servo system performed at that frequency of flutter. The measured servo responses of the four tape recorders are presented in figure 7. All four servo systems are shown to have regions of flutter frequency where the servo system amplifies the modulating frequency.

In this study, the peak deviation of the 100-kHz VCO was 50 Hz for three of the recorders and 10 Hz for recorder B. At higher peak deviations, all the servo loops broke into severe oscillation (at some modulation frequencies) for all tape recorders used. For example, figure 8 shows the flutter spectrum of recorder B with a 150-Hz modulating frequency and a peak deviation of 50 Hz. With this combination, the servo loop of B was unstable, and this caused the large low-frequency components, therefore a lower peak deviation had to be used. Normally, the 150-Hz component would be the largest component. This and the fact that the underdamping of the servo loop increases the amplitude of certain flutter components (see servo response curves and appendix A) strongly suggests that either the tape servo mode should be used very cautiously or servo systems should be readjusted for critical damping.

INTERCHANNEL TIME DISPLACEMENT ERROR PROCEDURES

The setup for the test is shown in figure 9. A 100-kHz sine wave was recorded on both track 2 and track 6. This was done for the four tape recorders that had the tape servo feature. These tapes were then reproduced on all four tape recorders. A signal proportional to the phase difference of the two 100-kHz signals was then derived (see appendix B) and differentiated to give the DITDE signal. This signal was passed through a 2 kHz low-pass filter and then used to modulate a 225-kHz VCO. The VCO output was recorded on a second tape recorder as in the flutter tests. The data tape playback procedure for the DITDE was the same as for the flutter (figure 3). The DITDE spectrums are presented in appendix G.

*Consultant, Del Mar, California.

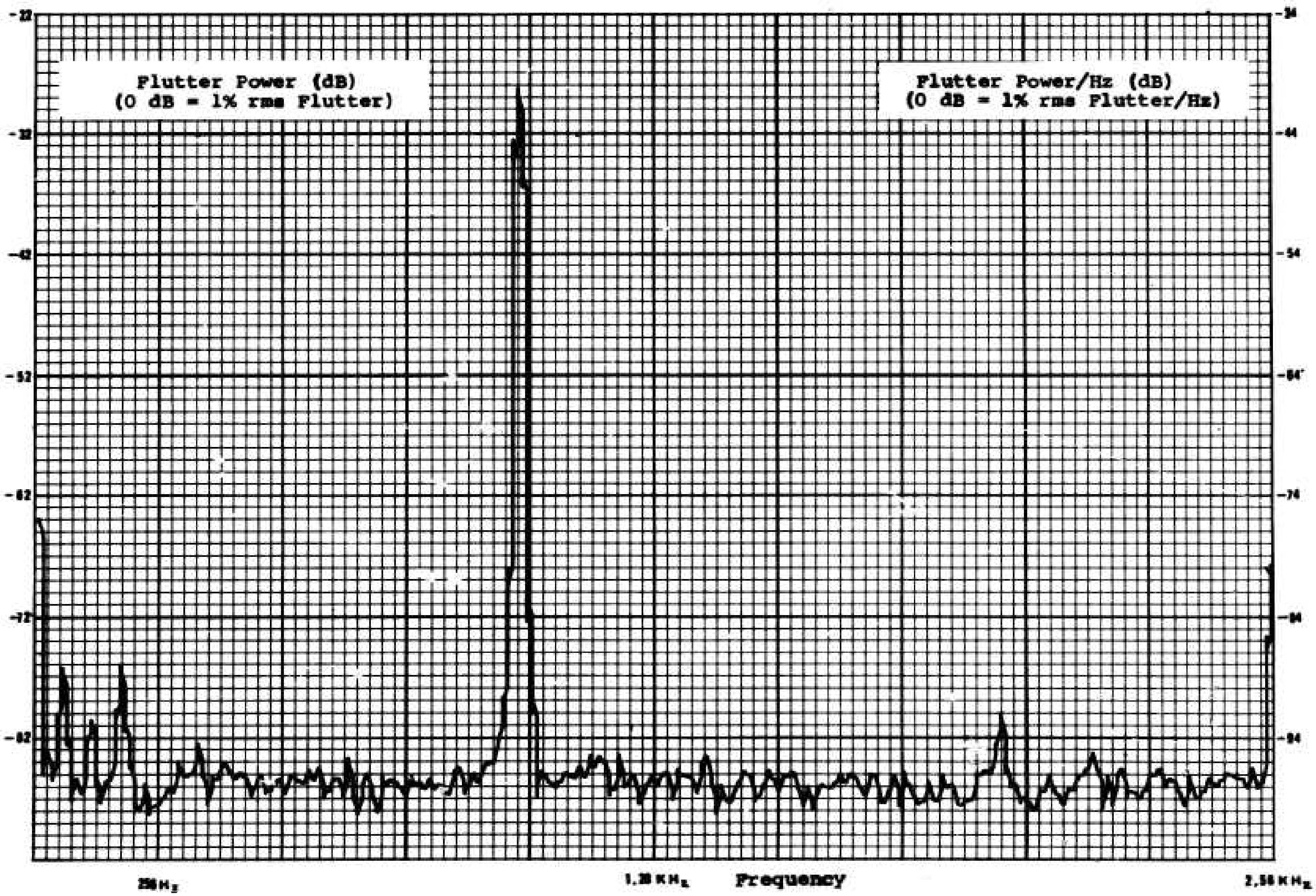

Figure 4. Spectrum of Reproduced Calibration Signal (2.56 kHz Bandwidth).

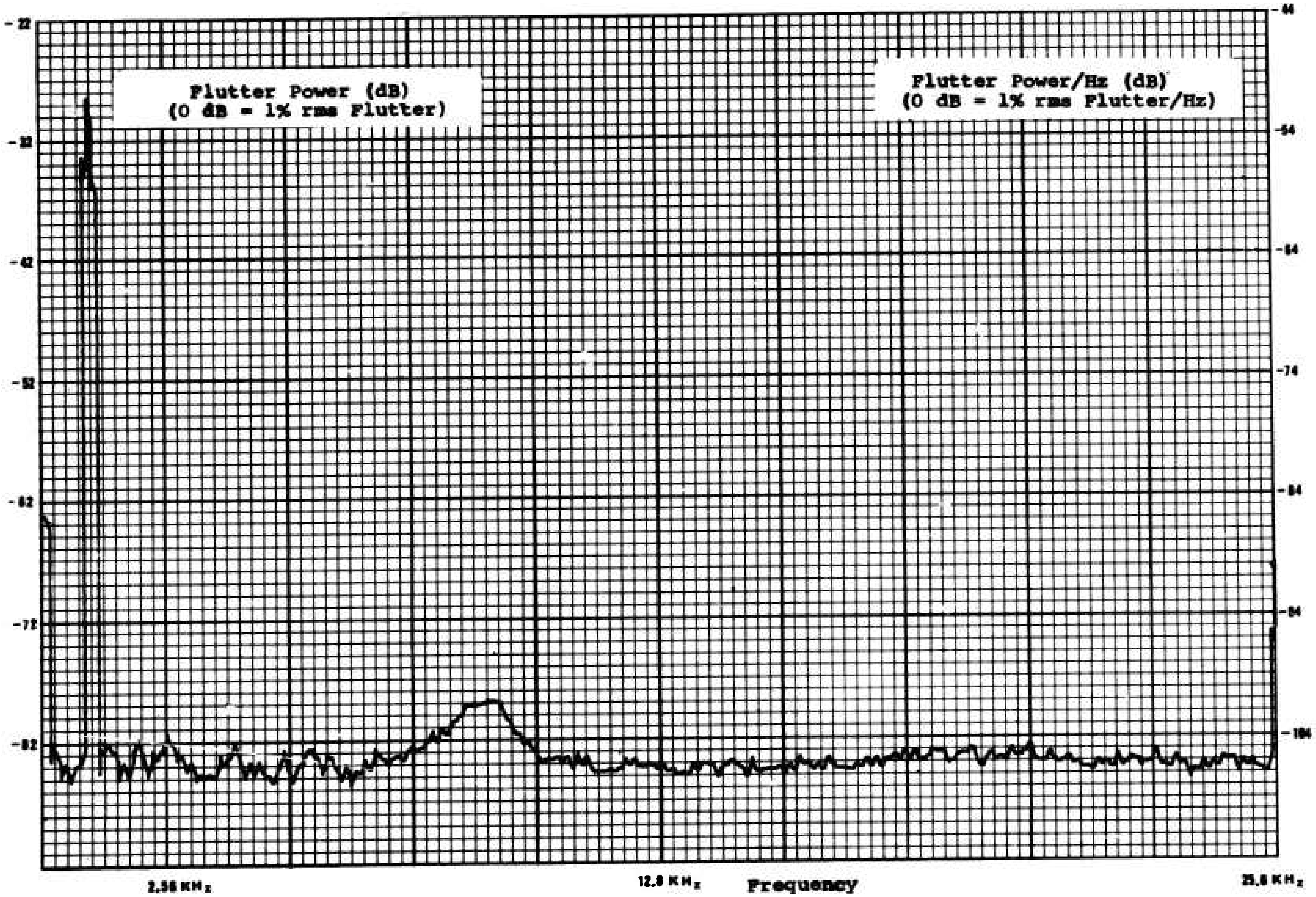

Figure 5. Spectrum of Reproduced Calibration Signal (25.6 kHz Bandwidth).

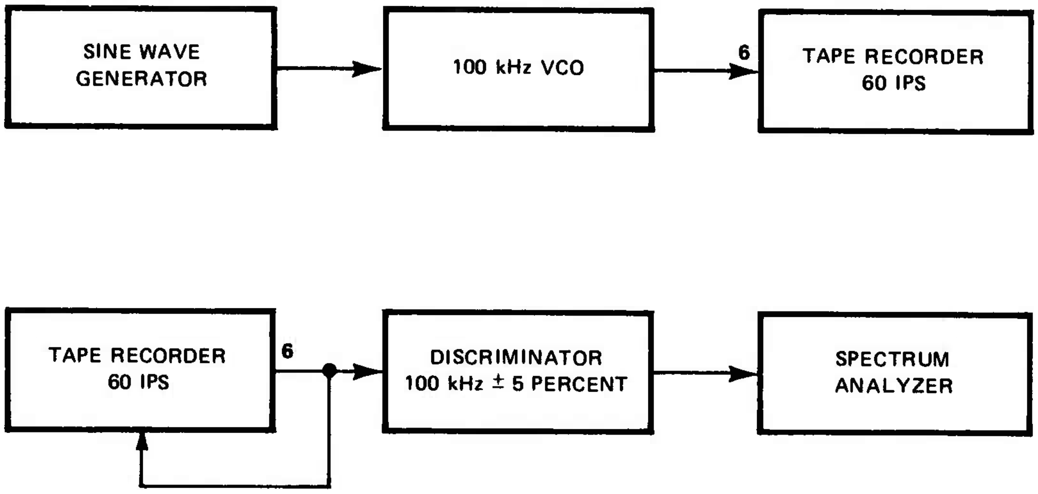

Figure 6. Setup for Servo Response Test.

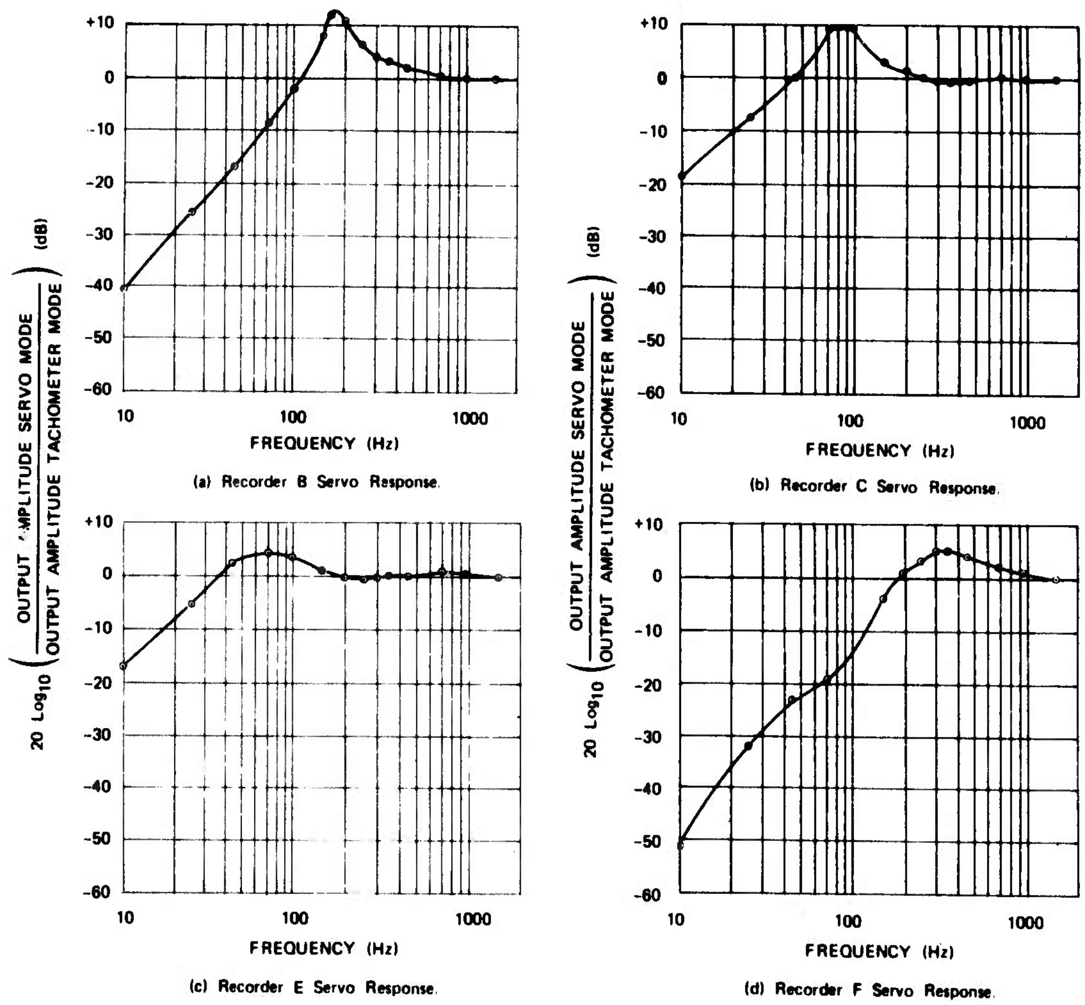

Figure 7. Tape Recorder Servo Responses.

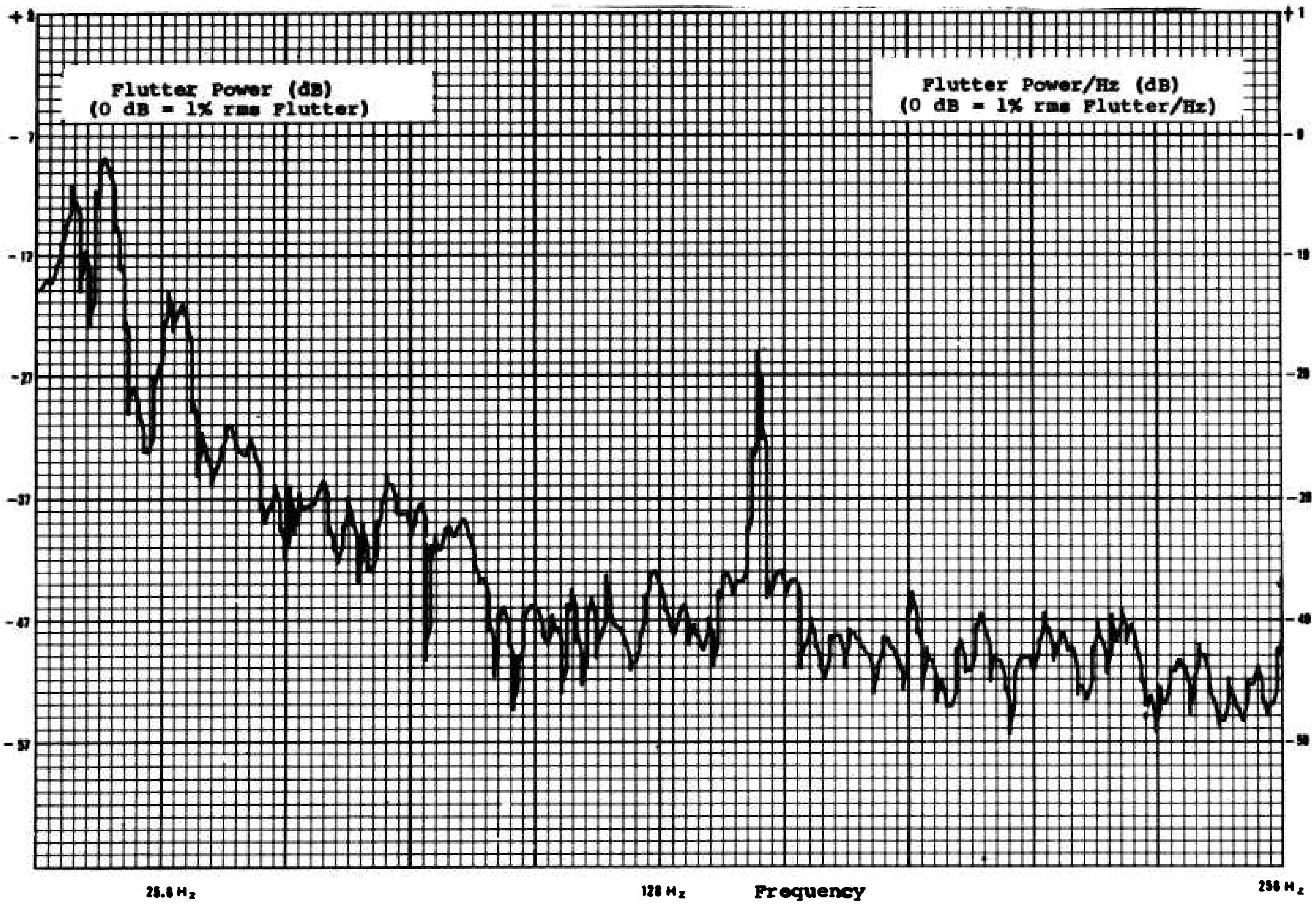

Figure 8. Flutter Spectrum in Tape Servo Mode (Unstable).

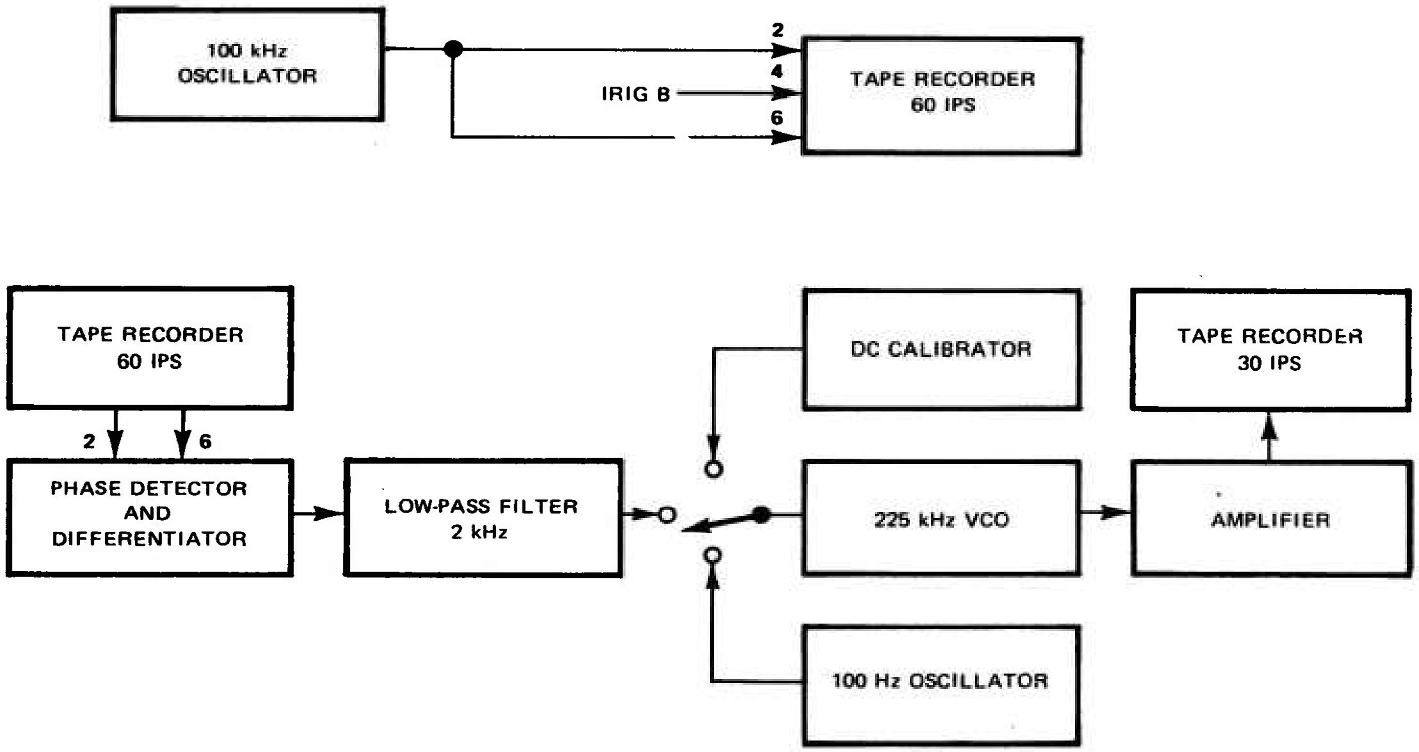

Figure 9. Setup for DITDE Measurements.

RESULTS

The results of the tests are as follows:

1. The low-frequency flutter components of the tape recorders tested were narrow-band sinusoidal processes, while high-frequency components were relatively wide-band random processes (see appendix A).

2. The servo systems of the tape recorders used in this study were all underdamped. This caused some flutter components to be amplified rather than attenuated in the tape servo mode.

3. Interchannel time displacement error does not appear to be a large contributor to total flutter in the tape servo mode (see appendix A).

4. Recordings made using brand x tape appear to have 1 to 3 db more high-frequency flutter power than those made using brand y tape (see appendix D).

5. Two different recorders of the same model can have significantly different flutter spectra (see appendix E).

CONCLUSIONS

1. The flutter spectrum resulting from a crossplay using two tape recorders can be predicted fairly well if the flutter spectra of each machine are known and it is known which components are record processes and which are reproduce processes.

2. There is a need for standard test procedures to measure tape recorder servo system response.

APPENDIX A

ANALYSIS OF FLUTTER AND DITDE SPECTRA

The flutter spectra of all six tape recorders used in this study are presented in appendix F. Analysis of these spectra shows that most of the spectral components below approximately 2 kHz are sinusoidal and the high-frequency components are random. Since the sum of several independent sinusoids tends toward a normal probability density function (central limit theorem*), the amplitude probability density function of the flutter is approximately normally distributed. A typical density function is shown in figure A-1.

Figure A-2 shows the low-frequency flutter spectrum recorder of A at the beginning and the middle of the reel of tape recorded and reproduced on A. The spectrum at the end of the tape was very similar to the spectrum at the beginning of the tape in this case. The large spectral component (beginning of tape) at approximately 3 Hz was due to the lower reel rate of 3 revolutions per second and the 1.5 Hz component was due to the upper reel rate of 1.5 revolutions per second. At the middle of the tape, the upper and lower reels both rotate at about 1.9 Hz. The only frequency components that changed with position on the reel of tape were the very-low-frequency components.

Figures A-3 through A-9 show that some flutter components were record phenomena (occurred only on reproductions involving the tape recorded on a certain machine), some were reproduce phenomena (occurred only when a tape was reproduced on a certain machine), and some were a combination of both (occurred whenever a tape was recorded or reproduced on a certain machine).

Figures A-3 and A-4 show that the crossplay spectra of A and B overlaid on the spectrum of A. Those overlays show that A had large combination components at 15, 30, and 45 Hz; large record components at 60, 75, and 90 Hz; and large reproduce components at 105, 135, 150, 180, and 225 Hz. B was shown to have a large combination component at 16.7 Hz (the capstan rotation rate); a large reproduce component at 50 Hz; and large record components at 133, 233, and 250 Hz. All of the above recorder A components are at multiples of 15 Hz and all of the above recorder B components are at multiples of 16.7 Hz.

*Hoel, Paul G. Introduction to Mathematical Statistics. Wiley, New York. 1971.

Figures A-5 and A-6 show the crossplay spectra of C and D overlaid on the spectrum of D. These figures show that D had large components at 150, 165, and 180 Hz that were mainly due to record phenomena. They also show that C had large combination effects at 5 and 20 Hz. Figure A-7 is an overlay of F record with D reproduce spectrum on the spectrum of D. This shows that the component at 165 Hz was a large reproduce component whereas the 150 Hz component was still a record component for this combination.

Figure A-8 consists of two overlays: the C record with the B reproduce spectrum overlaid on the C spectrum and the B record with C reproduce spectrum overlaid on the B spectrum. This figure shows that B had a large record component at approximately 13 kHz and a large combination component at approximately 9 kHz. The C had large record components at approximately 14 kHz and 8 kHz (crosstalk with 100-kHz reference signal). The C also had large reproduce components at 1.3 and 2.1 kHz.

Figure A-9 shows the C and E crossplay spectra overlaid on the E spectrum. This figure shows that the E had a reproduce component at 11 kHz and a record component at 13 kHz. It also shows the C record component at 14 kHz.

Figures A-10 and A-11 are overlays of B flutter spectra taken using the same recorded tape but played back 7 months apart. Figure A-10 shows that the high-frequency flutter components showed little change over this interval. Figure A-11 shows that some of the low-frequency flutter components changed considerably over this time interval. Figure A-12 shows an overlay of the greatest difference observed between low-frequency flutter components of several playbacks on one day. This shows that most low-frequency components show very little change but some components can change as much as 6 dB. This appears to be due to a lack of stationarity in the flutter rather than a lack of degrees of freedom of the plotted data. This means that accurate prediction of some flutter components may not be possible because they change from playback to playback. Also, some flutter components change due to various changes in the tape recorder transport. Changes in a tape recorder's flutter components can be used to detect possible problems in the tape recorder transport.

Figures A-13, A-14, and A-15 are overlays of the B flutter spectrum in tachometer mode and tape servo mode. These figures show that the B servo system attenuates flutter components below about 110 Hz, amplifies flutter components between 110 Hz and 300 Hz, and does not appear to affect flutter components above 750 Hz.

Figures A-16 and A-17 are sample overlays of the flutter in tape servo mode and the DITDE for the tape recorded on C and reproduced on F. Figure A-16 shows good correlation in the 7 Hz and 14 Hz components but no correlation in the 4-Hz component of flutter. Figure A-17 shows fair correlation in the 115 Hz and 230 Hz components. However, the important point is that the maximum DITDE component had an amplitude approximately equivalent to 0.001 percent rms flutter (see appendix G). Therefore, DITDE has a relatively minor effect upon total flutter in the tape servo mode.

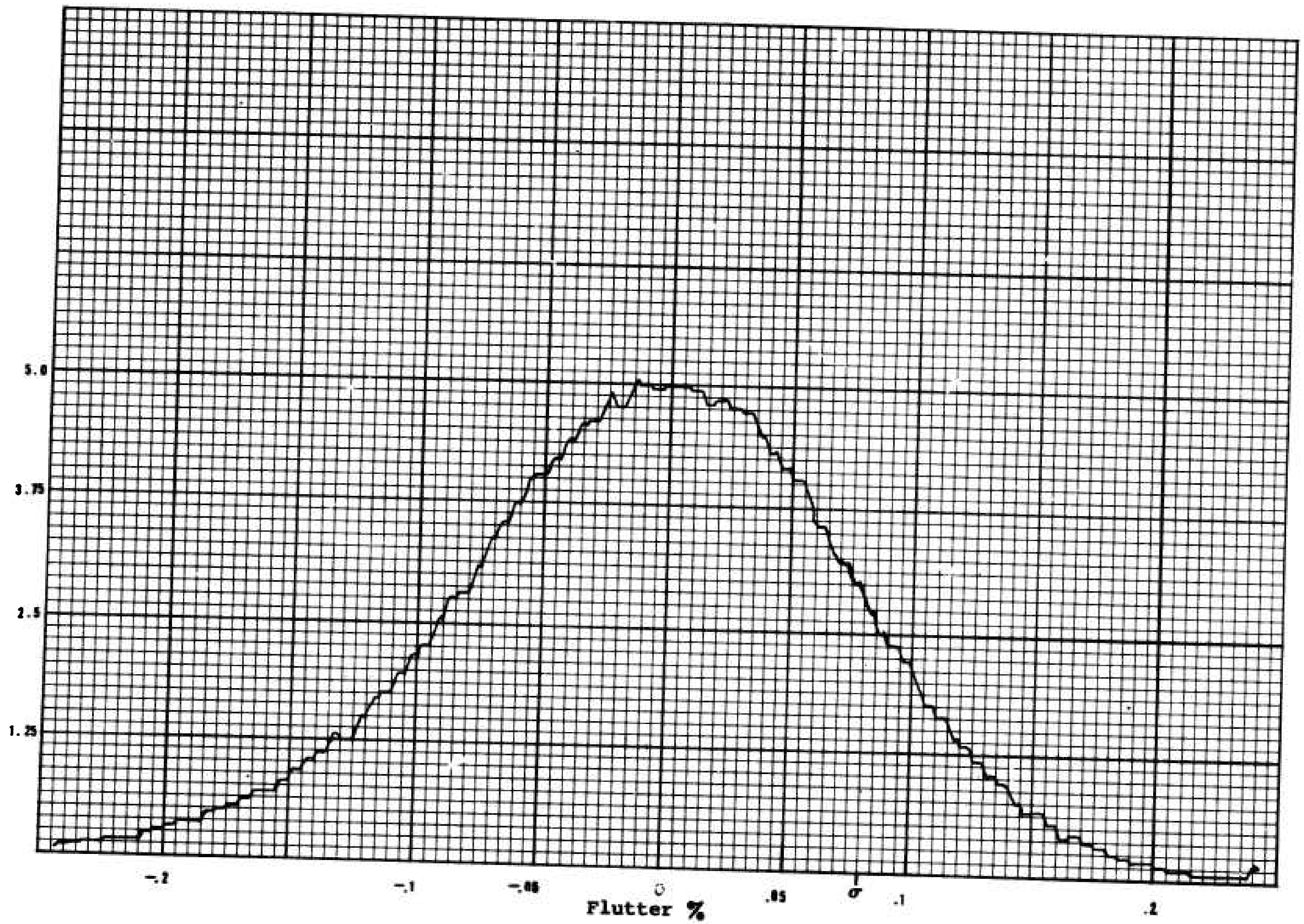

Figure A-1. Flutter Probability Density Function, Recorder B.

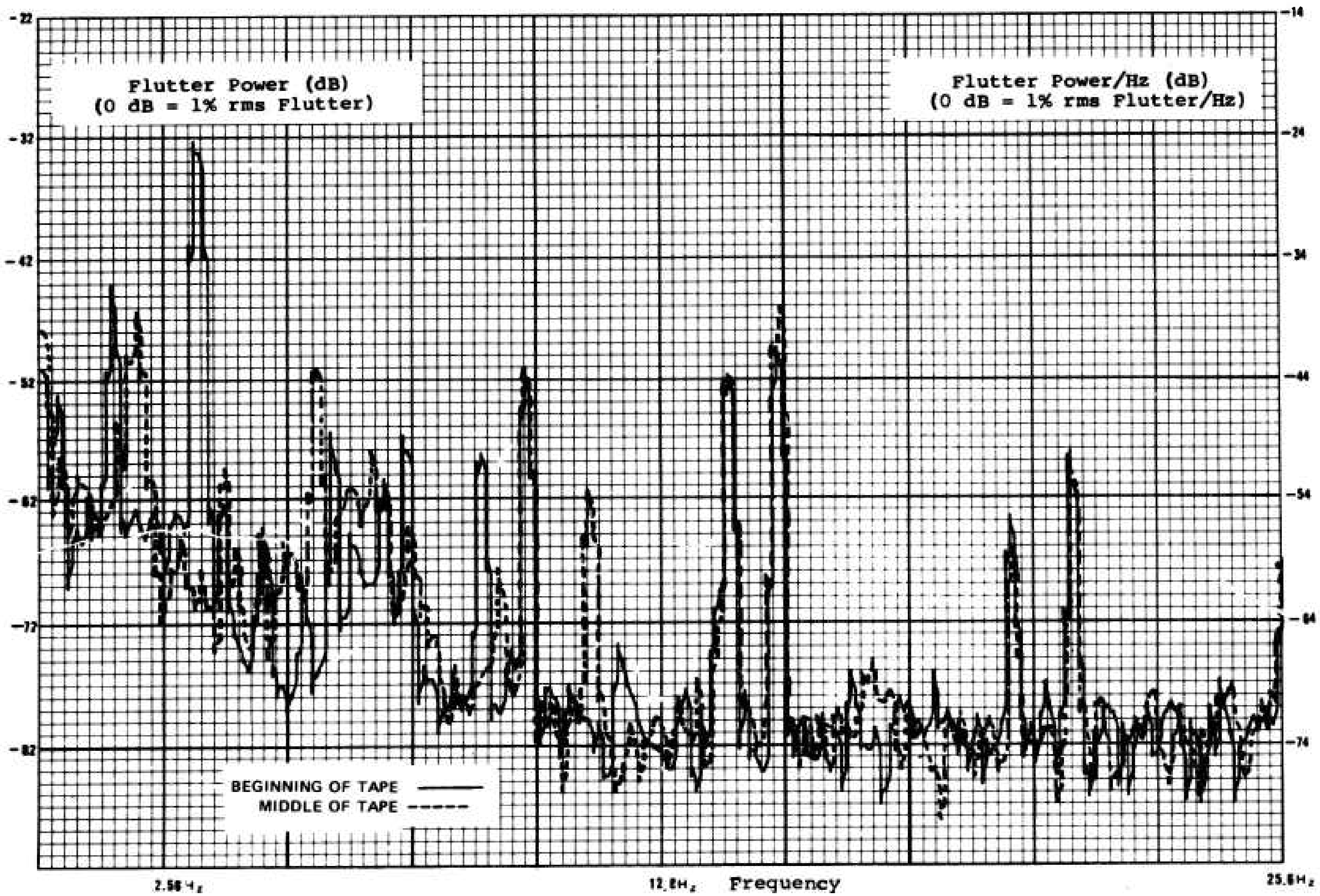

Figure A-2. Flutter Power Spectral Densities, Recorder A.

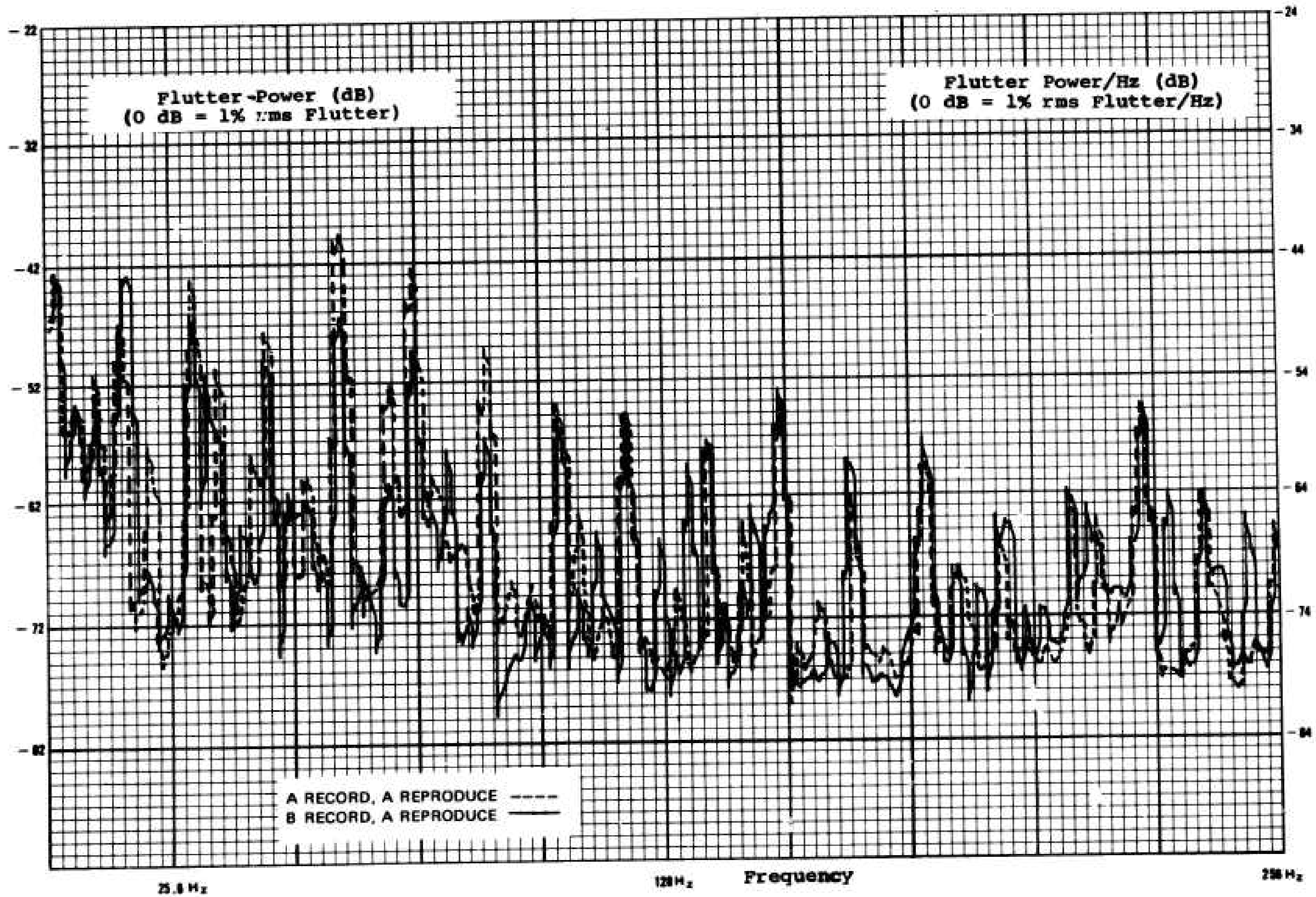

Figure A-3. Flutter Comparison of Recorder B Record and Recorder A Reproduce Versus Recorder A.

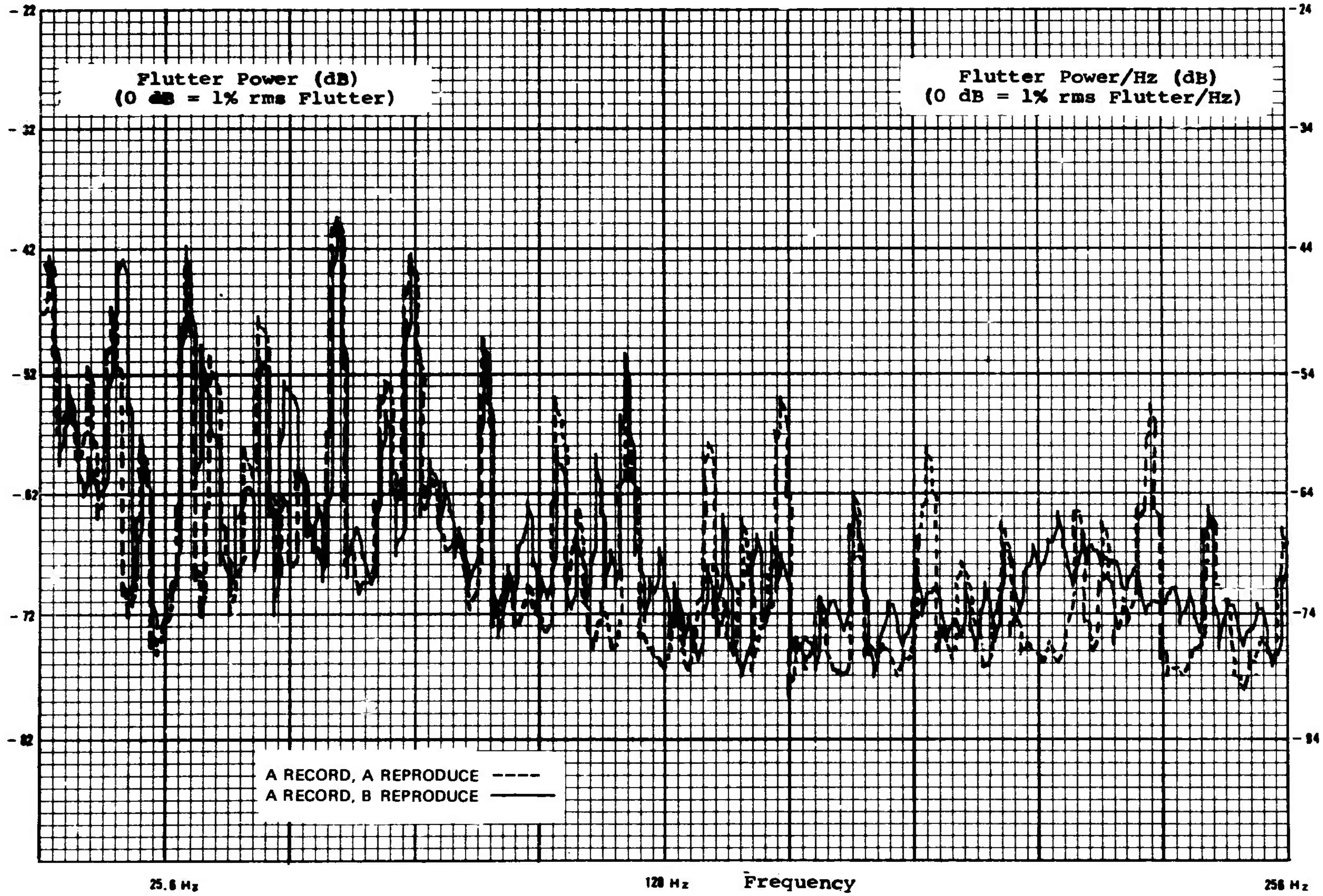

Figure A-4. Flutter Comparison of Recorder A Record and Recorder B Reproduce Versus Recorder A.

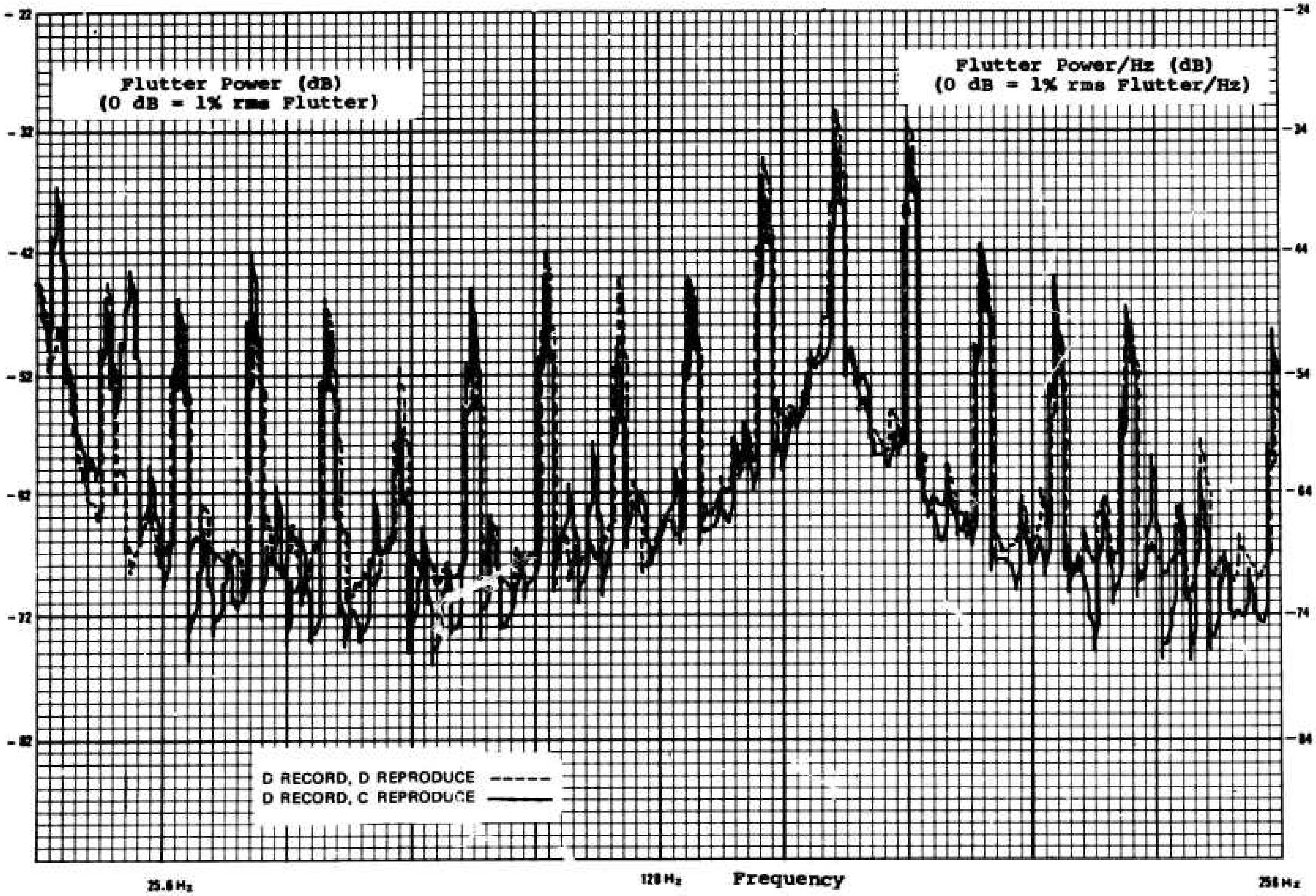

Figure A-5. Flutter Comparison of Recorder Record and Recorder C Reproduce Versus Recorder D.

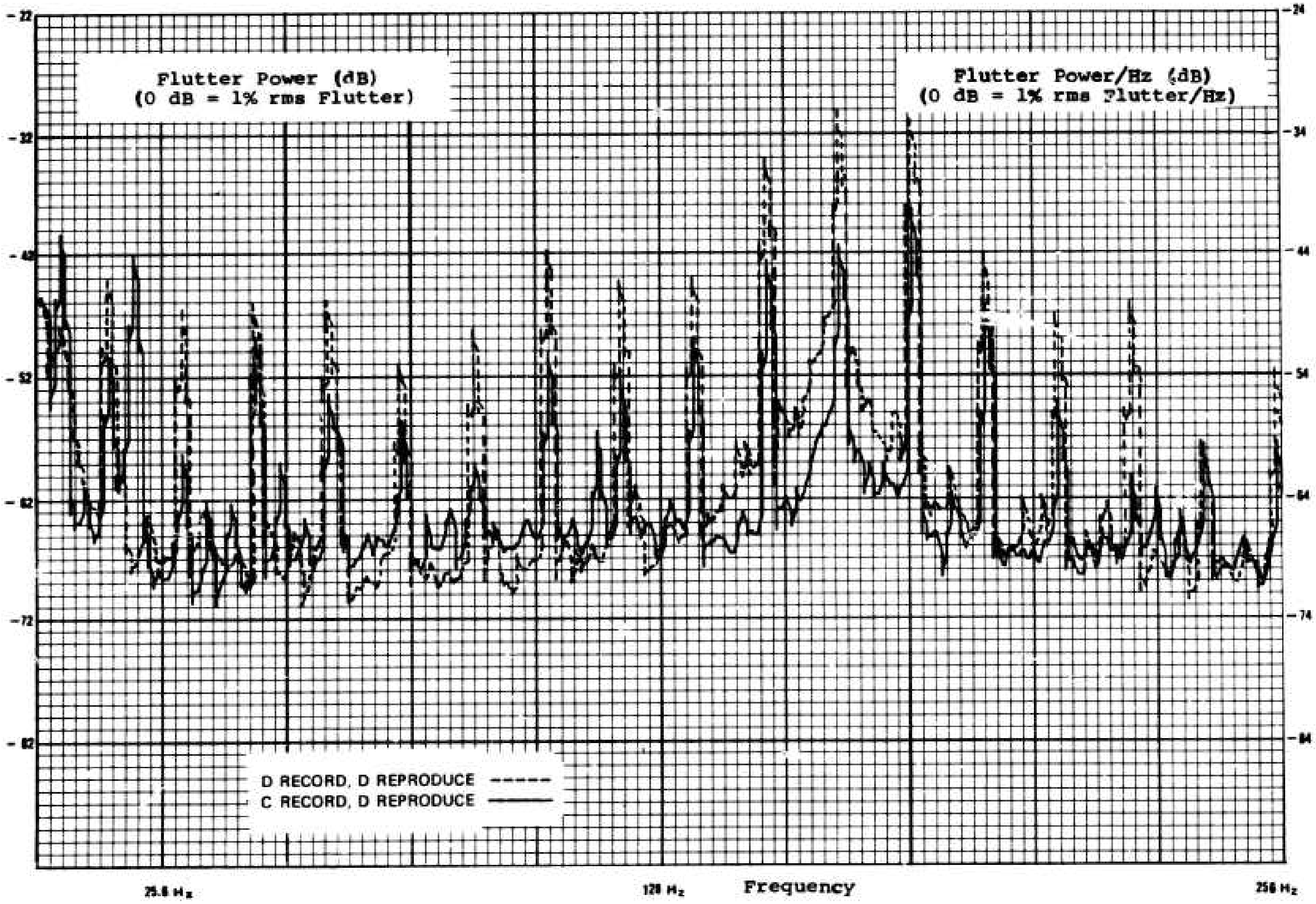

Figure A-6. Flutter Comparison of Recorder C Record and Recorder D Reproduce Versus Recorder D.

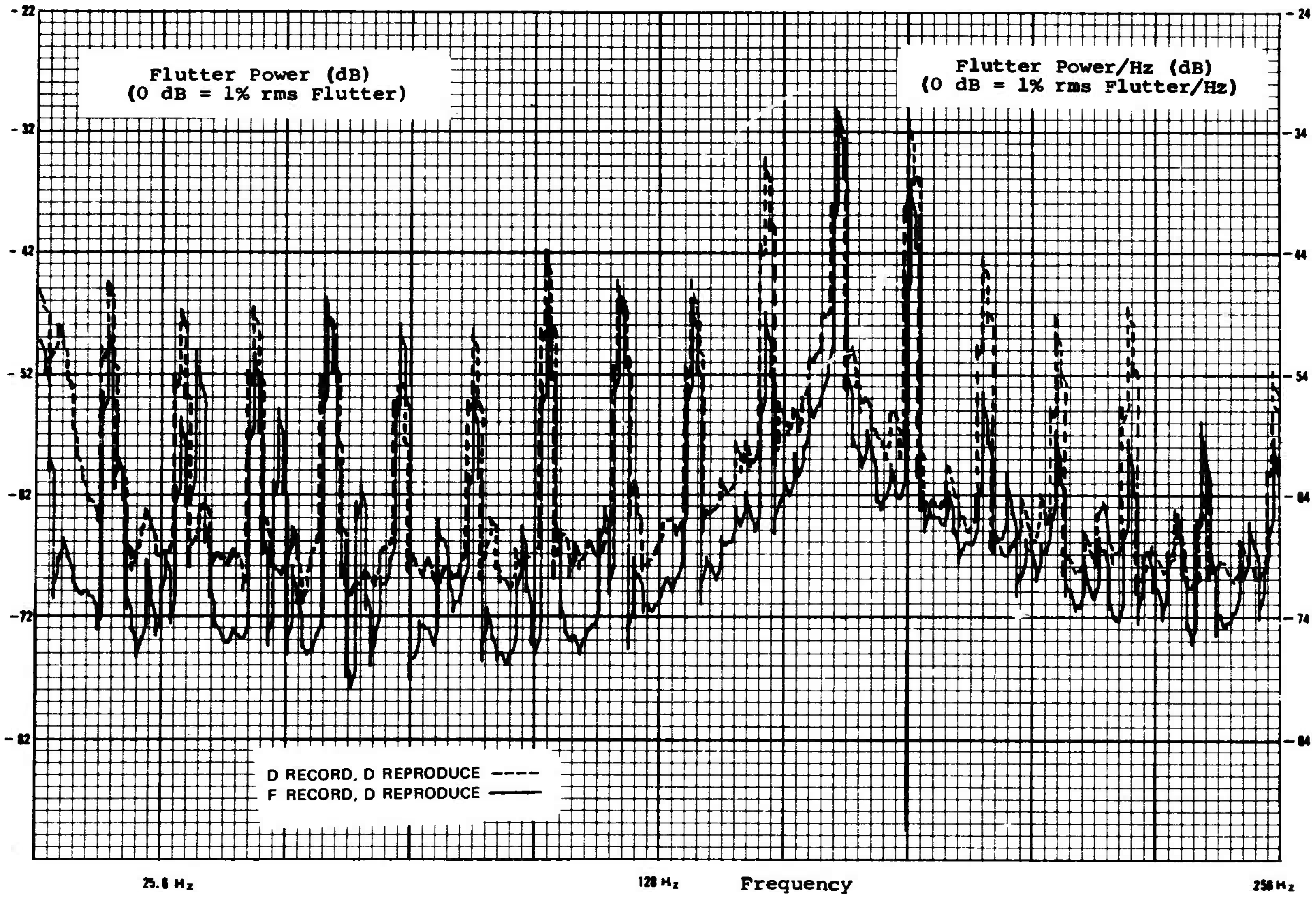

Figure A-7. Flutter Comparison of Recorder F Record and Recorder D Reproduce Versus Recorder D.

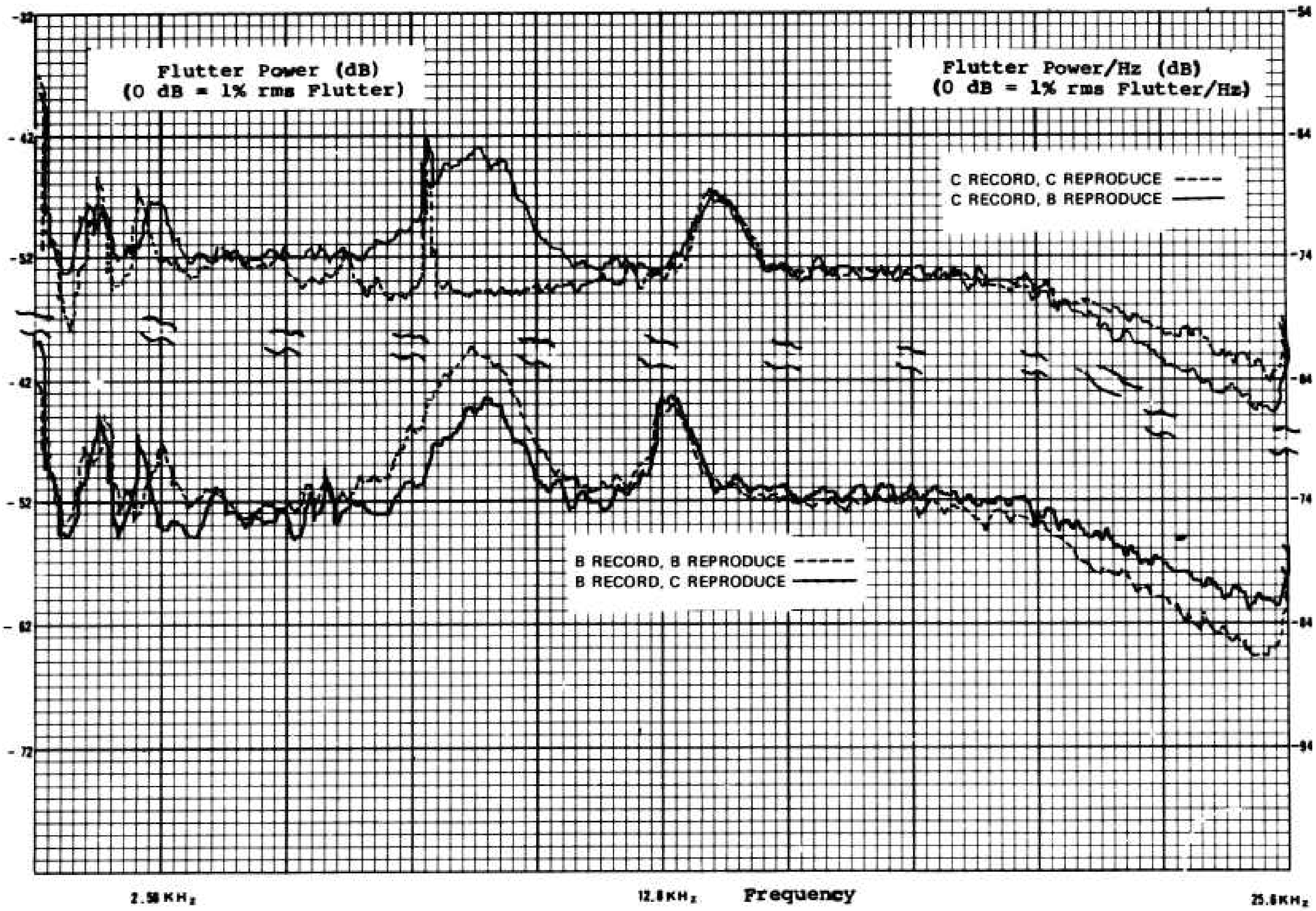

Figure A-8. Comparison of Recorders B and C in Record and Reproduce Modes.

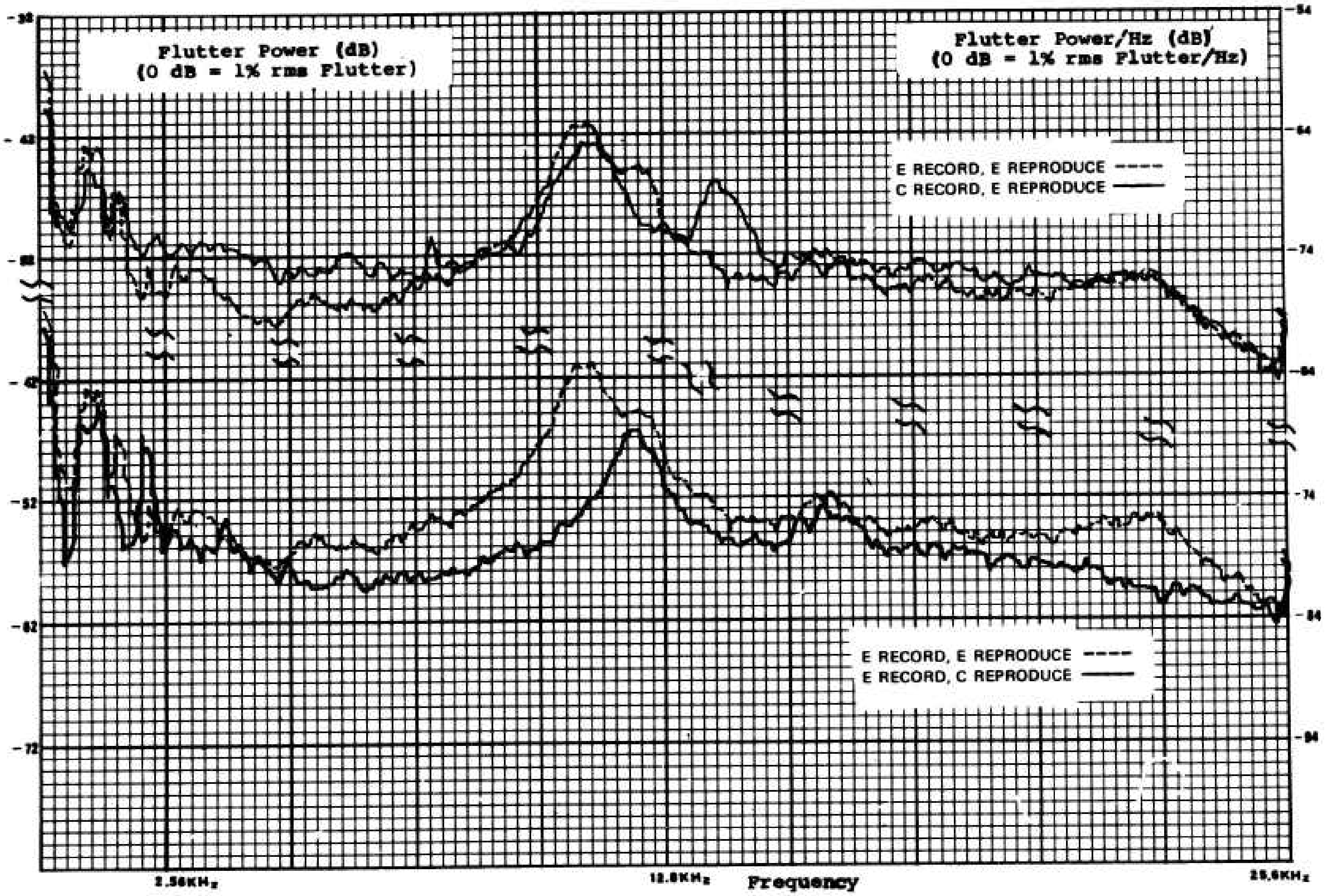

Figure A-9. Comparison of Recorders C and E in Record and Reproduce Modes.

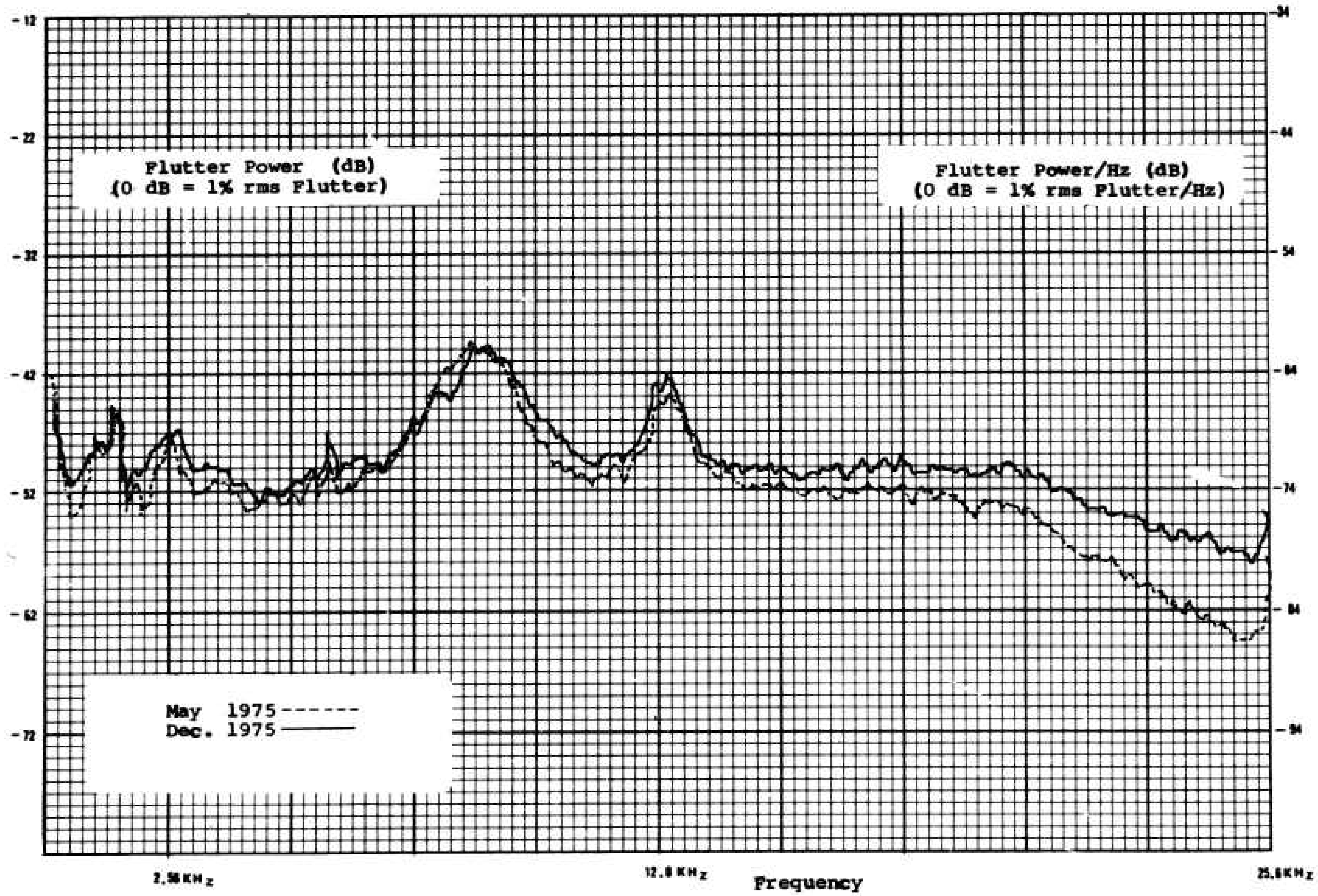

Figure A-10. May and December 1975 Flutter Power Spectral Densities, 25.6 kHz Bandwidth.

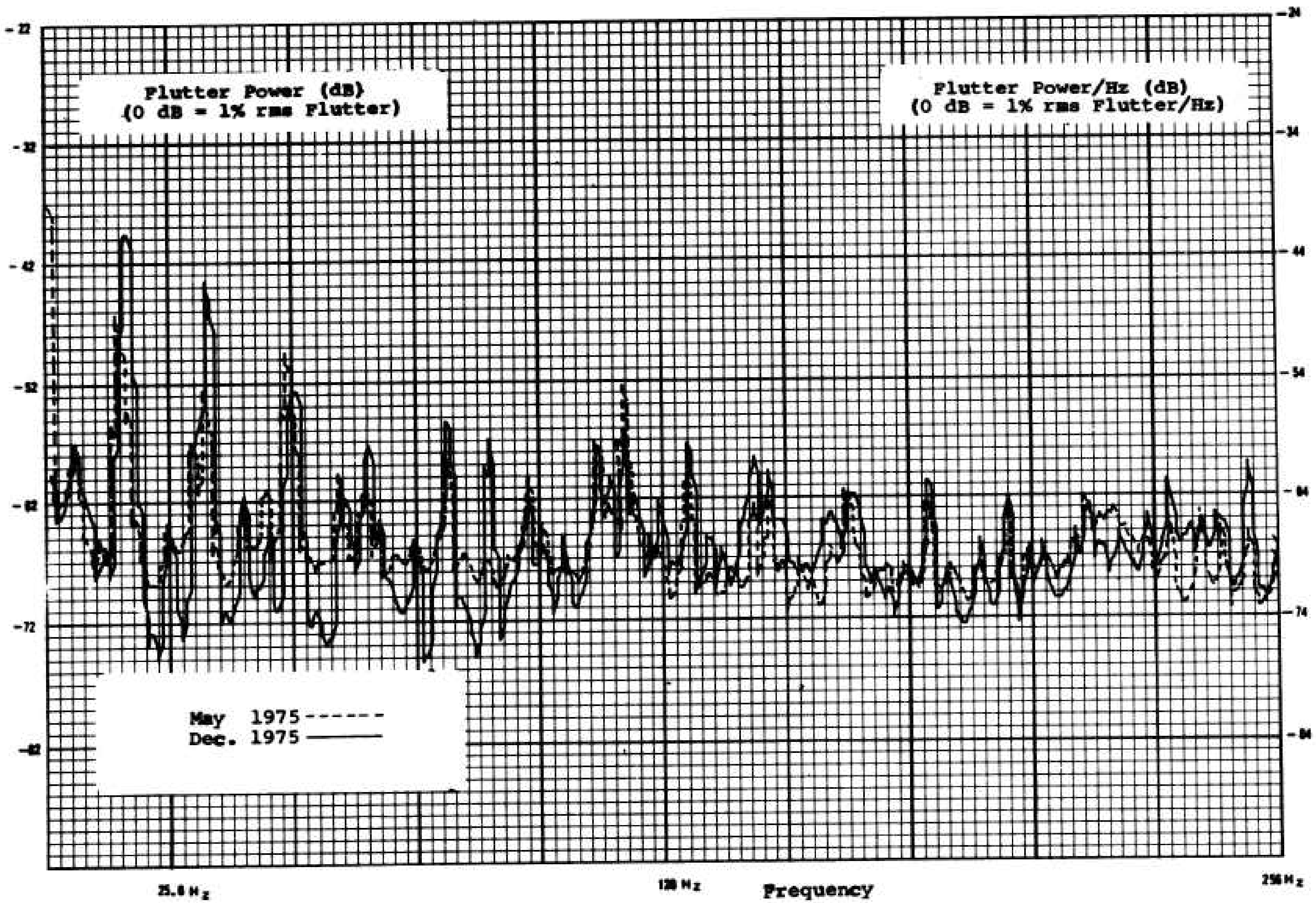

Figure A-11. May and December 1975 Flutter Power Spectral Densities, 256 Hz Bandwidth.

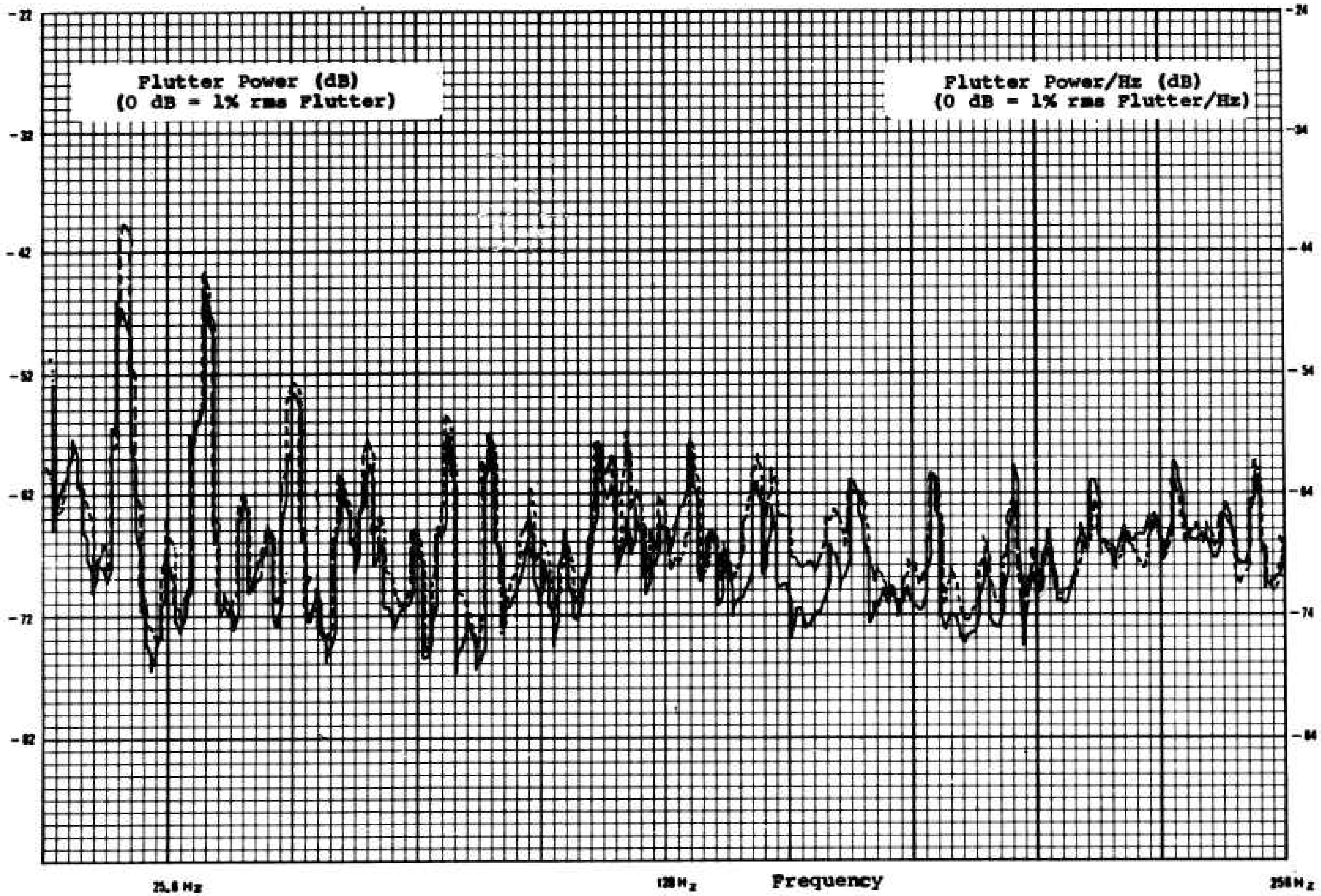

Figure A-12. Maximum Difference in Low-Frequency Flutter Components From Several Reproductions in a Single Day.

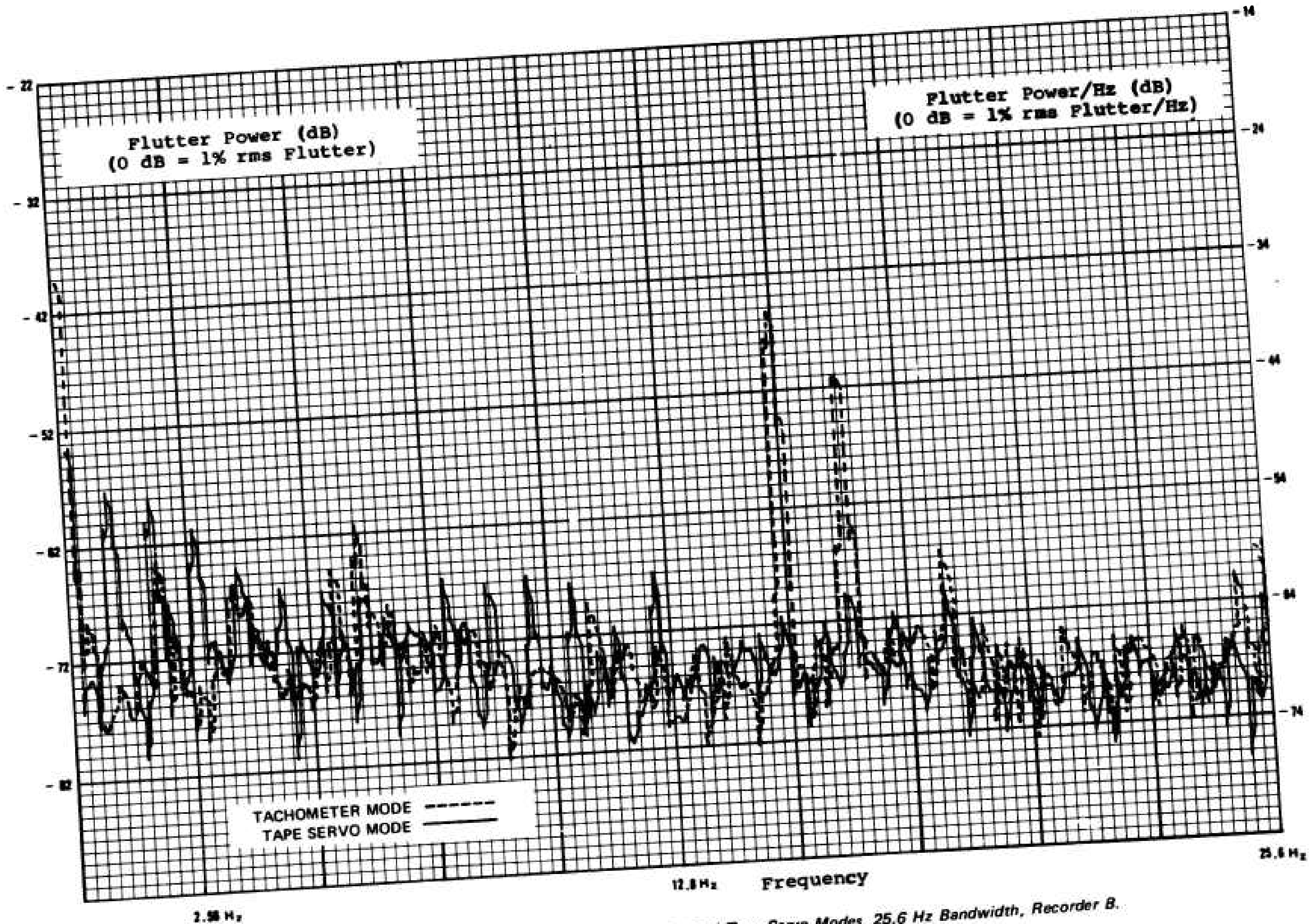

Figure A-13. Flutter Power Spectral Density in Tachometer and Tape Servo Modes, 25.6 Hz Bandwidth, Recorder B.

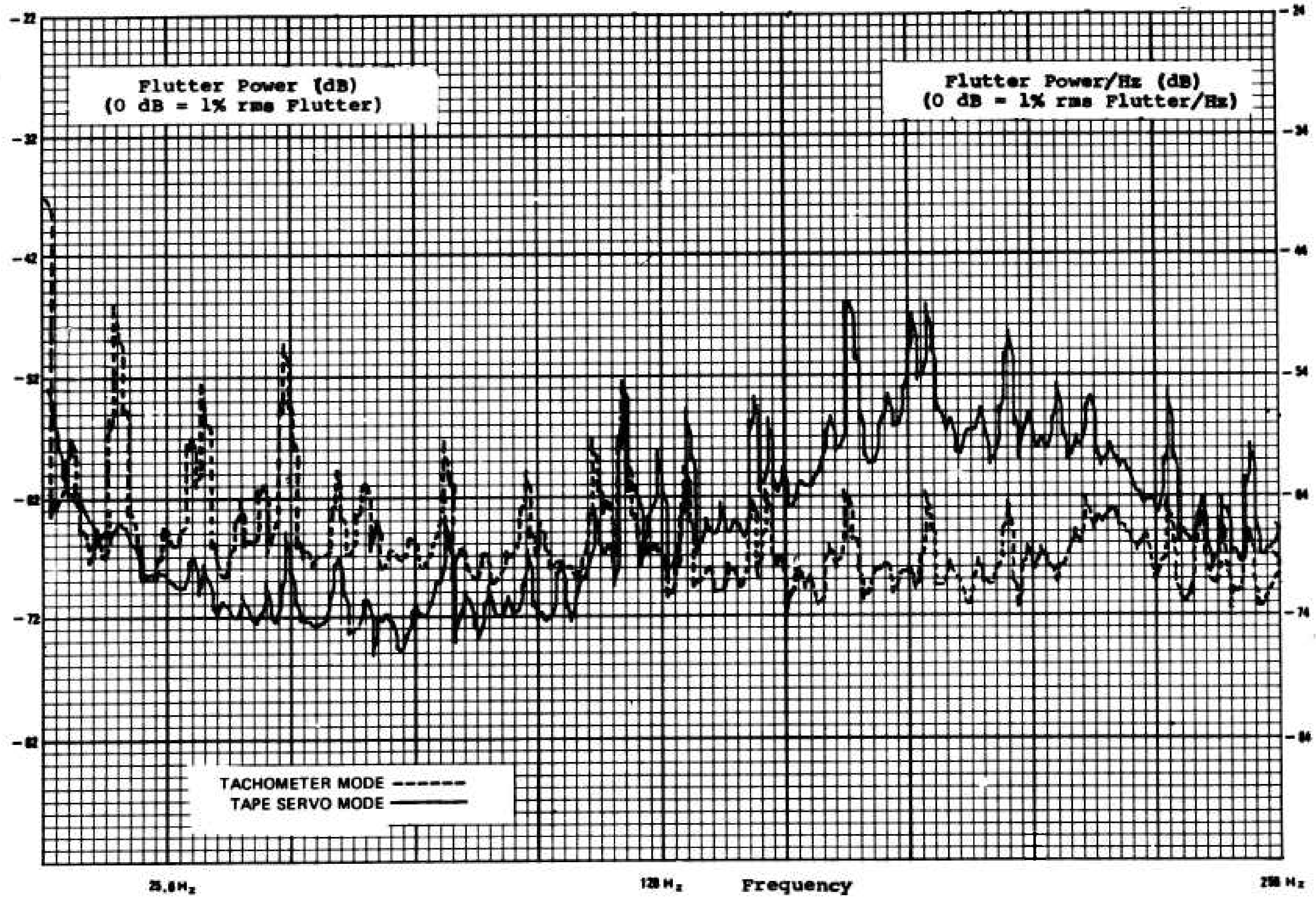

Figure A-14. Flutter Power Spectral Density in Tachometer and Tape Servo Modes, 256 Hz Bandwidth, Recorder B.

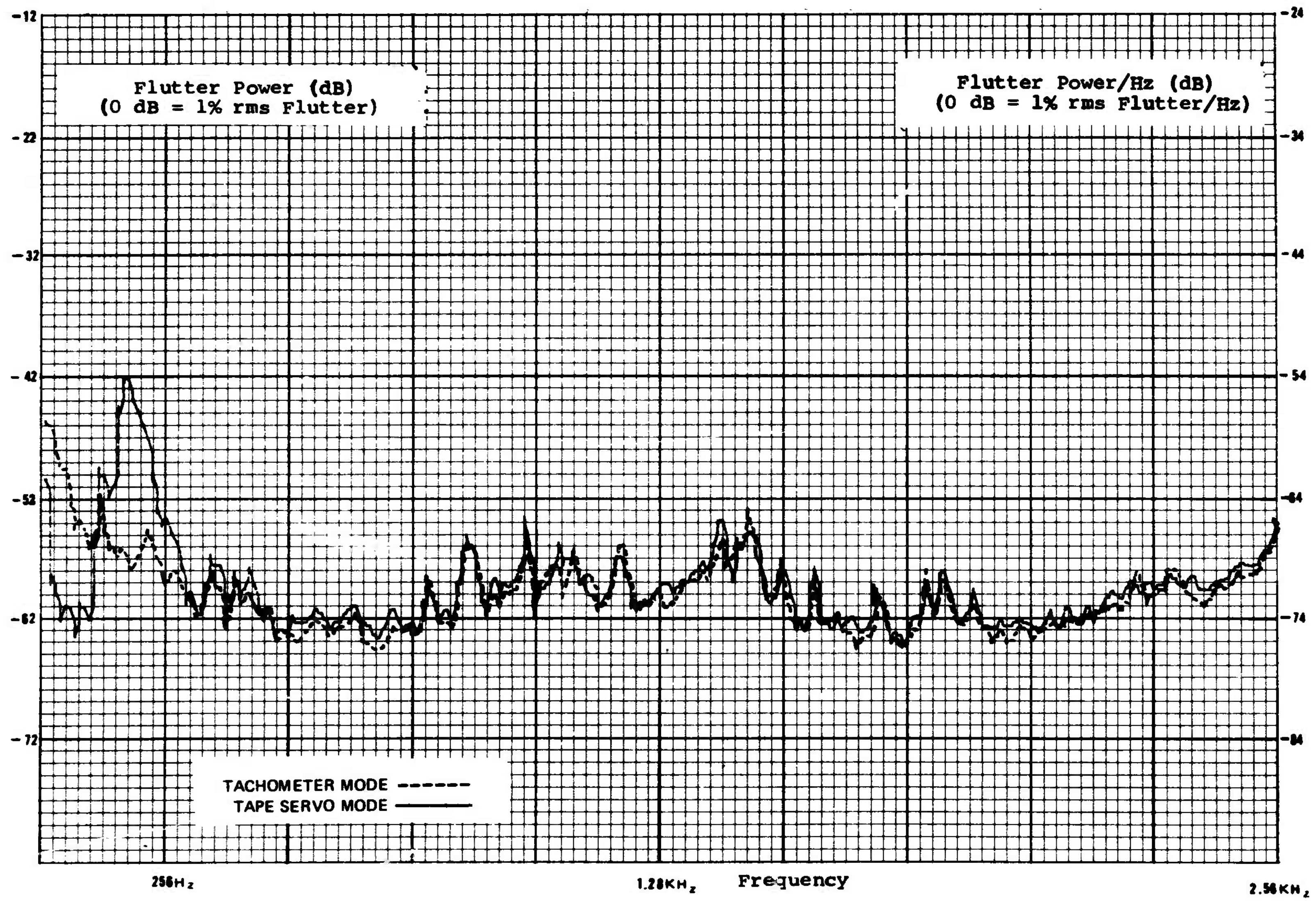

Figure A-15. Flutter Power Spectral Density in Tachometer and Tape Servo Modes, 2.56 kHz Bandwidth, Recorder B.

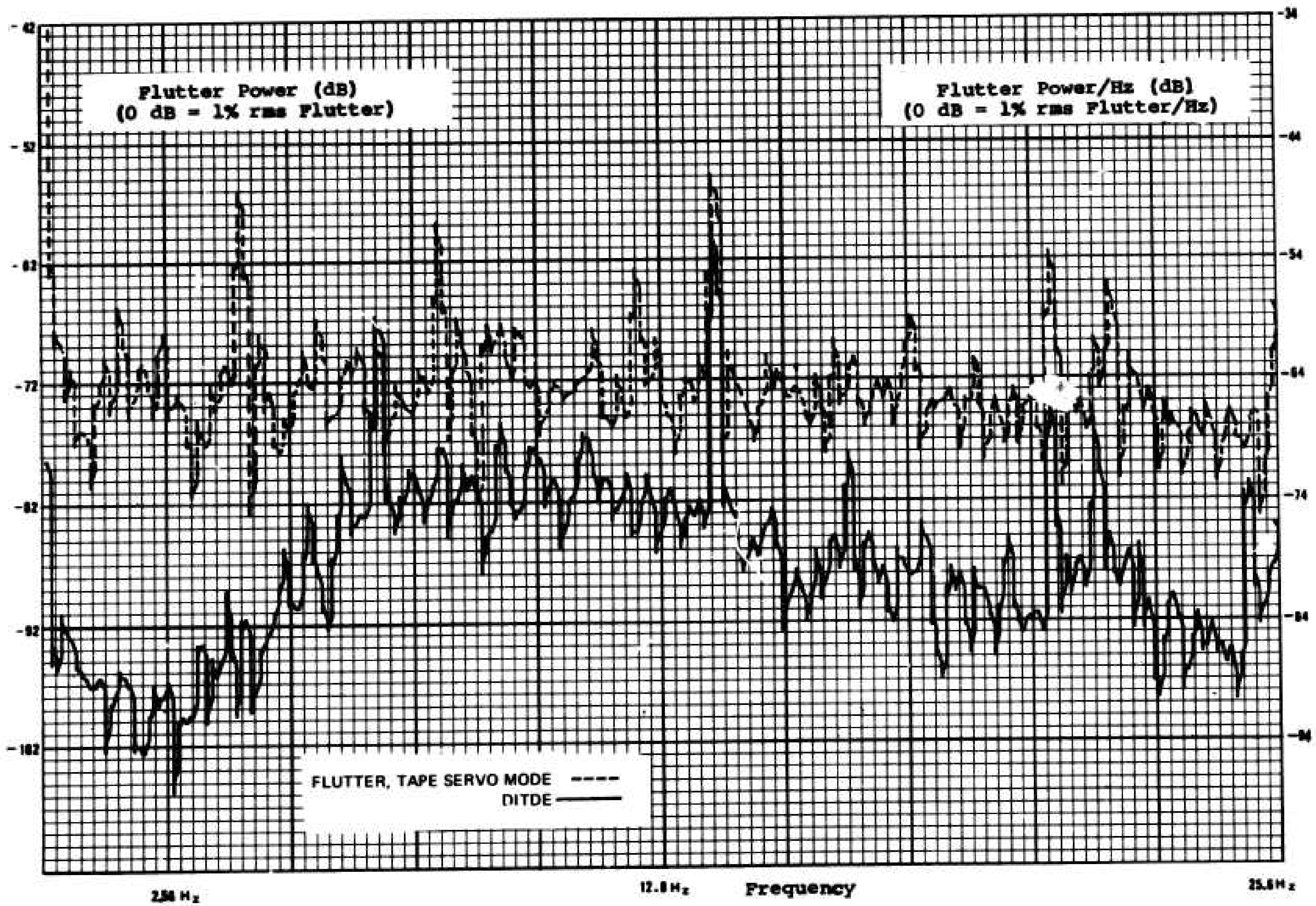

Figure A-16. Comparison of Flutter and DITDE Power Spectral Densities, 25.6 Hz Bandwidth, C Record, F Reproduce.

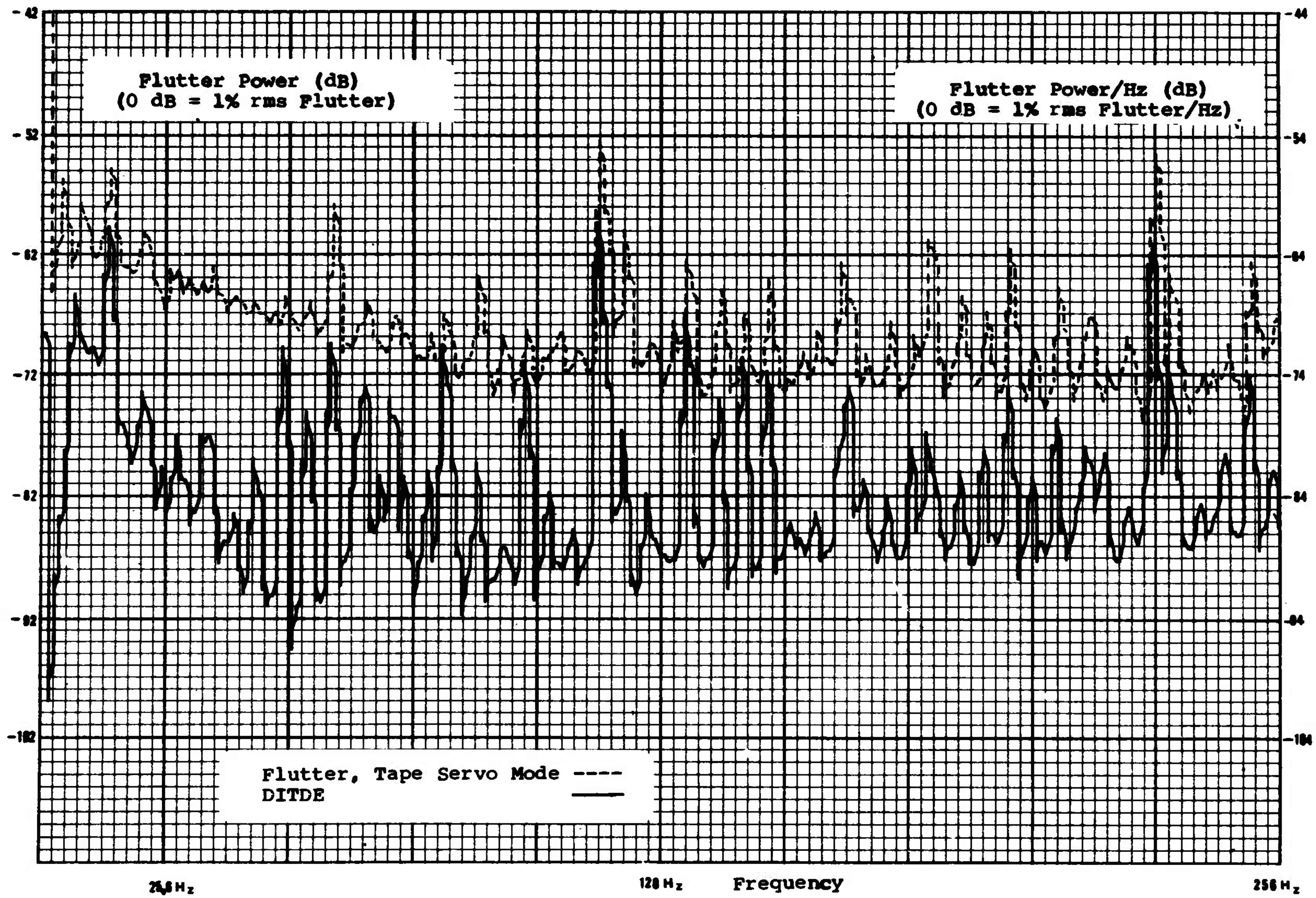

Figure A-17. Comparison of Flutter and DITDE Power Spectral Densities, 256 Hz Bandwidth, C Record, F Reproduce.

APPENDIX B

DESCRIPTION OF PHASE DETECTOR AND DIFFERENTIATOR

Figure B-1 is a schematic of the differential phase detector and differentiator designed and built for this project. The two 100-kHz signals from the tape recorder are applied to inputs No. 1 and No. 2. Input No. 1 contains a network which has a 45-degree lead of input versus output phase at 100 kHz. Input No. 2 contains a network which has a 45 degree lag of input versus output phase at 100 kHz. This gives a net 90 degrees phase shift between the inputs. The MC1596L is a balanced modulator-demodulator which operates as a linear phase detector provided that the inputs have an amplitude greater than 100 mV. Amplifier AR1 sums the differential outputs of the MC1596L.

The output of amplifier AR1 contains a component directly proportional to the phase difference between the two inputs (provided that this angle is less than 90 degrees) and a component at 200 kHz. This signal then goes to a 3-pole, Butterworth active filter with a 3 dB bandwidth of 10 kHz. The output of the filter is a signal proportional to the phase difference between the two inputs, with a sensitivity of 100 mV/degree. This signal then goes to a differentiator with selectable RC time constants of 0.03 ms, 0.1 ms, and 0.3 ms.

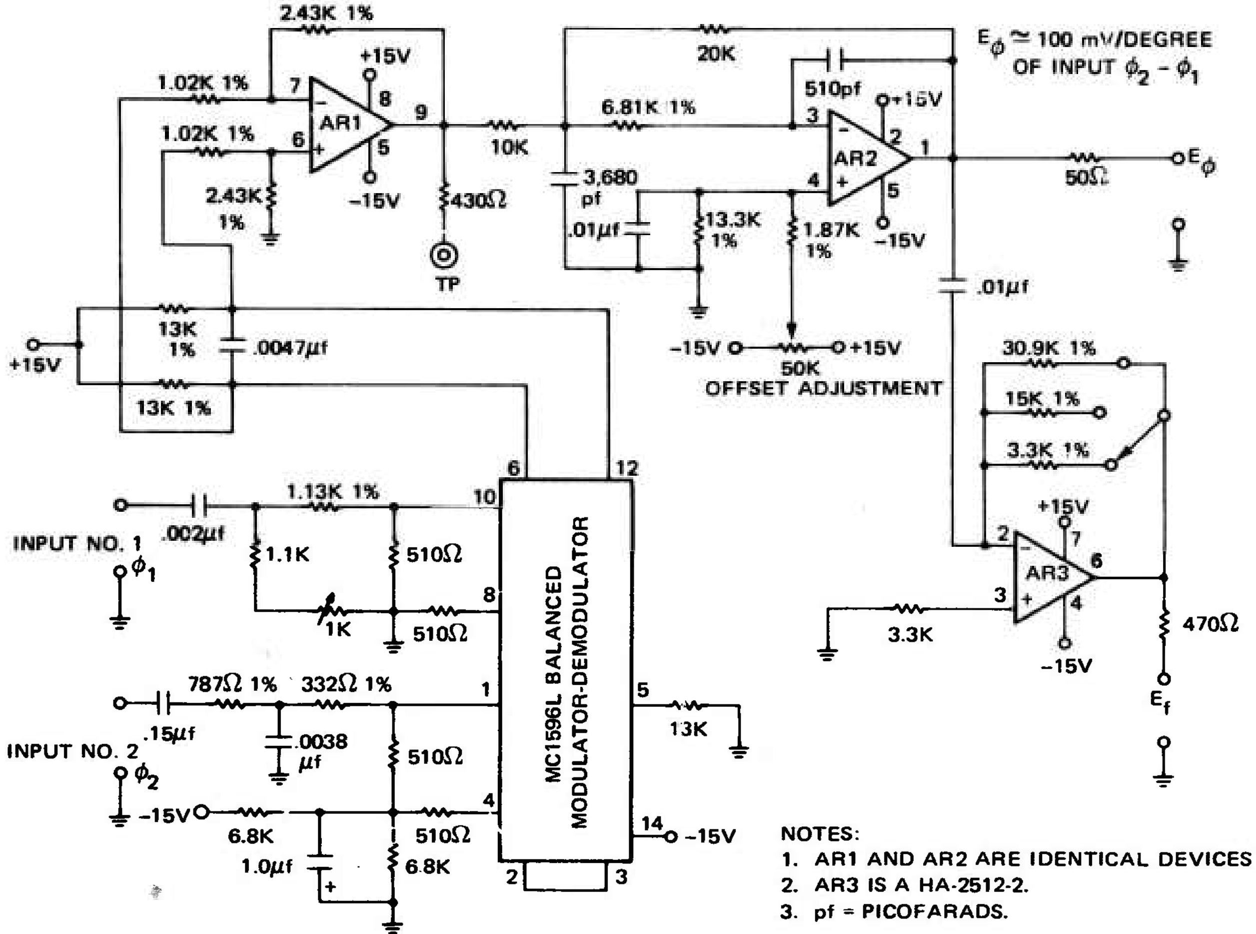

NOTES:
1. AR1 AND AR2 ARE IDENTICAL DEVICES (CA747CT).
2. AR3 IS A HA-2512-2.
3. pf = PICOFARADS.

Figure B-1. Schematic of PMTC Phase Detector and Differentiator.

APPENDIX C

PROCEDURE FOR CALCULATION OF TIME BASE ERROR SPECTRUM FROM FLUTTER SPECTRUM

The rms time base error at a frequency f_i can be calculated from the rms flutter as follows: time base error is proportional to the integral of flutter with time error

$$\tau = \frac{\phi T}{2\pi}$$

and the derivative of phase with respect to time equals frequency, therefore:

$$\int d\phi = \int \Delta w_i \cos (w_i t) dt$$

or

$$\phi = \frac{\Delta w_i}{w_i} \sin (w_i t)$$

$$\therefore \text{peak amplitude of } \phi = \frac{\Delta w_i}{w_i} = \frac{\Delta f_i}{f_i}$$

and

$$\tau \text{ peak} = \frac{T \Delta f_i}{2\pi f_i}$$

or

$$\tau \text{ rms} = \frac{T \Delta f_i \text{ rms}}{2\pi f_i}$$

where

T = period of recorded signal in seconds

Δf_i = peak frequency deviation in Hz at frequency f_i

Δf_i rms = rms frequency deviation in Hz at frequency f_i

ϕ = angular displacement in radians

For the data presented in this report

$$T = \frac{1}{(1.08)\,(10^5)} \text{ second and}$$

$$\Delta\, f_i \text{ rms} = (1.08)\,(10^3)\left(10^{\frac{y_i}{20}}\right) \text{ Hz}$$

where y_i is the left ordinate value at frequency f_i in decibels with respect to 1 percent rms deviation.

$$\therefore T\ \Delta\, f_i \text{ rms} = \frac{(1.08)\ (10^3)\left(10^{\frac{y_i}{20}}\right)}{(1.08)\ (10^5)} = \frac{10^{\frac{y_i}{20}}}{100}$$

$$\therefore \tau \text{ rms} = \frac{10^{\frac{y_i}{20}}}{200\ \pi\ f_i}$$

This same equation for τ can be also be used to convert DITDE to ITDE.

APPENDIX D

COMPARISON OF FLUTTER POWER SPECTRAL DENSITIES OF TWO BRANDS OF TAPE

Flutter tests were also conducted on several tape recorders using both brand x and brand y tape. Both were the two most commonly used wide-band, group II-type tapes. Typical flutter spectra are presented in figures D-1 and D-2. Figure D-1 shows that the low frequency flutter components are nearly identical. Figure D-2 shows that the brand x tape used has about 1 to 3 dB more flutter power in the frequencies above 2.5 kHz. This occurred for all samples of tape used, all tape recorders used, and all record levels. This difference is probably not a problem because the most important flutter components are the low frequency components.*

*Ratz, A. G. The Effect of Tape Transport Flutter on Spectrum and Correlation Analysis. IEEE TRANS ON SPACE ELECTRONICS AND TELEMETRY, Vol. SET-10, December 1964, Pp. 129–134.

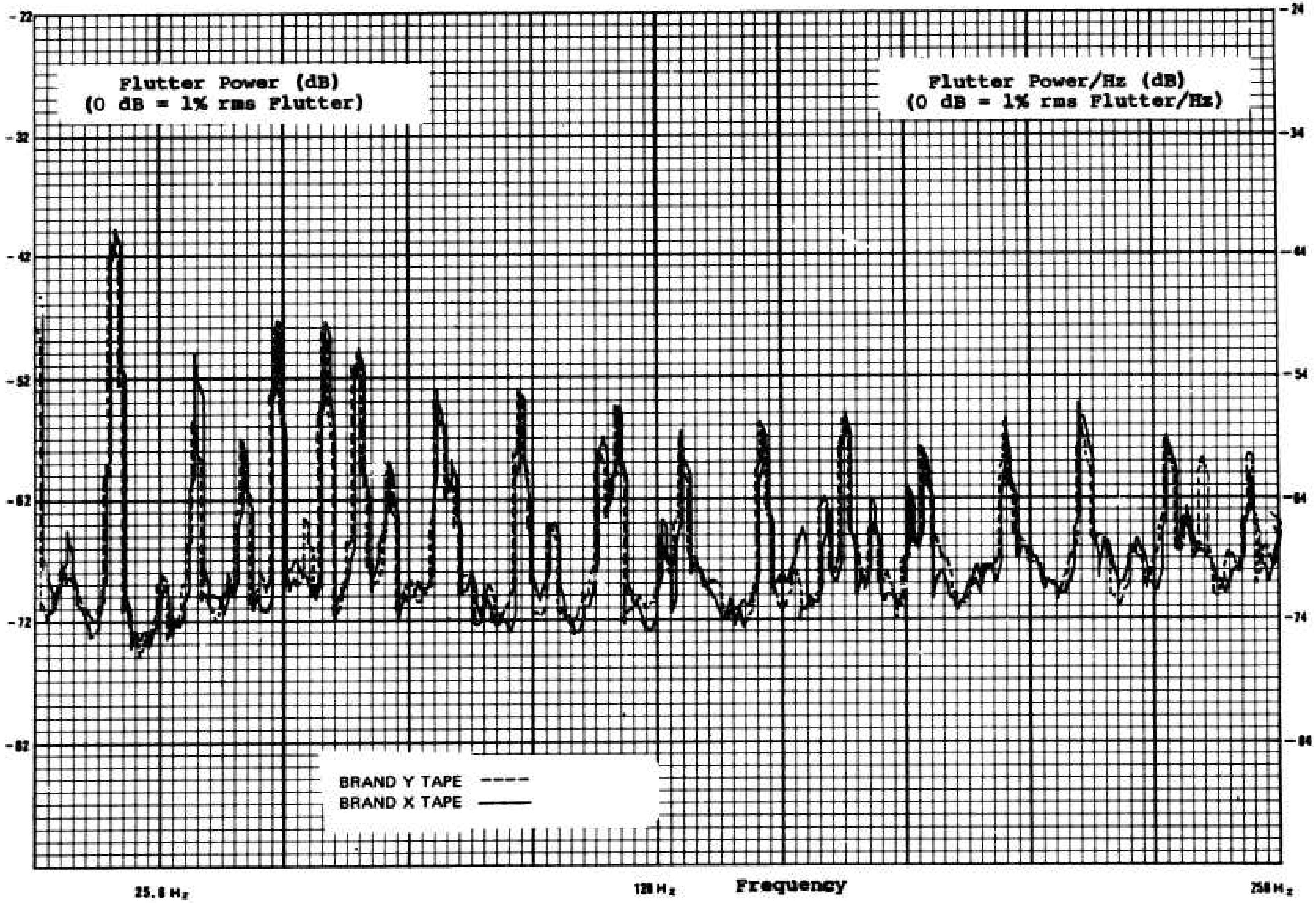

Figure D-1. Tape x and Tape y Flutter Power Spectral Densities, 256 Hz Bandwidth.

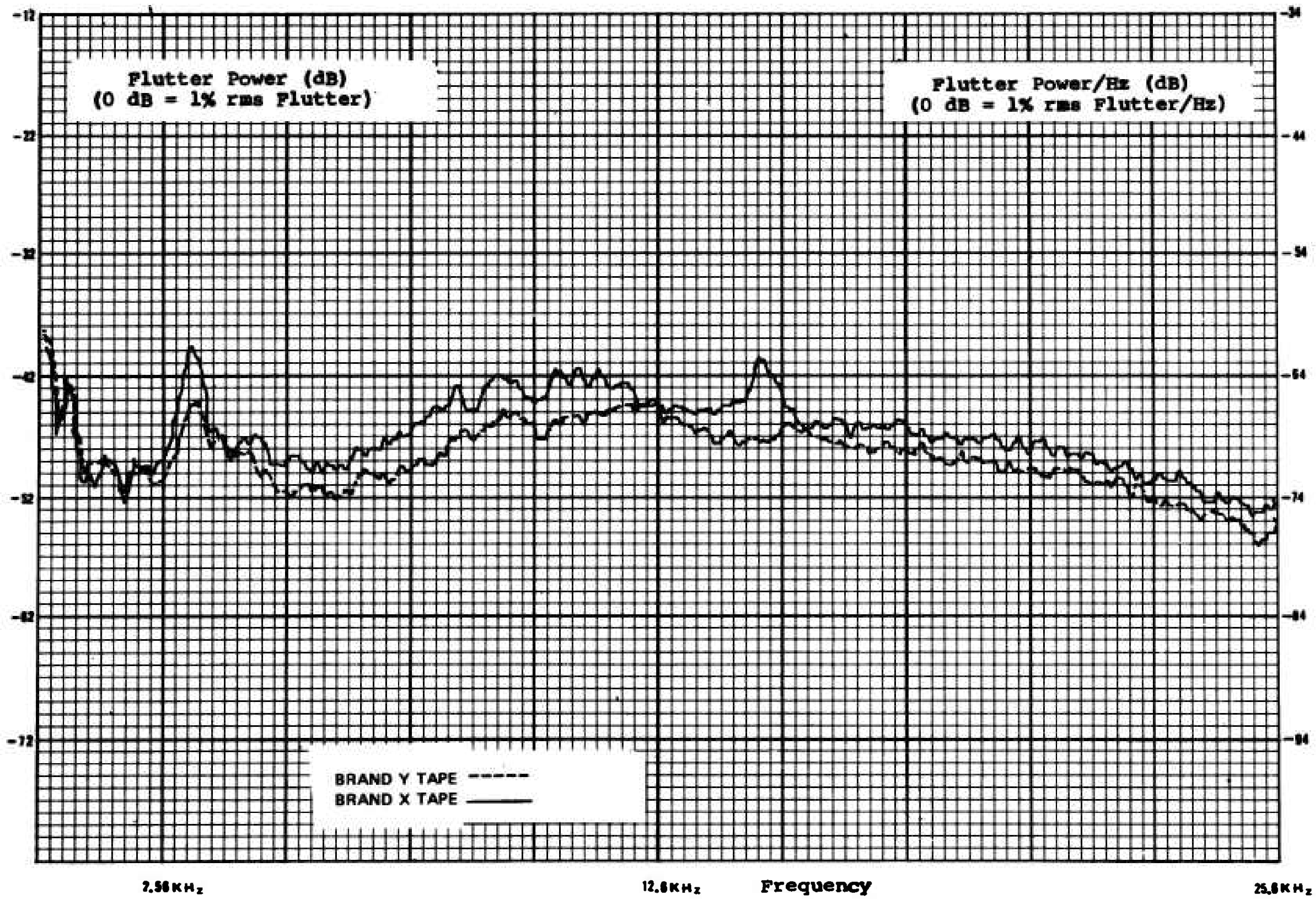

Figure D-2. Tape x and Tape y Flutter Power Spectral Densities, 25.6 kHz Bandwidth.

APPENDIX E

COMPARISON OF FLUTTER POWER SPECTRAL DENSITIES OF TAPE RECORDERS OF THE SAME MODEL

Tests were conducted to measure the flutter spectrums of two tape recorders of the same model (recorder 1 and recorder 2). These tests were conducted exactly the same as the other flutter tests. The flutter spectrums of the two recorders are shown in figures E-1, E-2, and E-3. Figure E-1 shows that recorder 1 had no components under 256 Hz that recorder 2 does not have. However, recorder 2 also had components at 43, 86, 129, 172, and 215 Hz. Figure E-2 shows that recorder 1 had large components at approximately 1 kHz, 1.48 kHz, and 1.93 kHz, while recorder 2 had large components at approximately 640 Hz and 1.97 kHz. Figure E-3 is an overlay of the crossplays between recorders 1 and 2. A comparison with figure E-2 shows that recorder 1 had large reproduce components at 1 kHz, 1.48 kHz, and 1.93 kHz, while recorder 2 had a record component at 280 Hz and large reproduce components at 215 Hz and 640 Hz. This figure also shows that the flutter spectra of the crossplays of two recorders show a strong dependence upon which recorder was the recording machine and which was the reproducing machine even for two recorders of the same model.

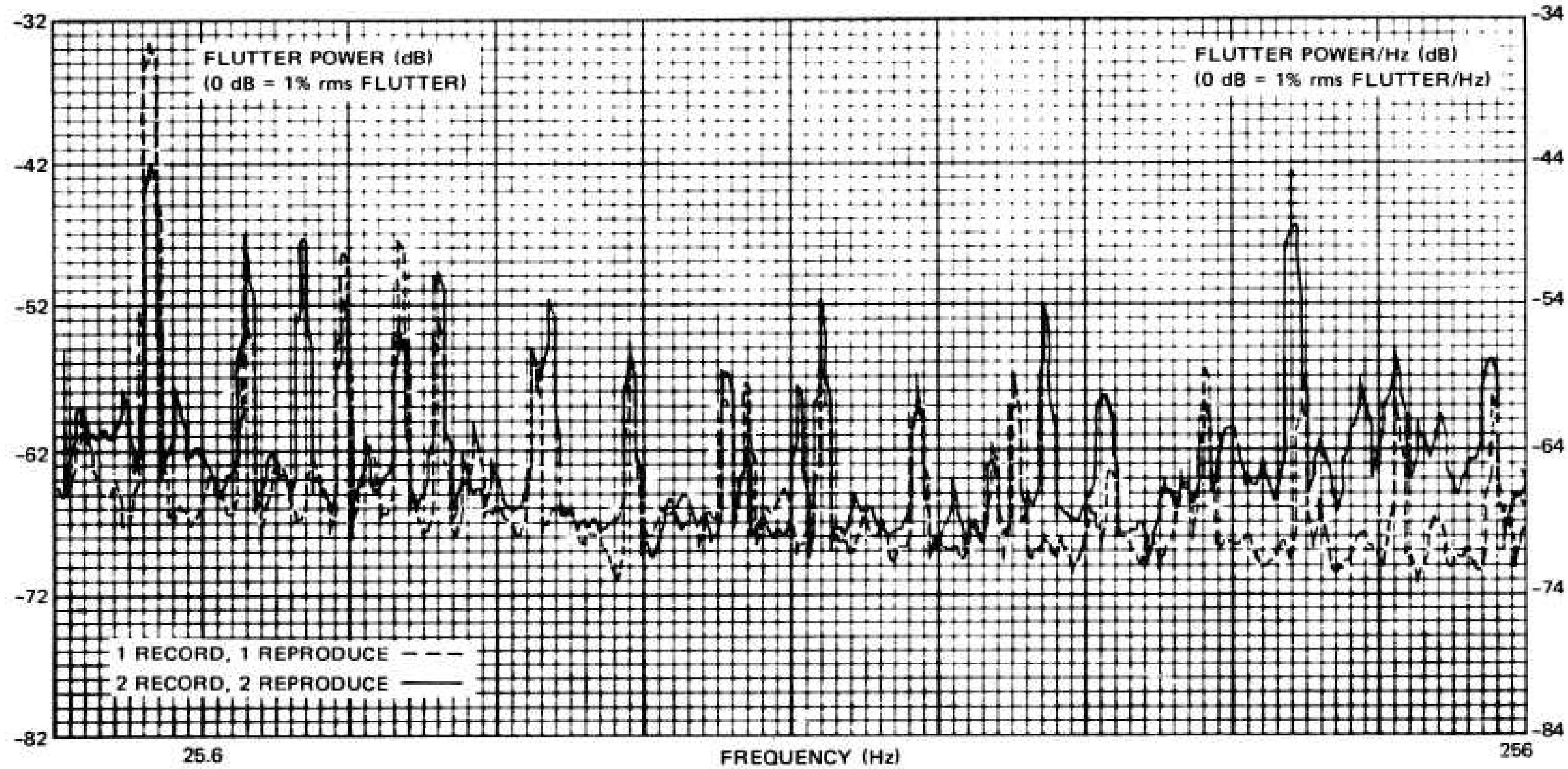

Figure E-1. Flutter Power Spectral Densities of Two Recorders of the Same Model (256 Hz Bandwidth).

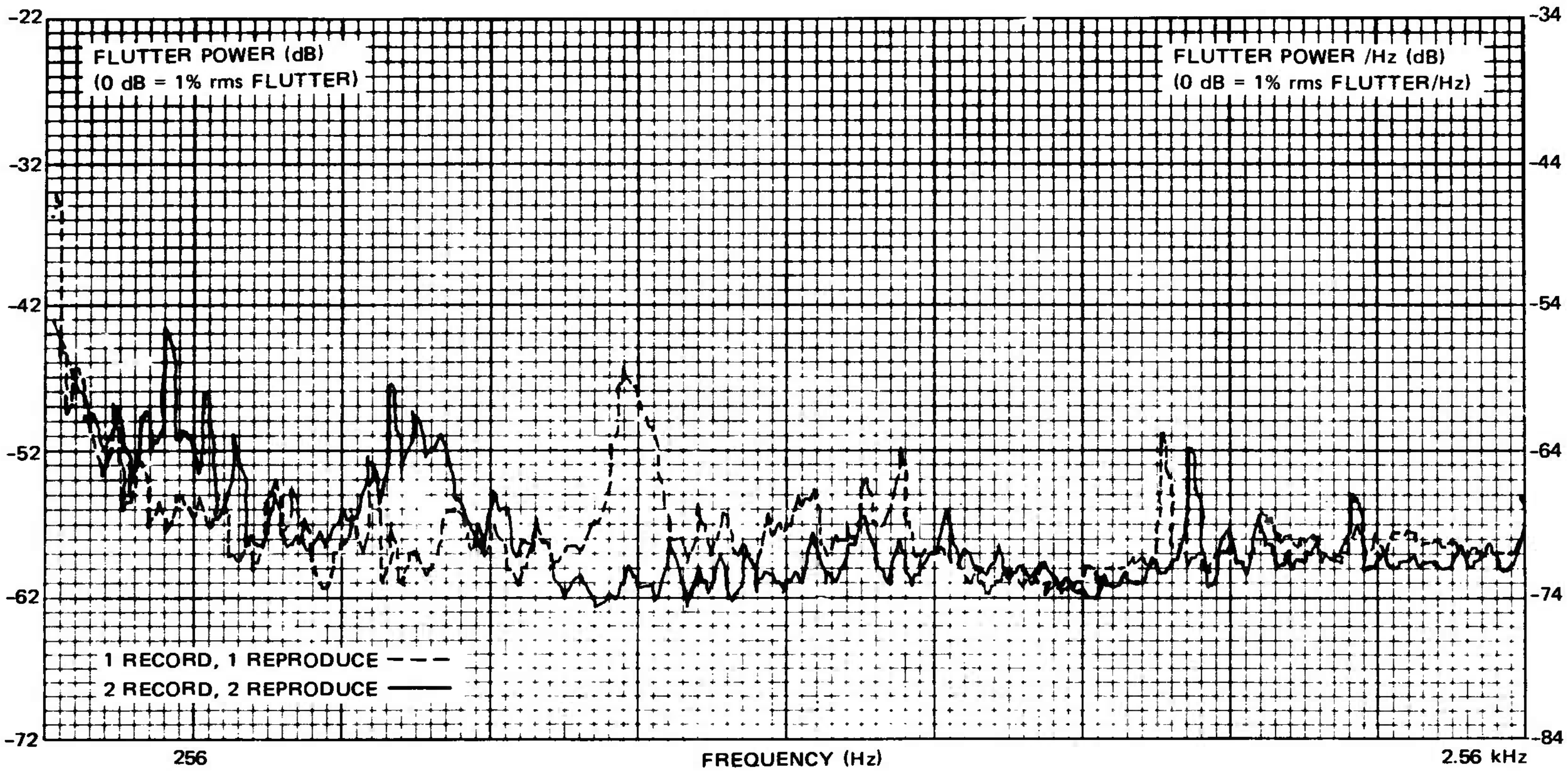

Figure E-2. Flutter Power Spectral Densities of Two Recorders of the Same Model (2.56 kHz Bandwidth).

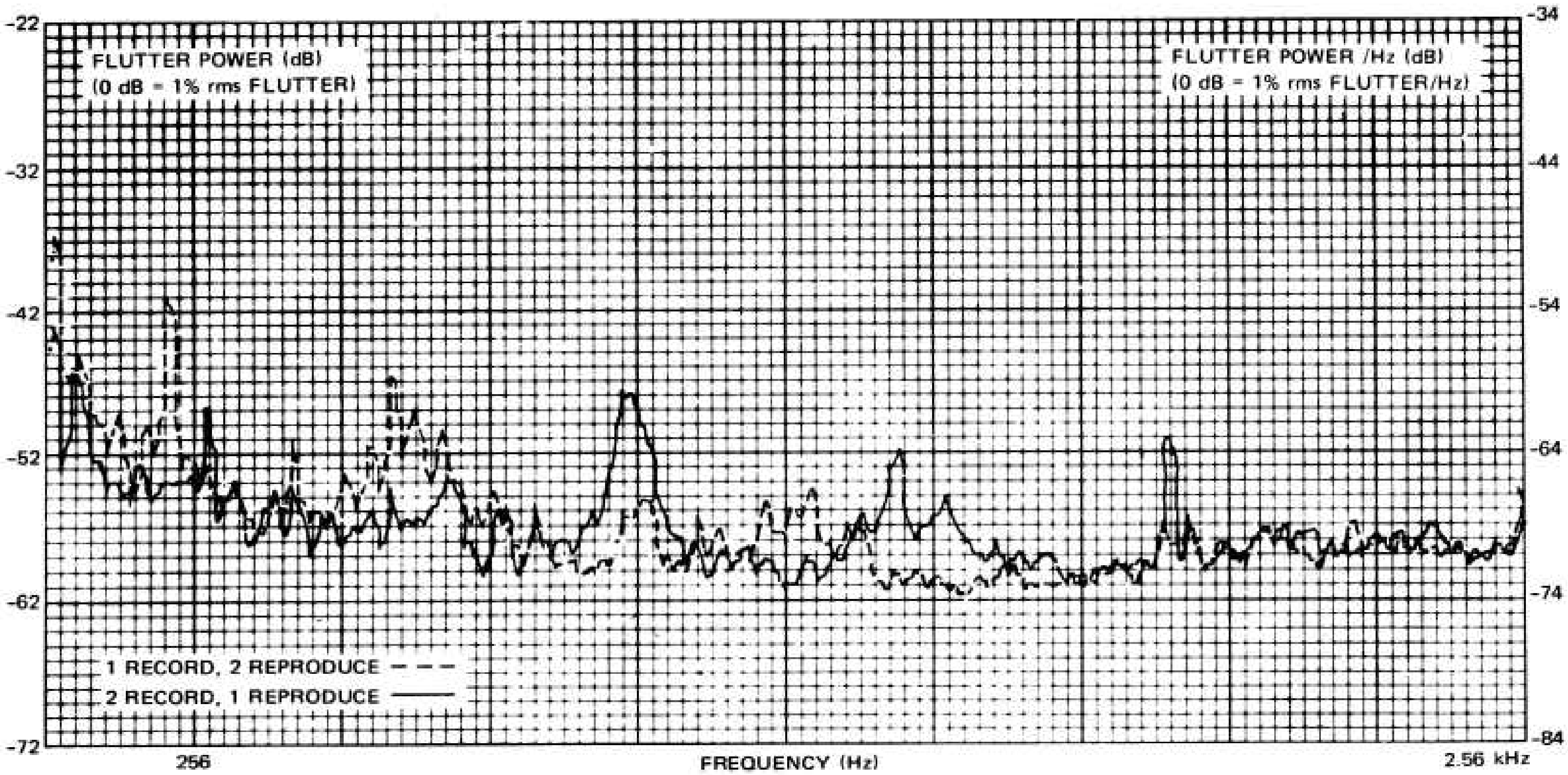

Figure E-3. Flutter Power Spectral Densities of Two Recorders of the Same Model (2.56 kHz Bandwidth).

APPENDIX F

FLUTTER POWER SPECTRAL DENSITY PLOTS

Figures F-1 through F-24 present the flutter spectra of the six tape recorders used in this study.

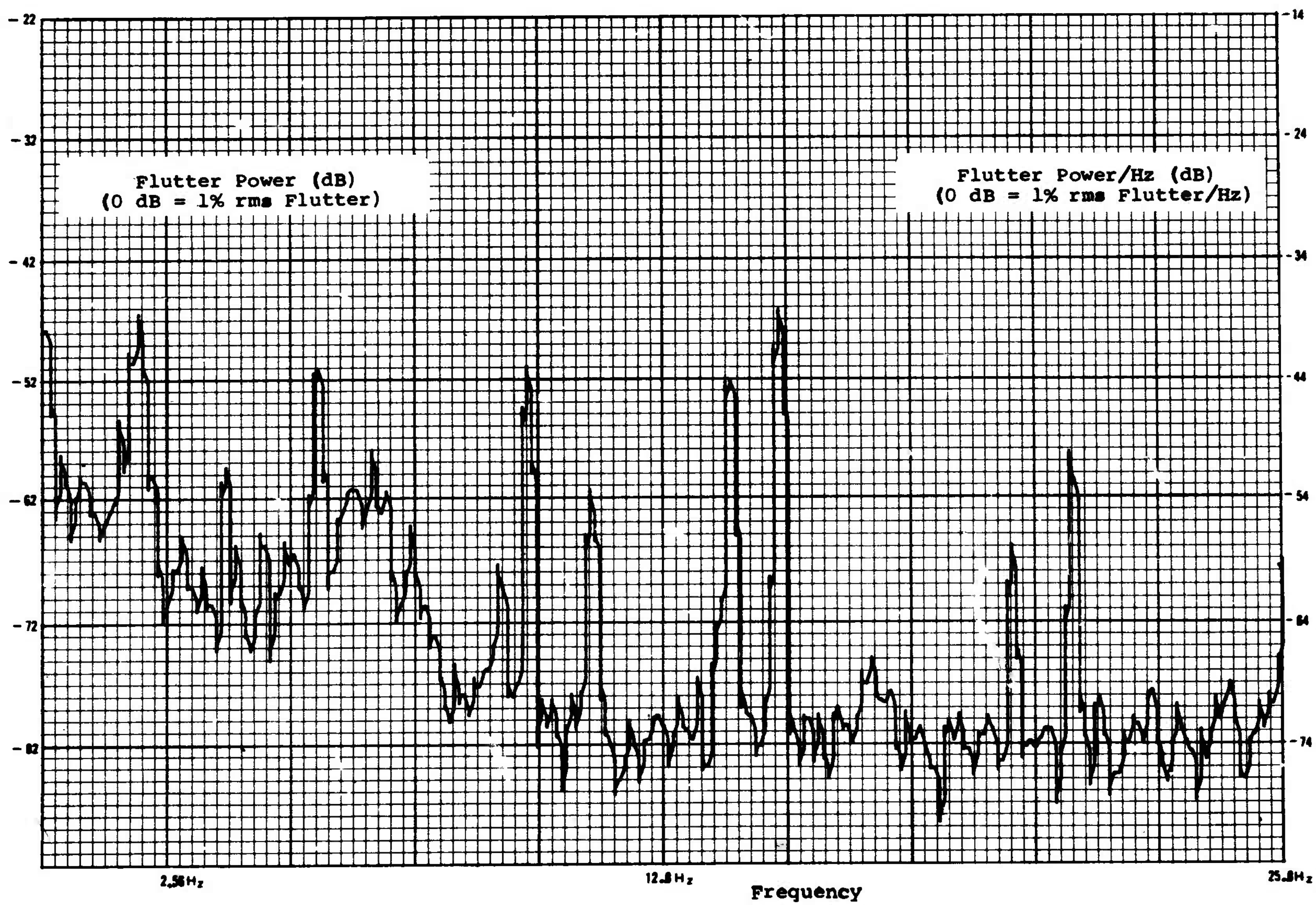

Figure F-1. Flutter Power Spectral Density, Recorder A, 25.6 Hz Bandwidth.

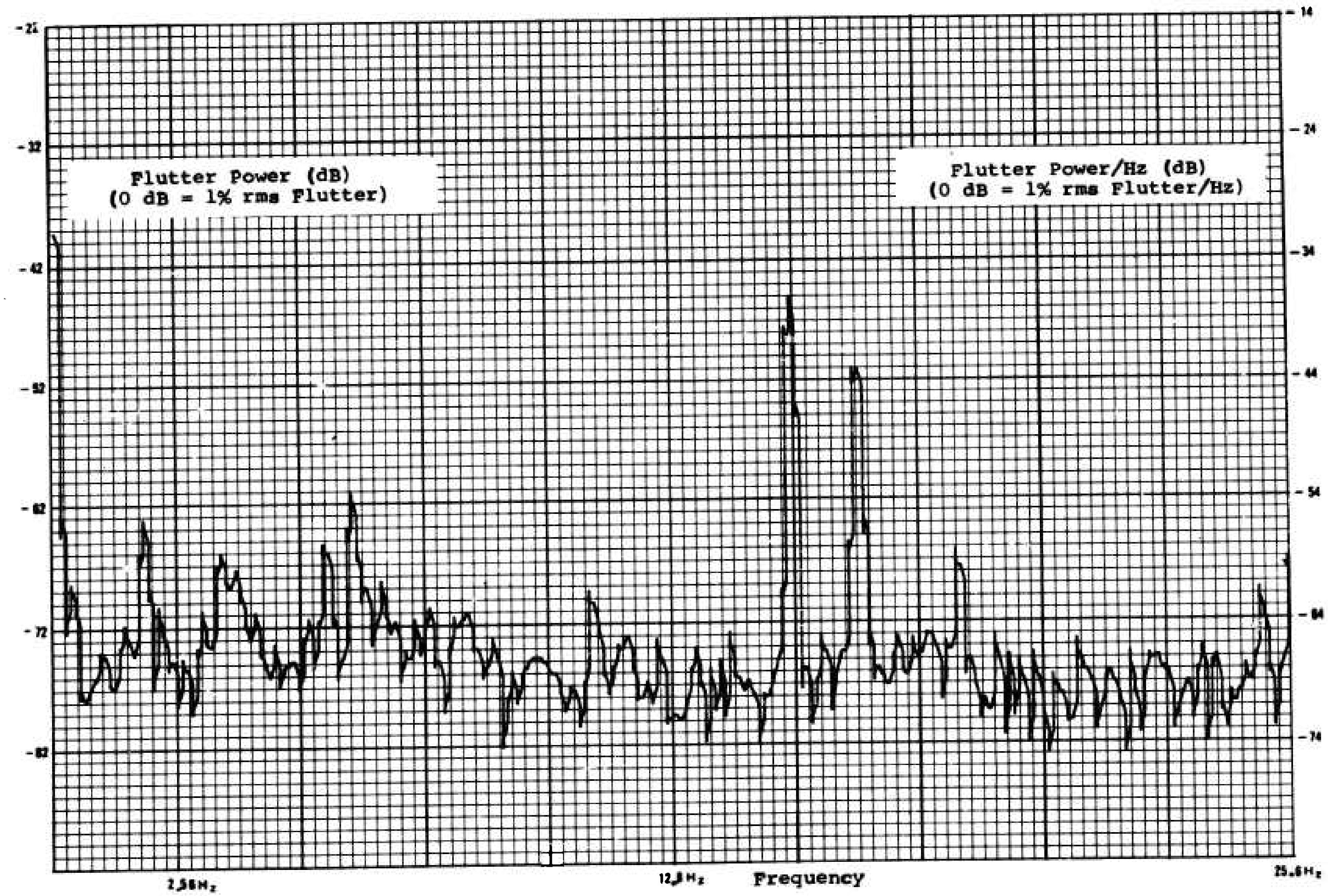

Figure F-2. Flutter Power Spectral Density, Recorder B, 25.6 Hz Bandwidth.

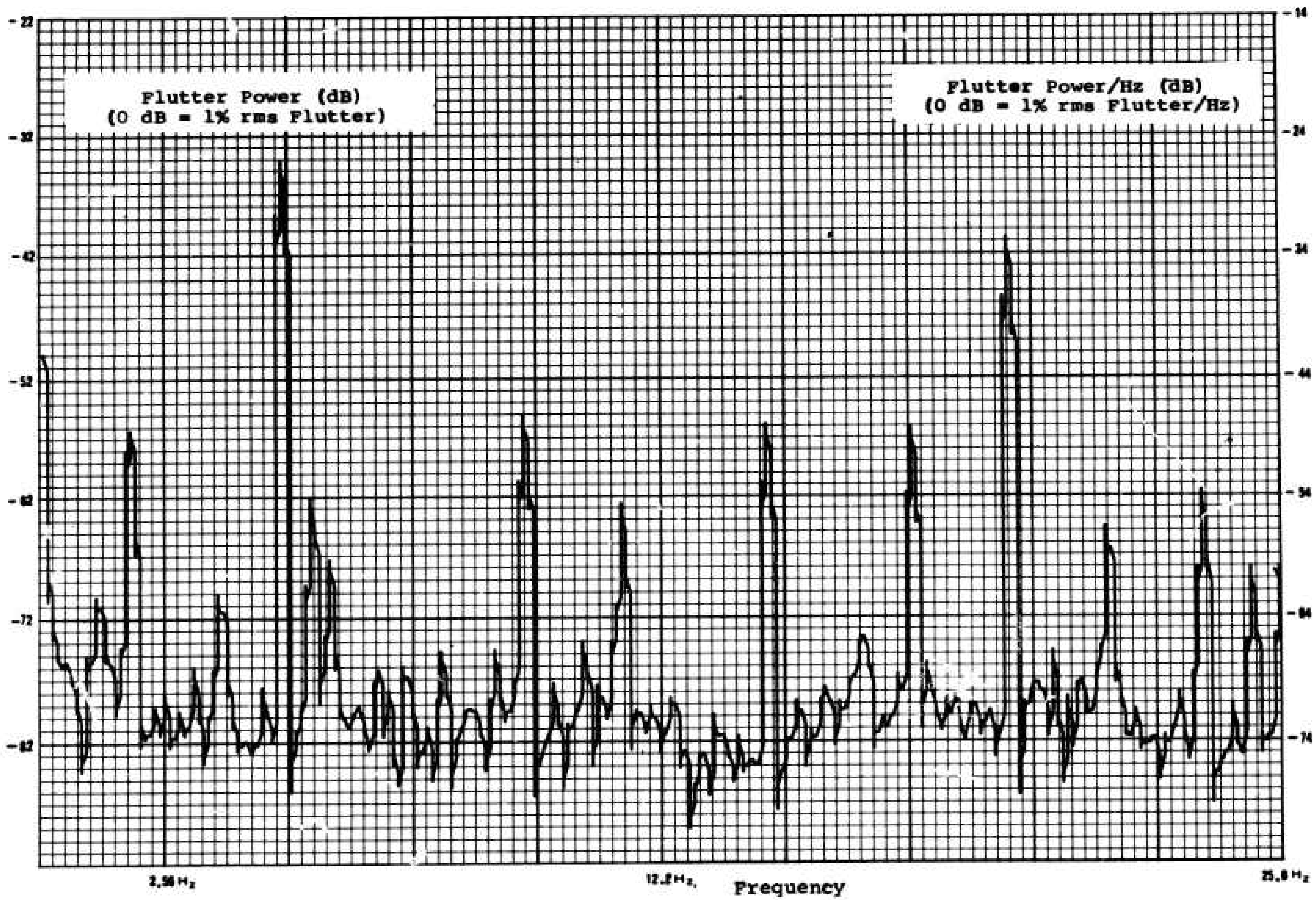

Figure F-3. Flutter Power Spectral Density, Recorder C, 25.6 Hz Bandwidth.

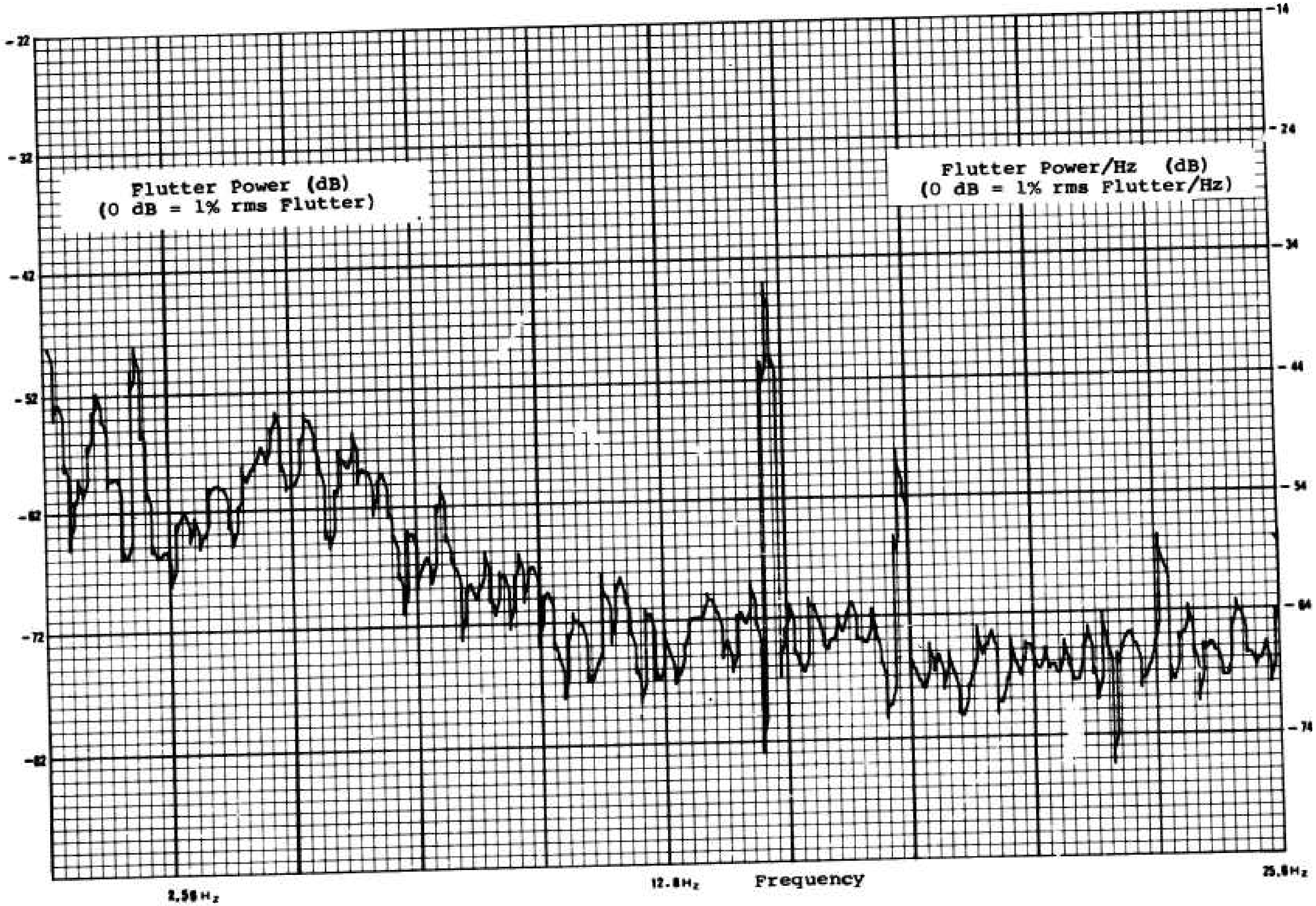

Figure F-4. Flutter Power Spectral Density, Recorder D, 25.6 Hz Bandwidth.

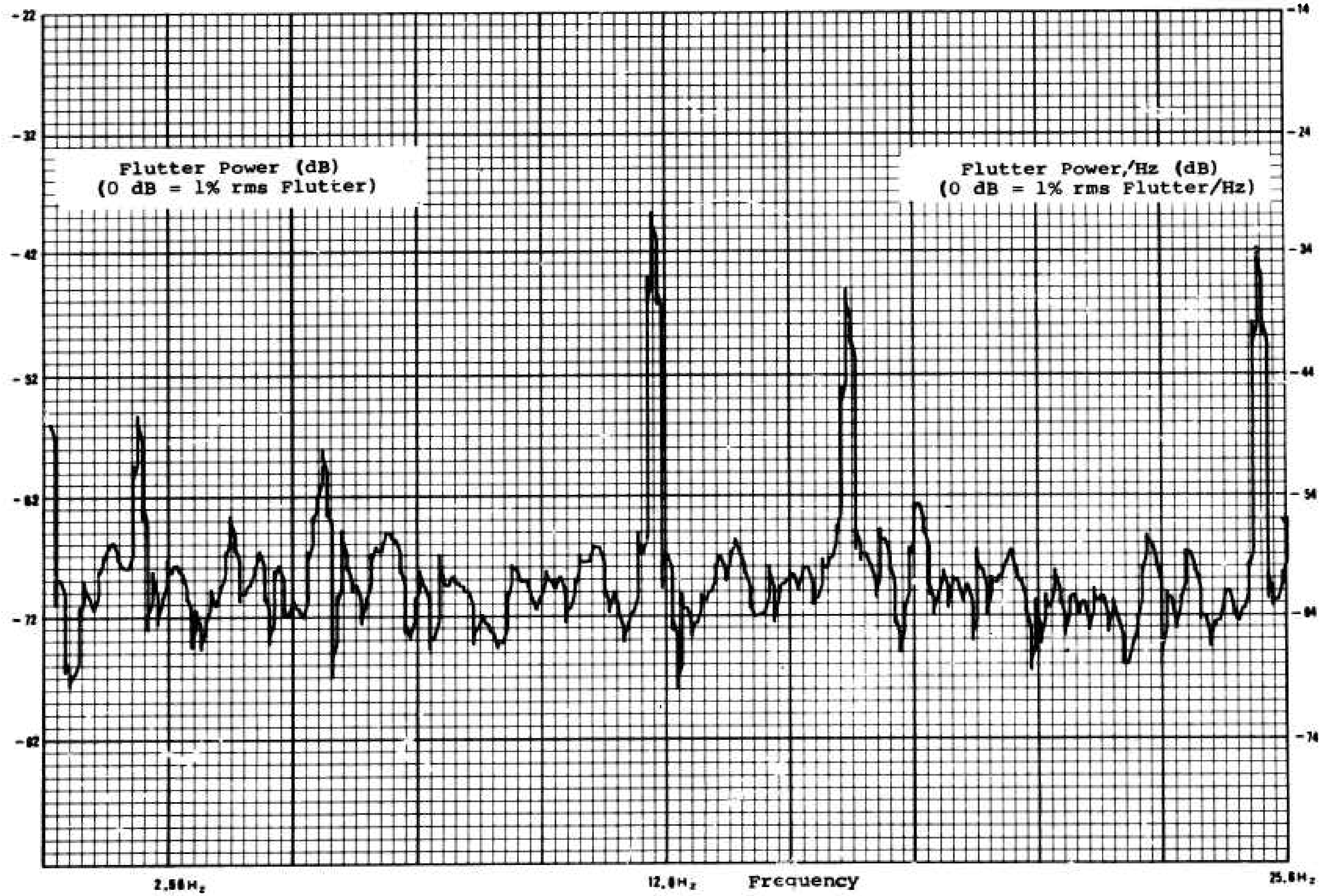

Figure F-5. Flutter Power Spectral Density, Recorder E, 25.6 Hz Bandwidth.

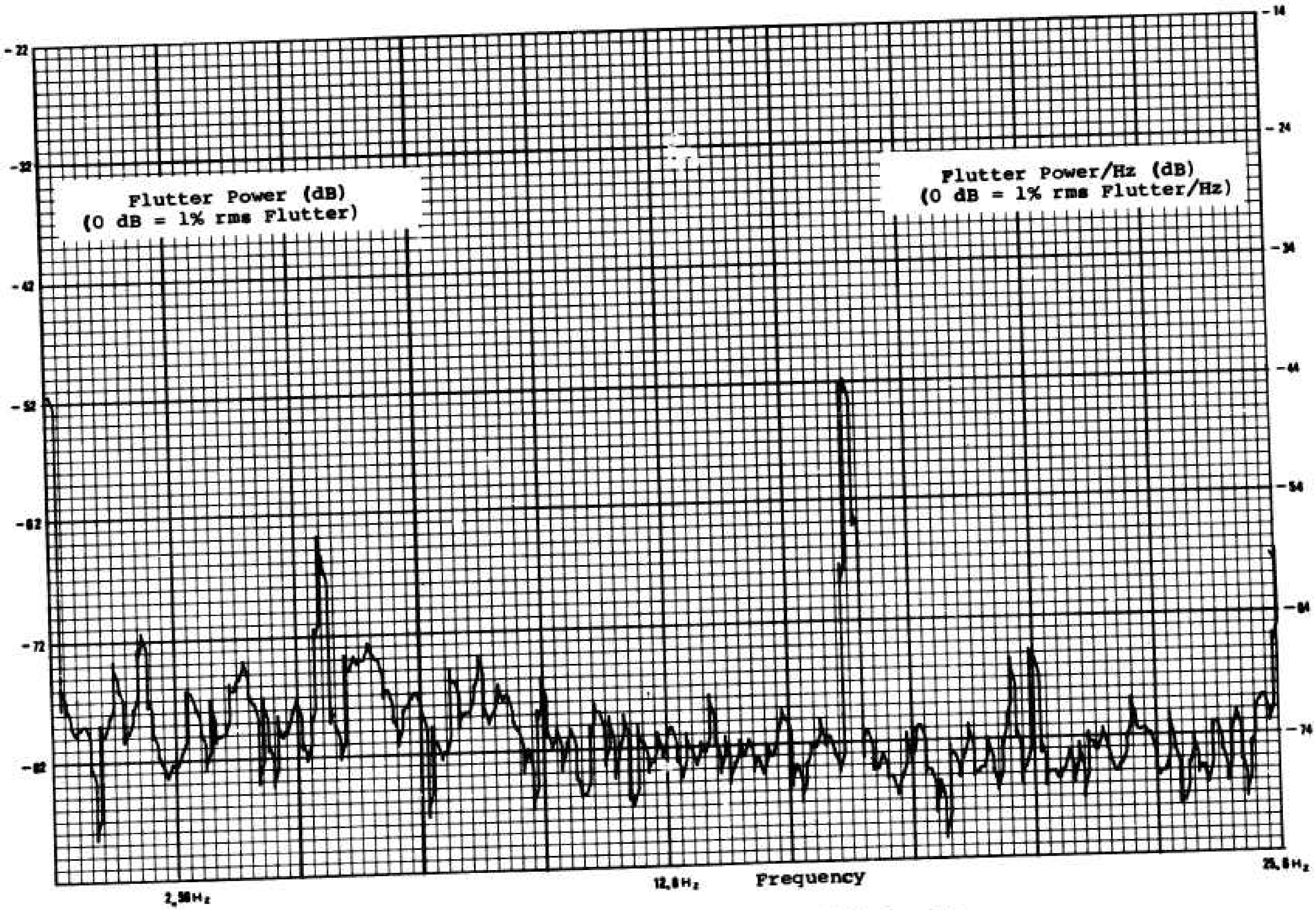

Figure F-6. Flutter Power Spectral Density, Recorder F, 25.6 Hz Banowidth.

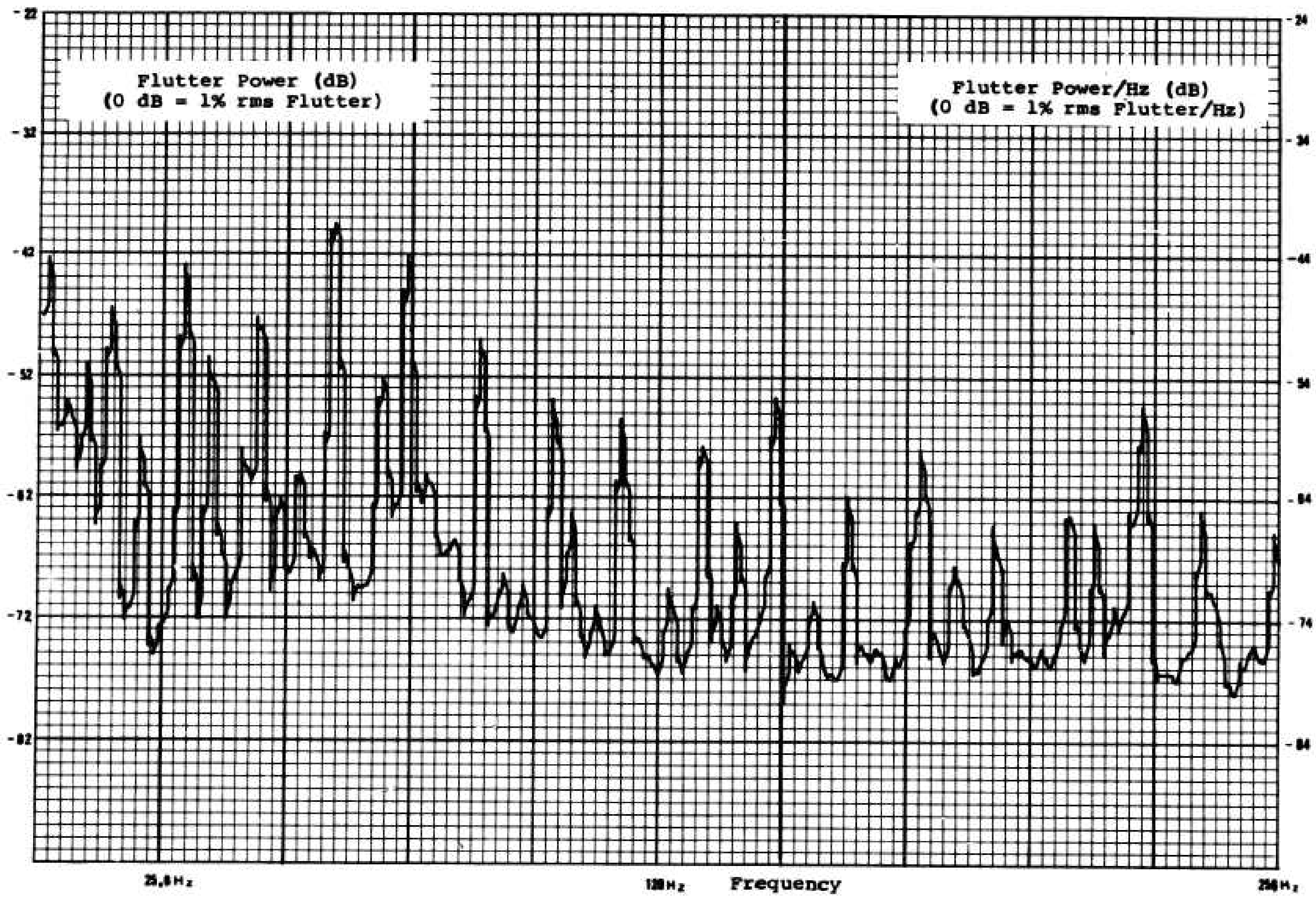

Figure F-7. Flutter Power Spectral Density, Recorder A, 256 Hz Bandwidth.

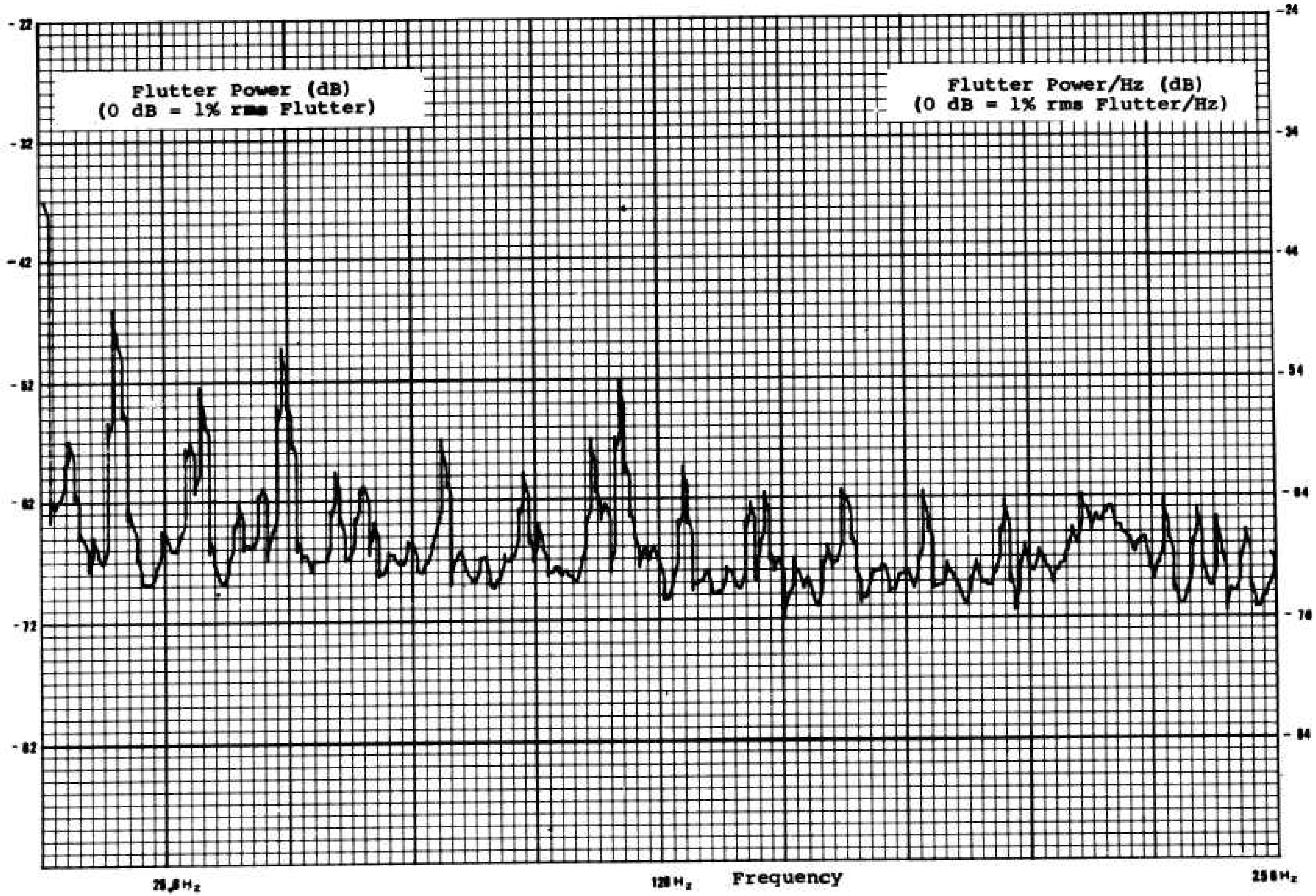

Figure F-8. Flutter Power Spectral Density, Recorder B, 256 Hz Bandwidth.

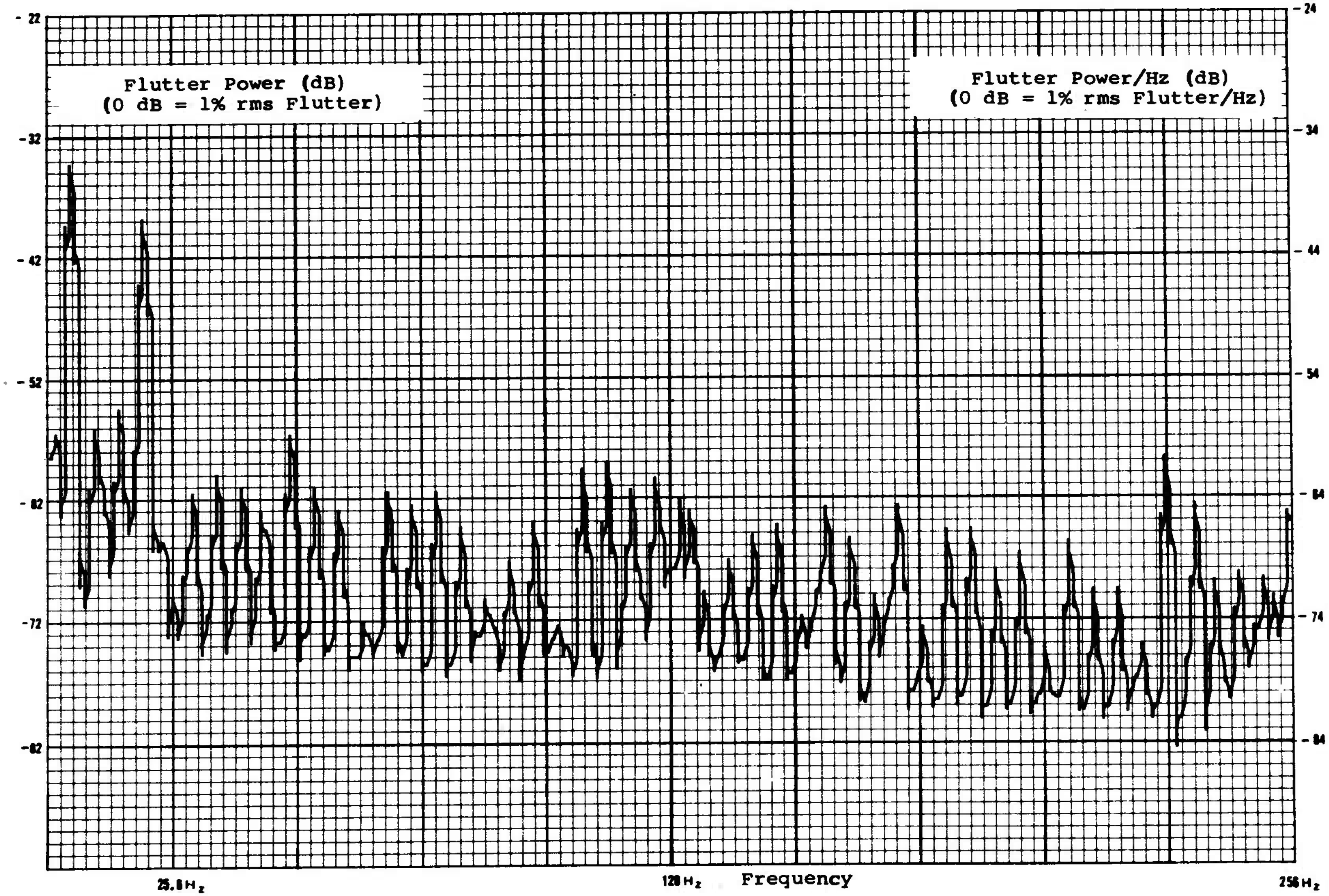

Figure F-9. Flutter Power Spectral Density, Recorder C, 256 Hz Bandwidth.

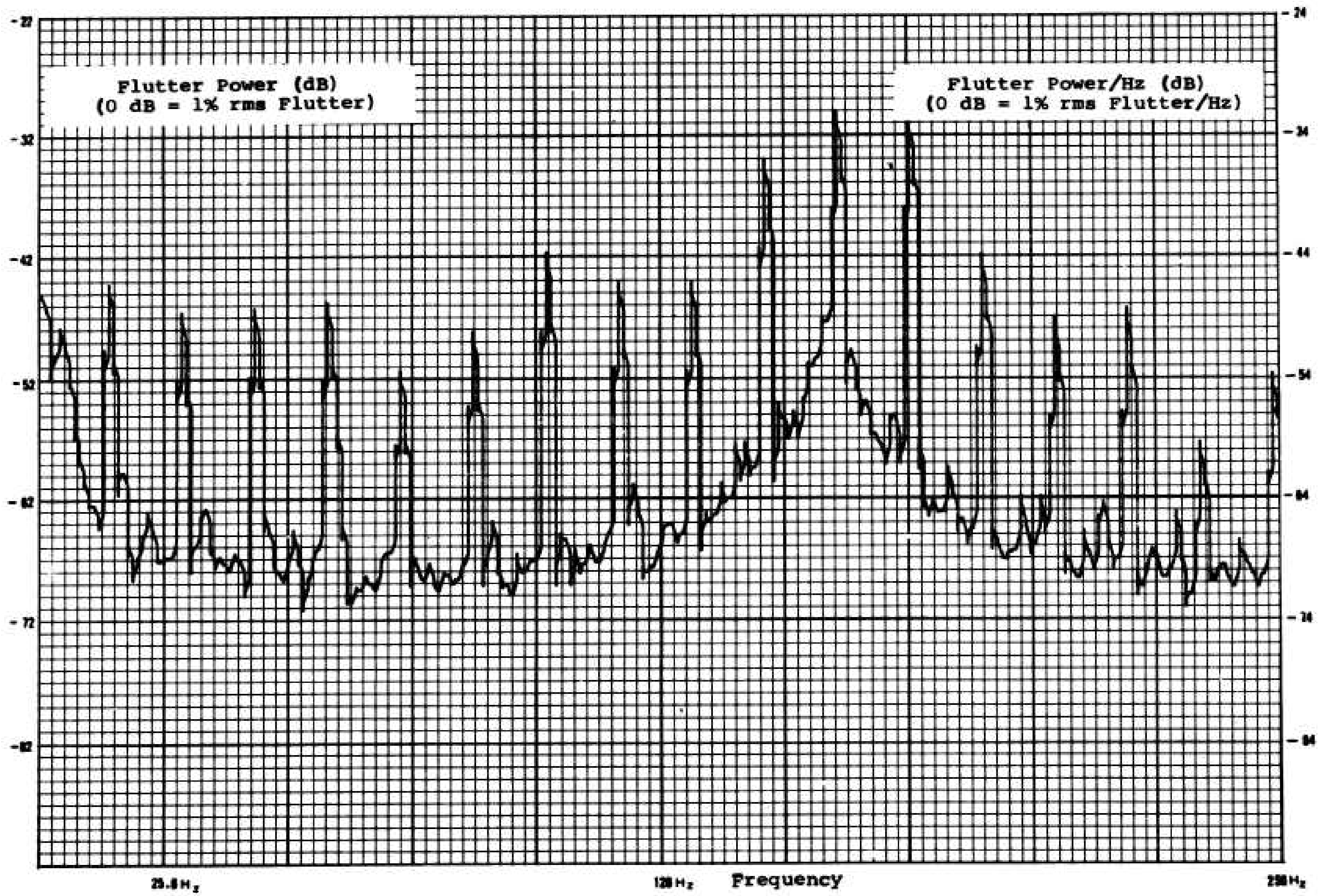

Figure F-10. Flutter Power Spectral Density, Recorder D, 256 Hz Bandwidth.

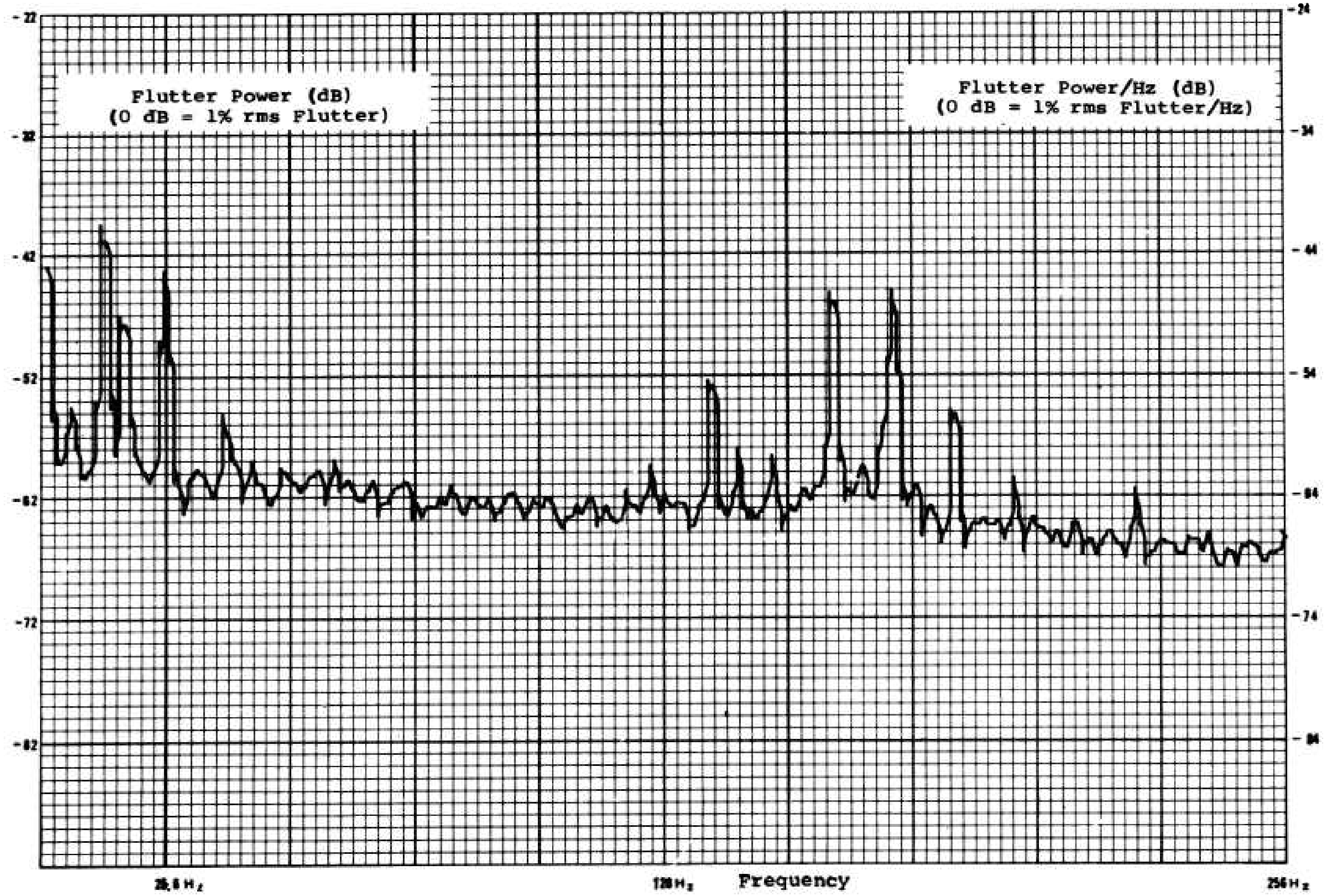

Figure F-11. Flutter Power Spectral Density, Recorder E, 256 Hz Bandwidth.

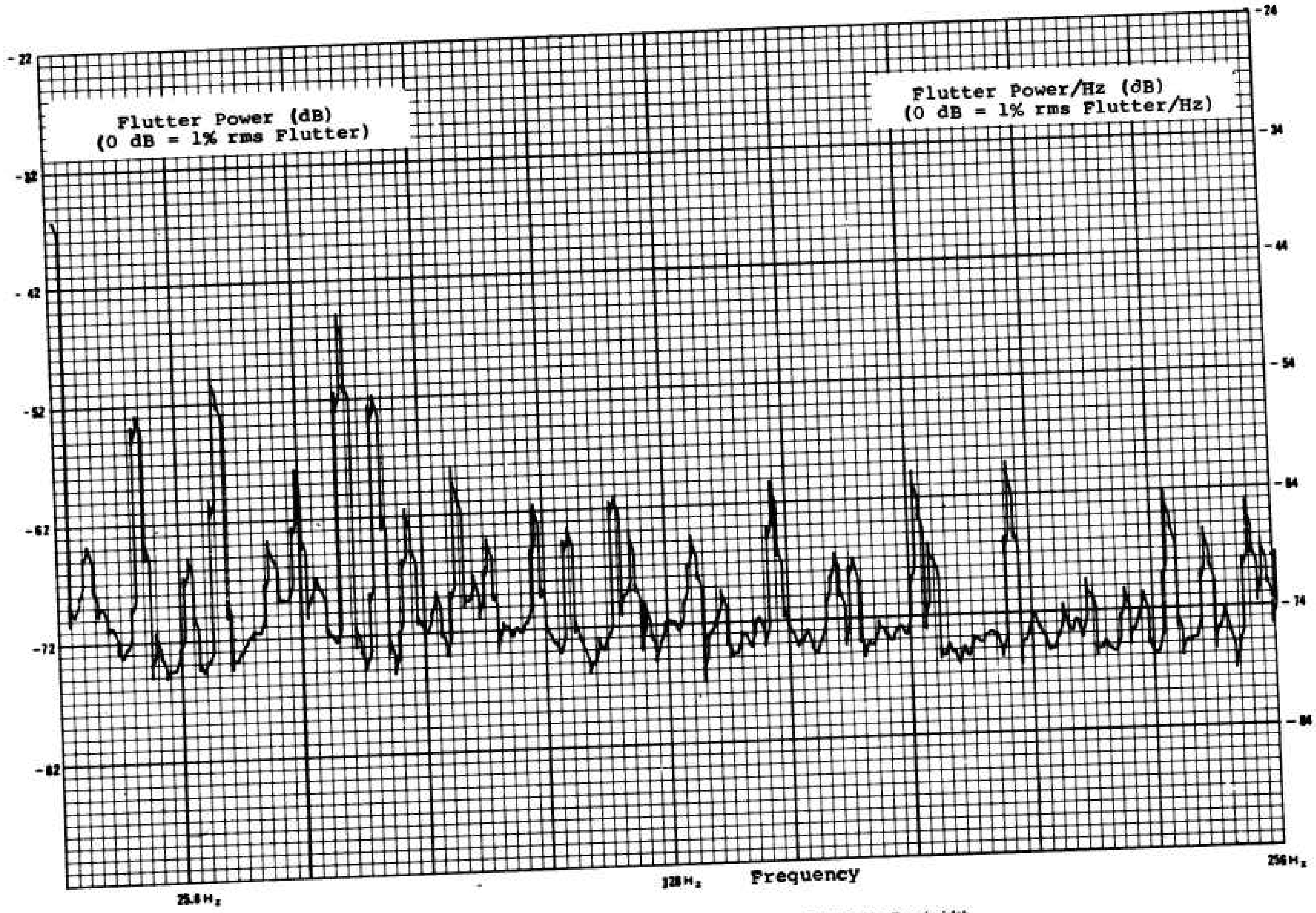

Figure F-12. Flutter Power Spectral Density, Recorder F, 256 Hz Bandwidth.

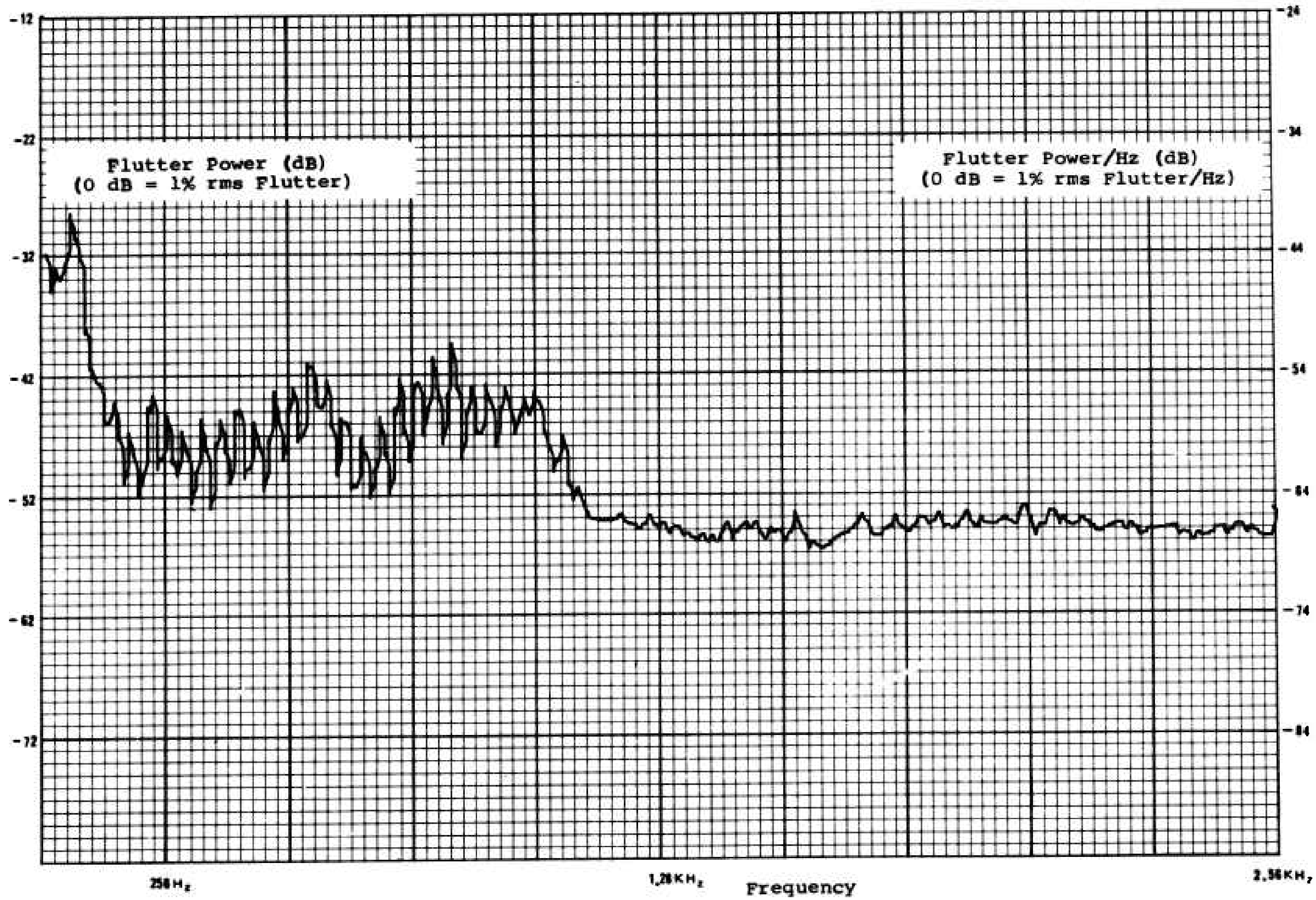

Figure F-13. Flutter Power Spectral Density, Recorder A, 2.56 kHz Bandwidth.

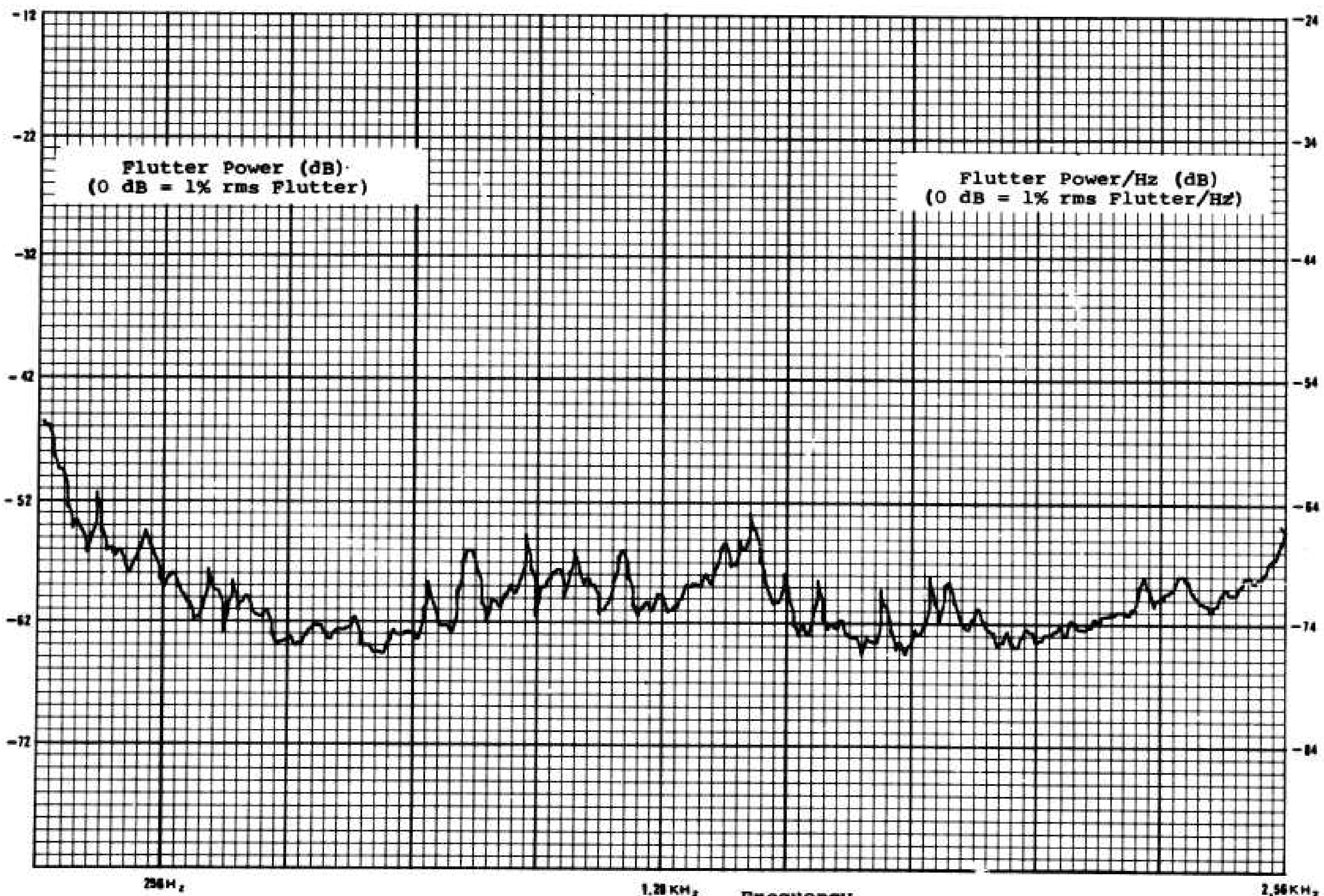

Figure F-14. Flutter Power Spectral Density, Recorder B, 2.56 kHz Bandwidth.

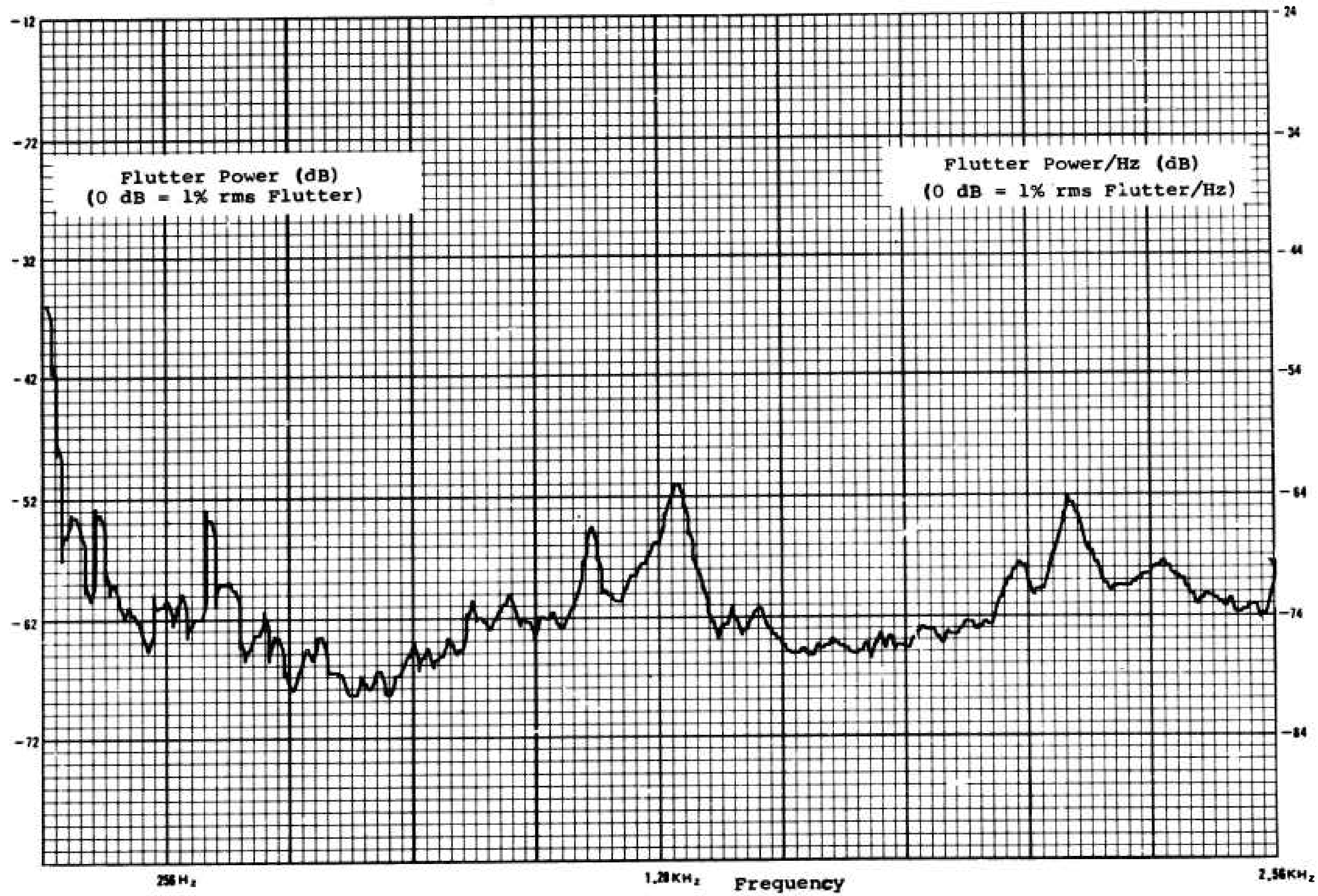

Figure F-15. Flutter Power Spectral Density, Recorder C, 2.56 kHz Bandwidth.

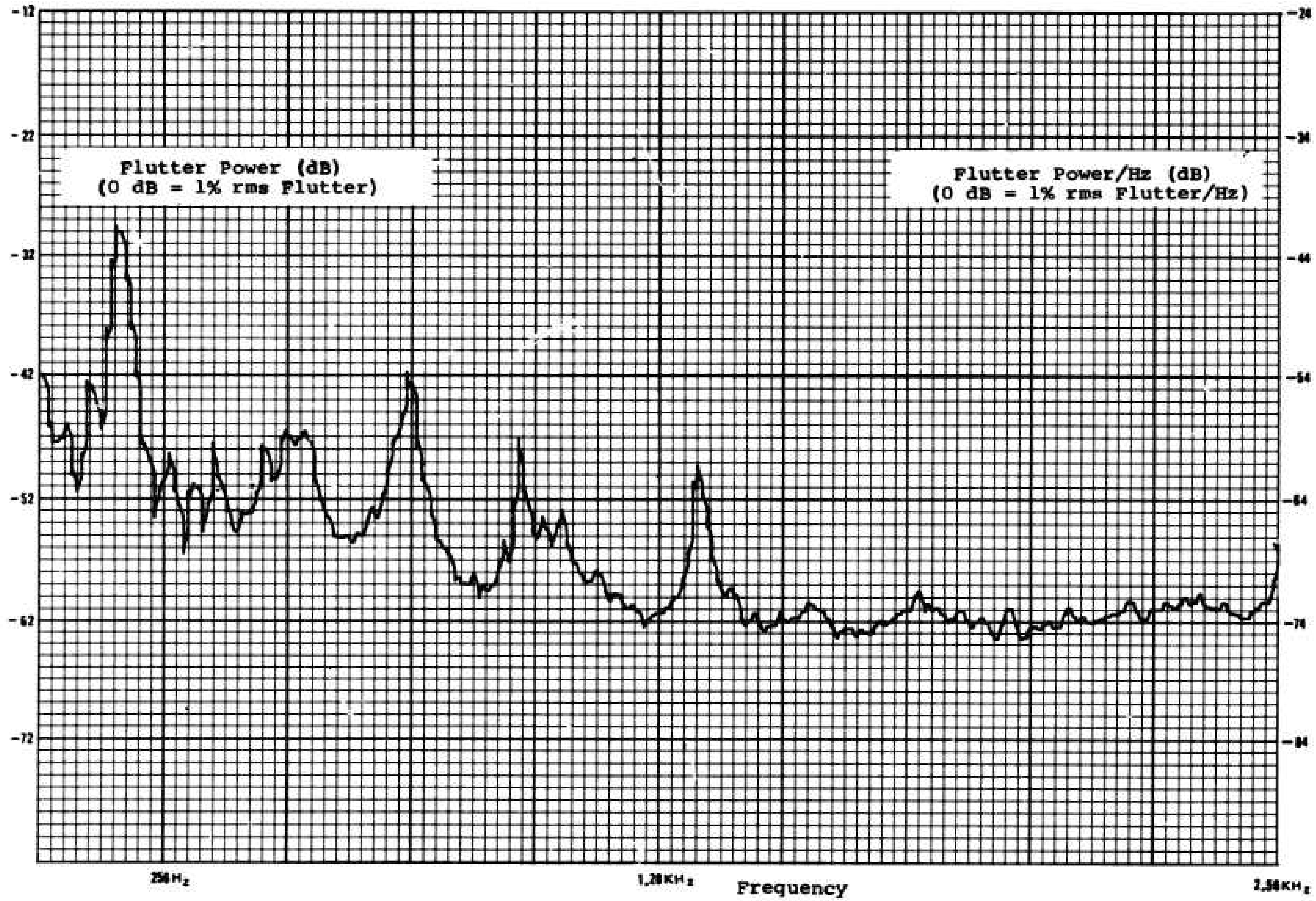

Figure F-16. Flutter Power Spectral Density, Recorder D, 2.56 kHz Bandwidth.

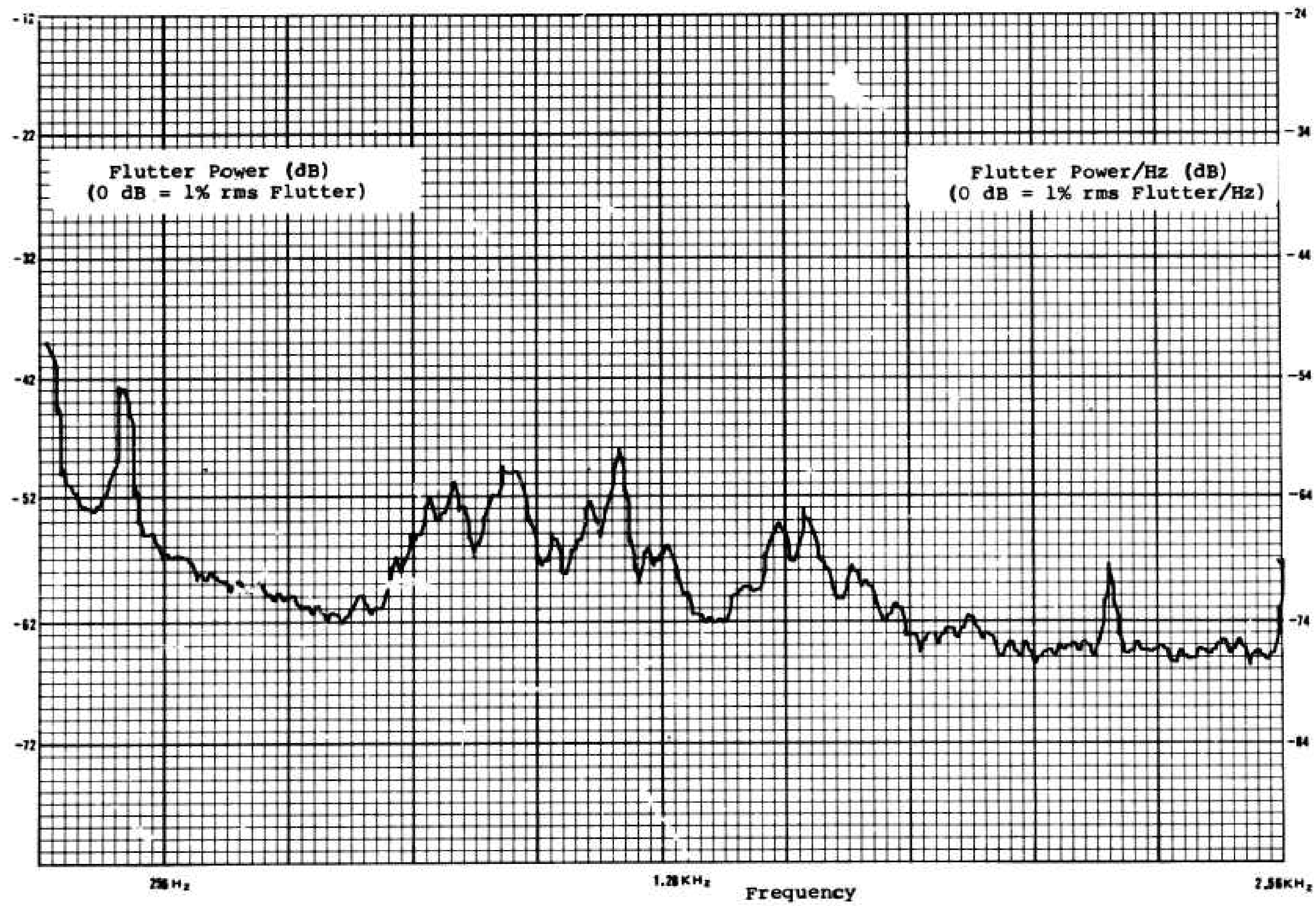

Figure F-17. Flutter Power Spectral Density, Recorder E, 2.56 kHz Bandwidth.

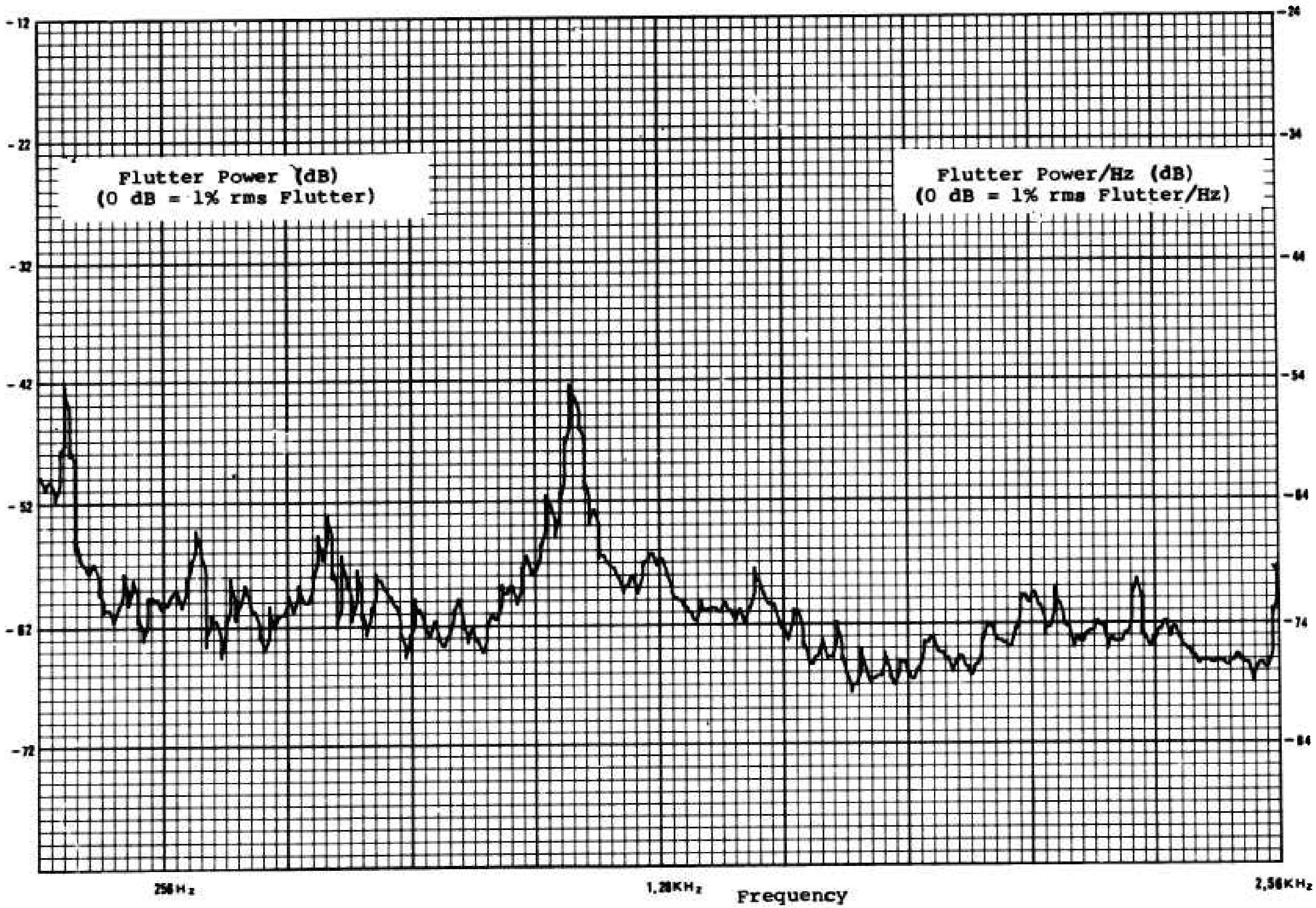

Figure F-18. Flutter Power Spectral Density, Recorder F, 2.56 kHz Bandwidth.

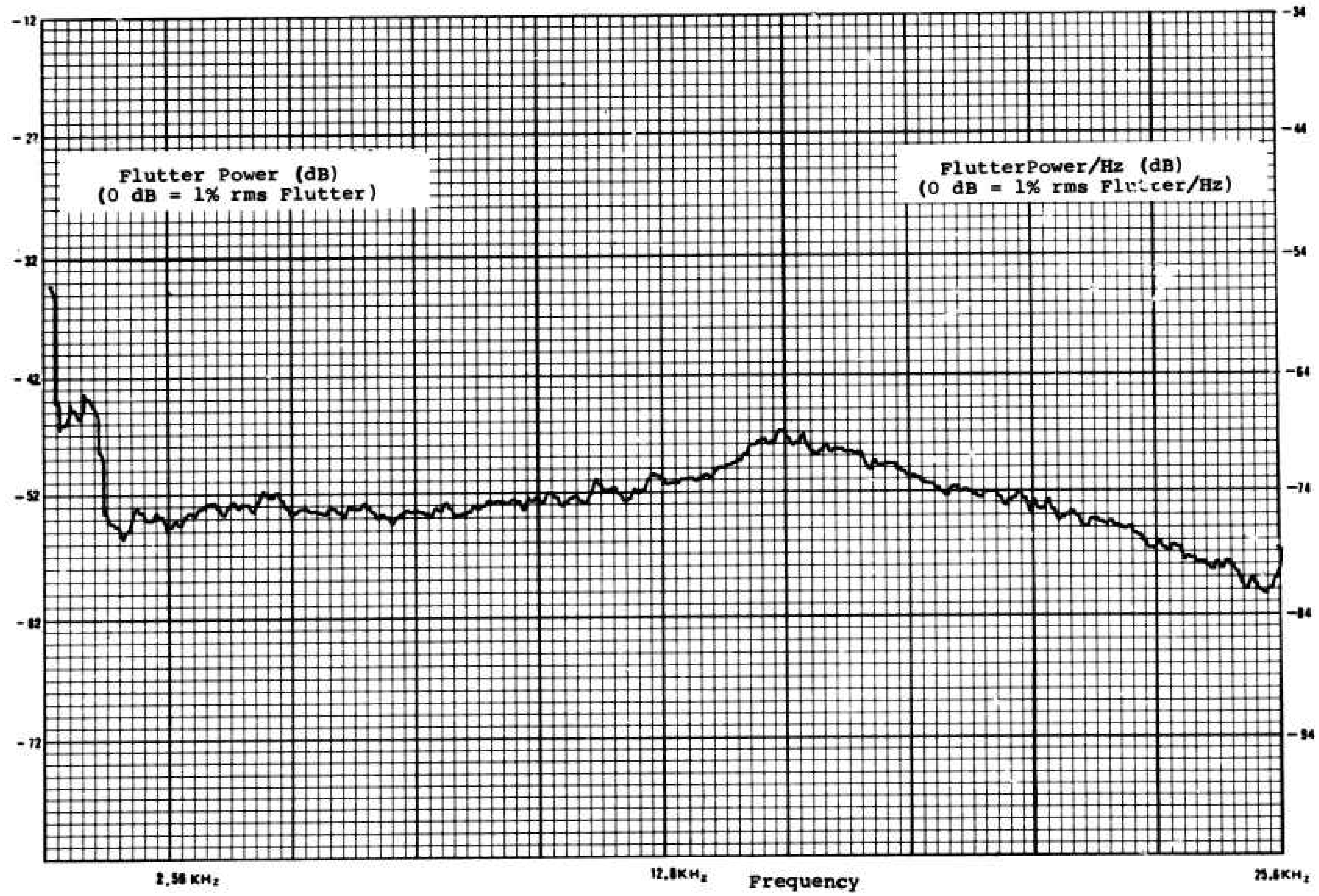

Figure F-19. Flutter Power Spectral Density, Recorder A, 25.6 kHz Bandwidth.

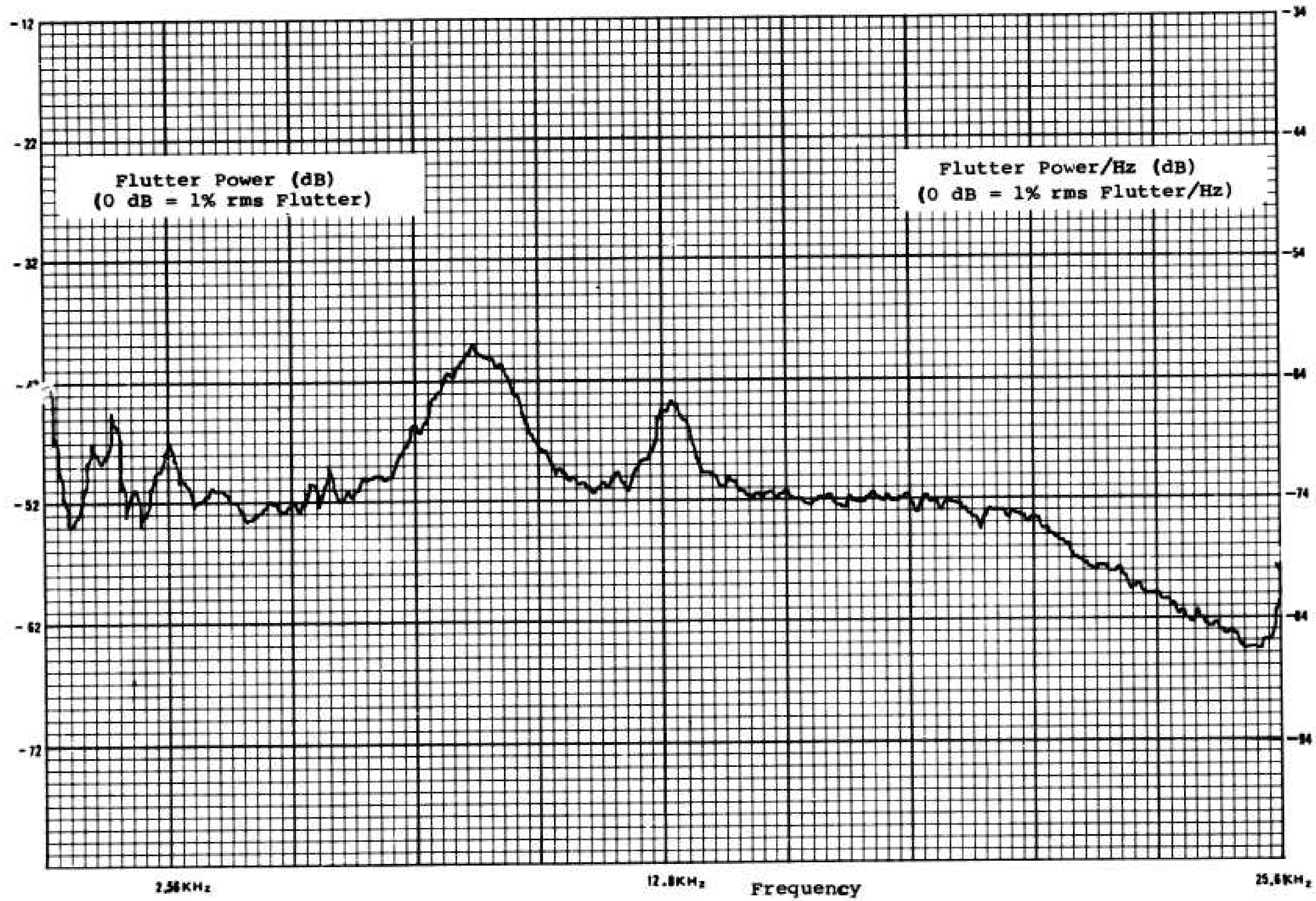

Figure F-20. Flutter Power Spectral Density, Recorder B, 25.6 kHz Bandwidth.

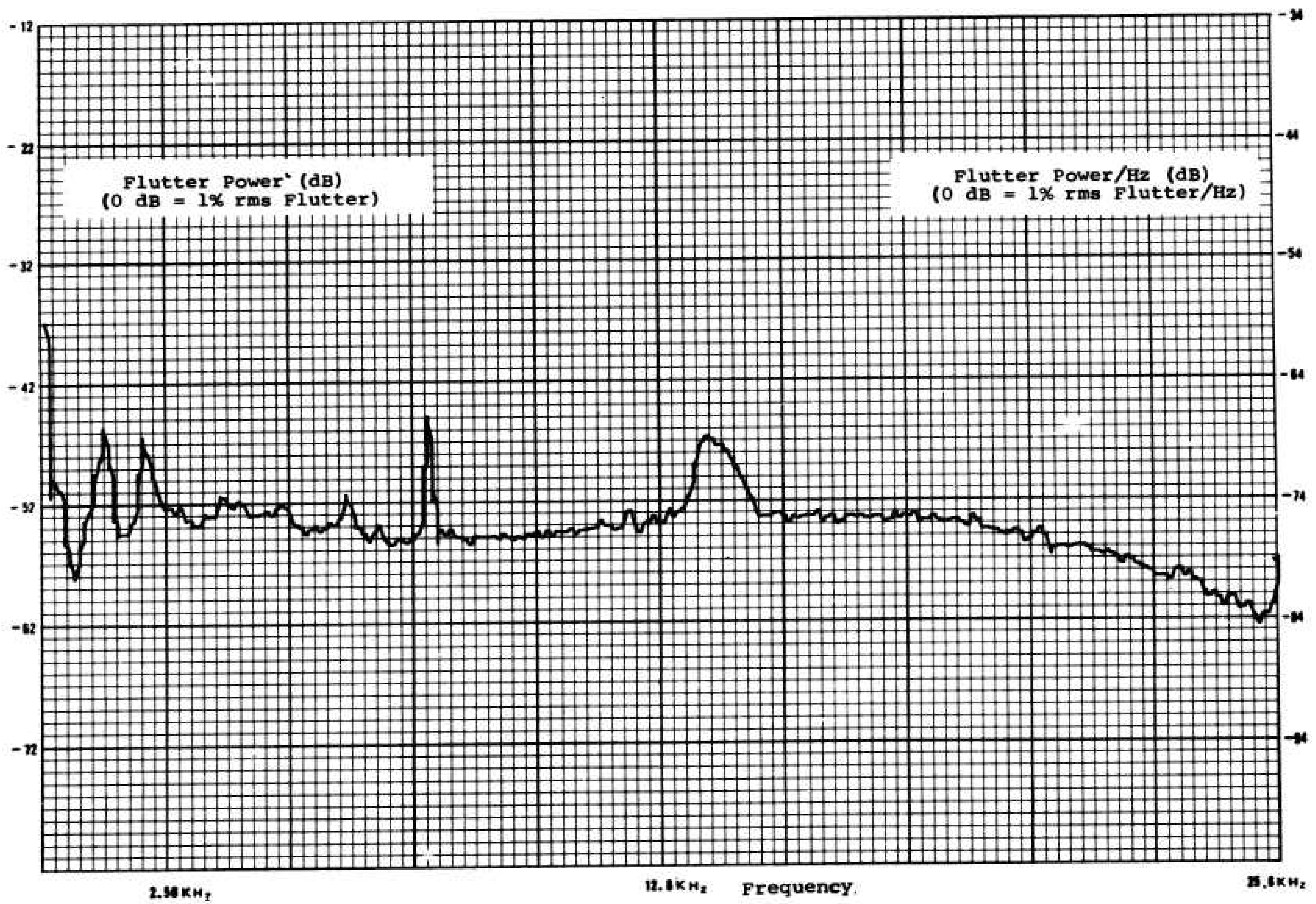

Figure F-21. Flutter Power Spectral Density, Recorder C, 25.6 kHz Bandwidth.

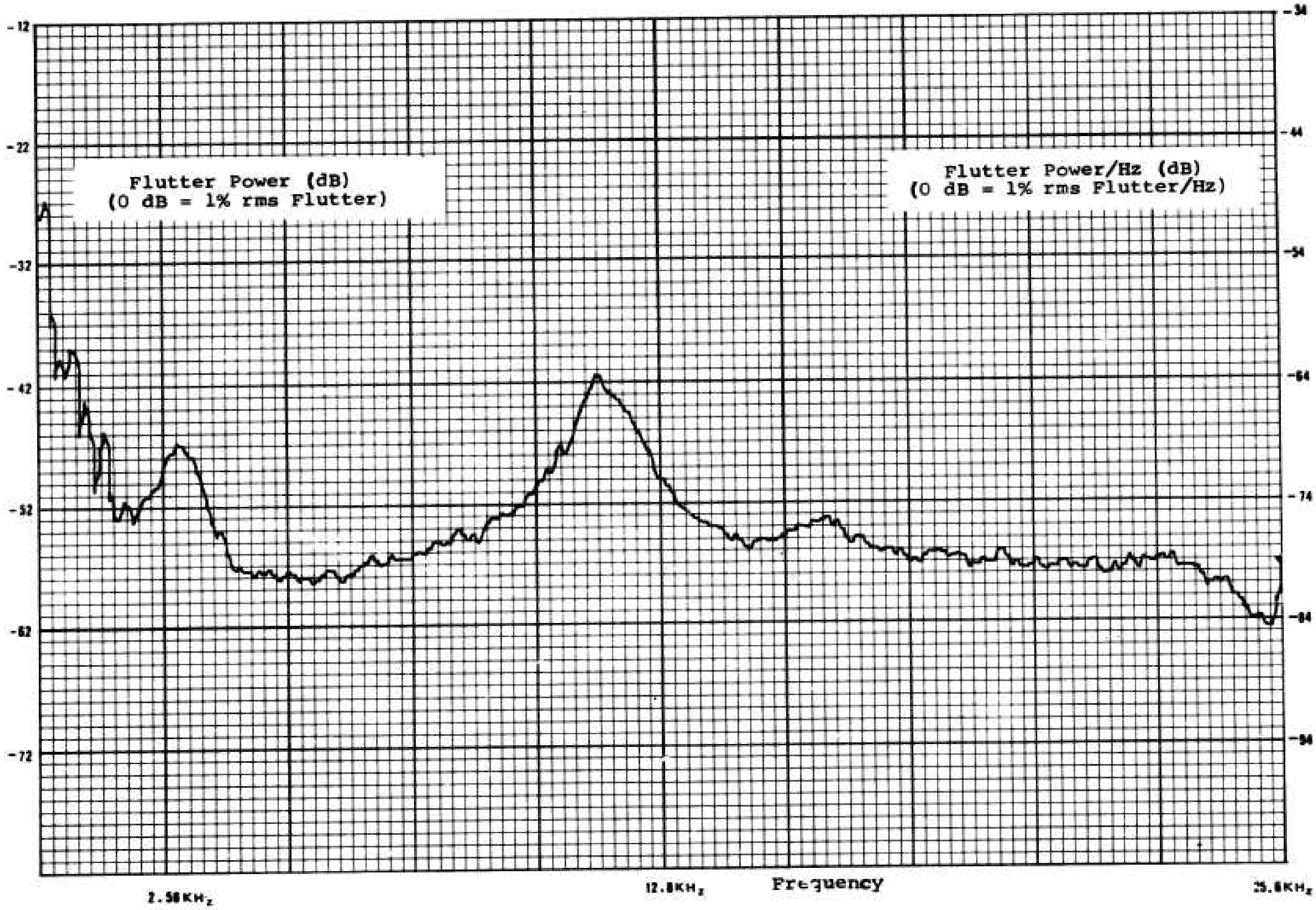

Figure F-22. Flutter Power Spectral Density, Recorder D, 25.6 kHz Bandwidth.

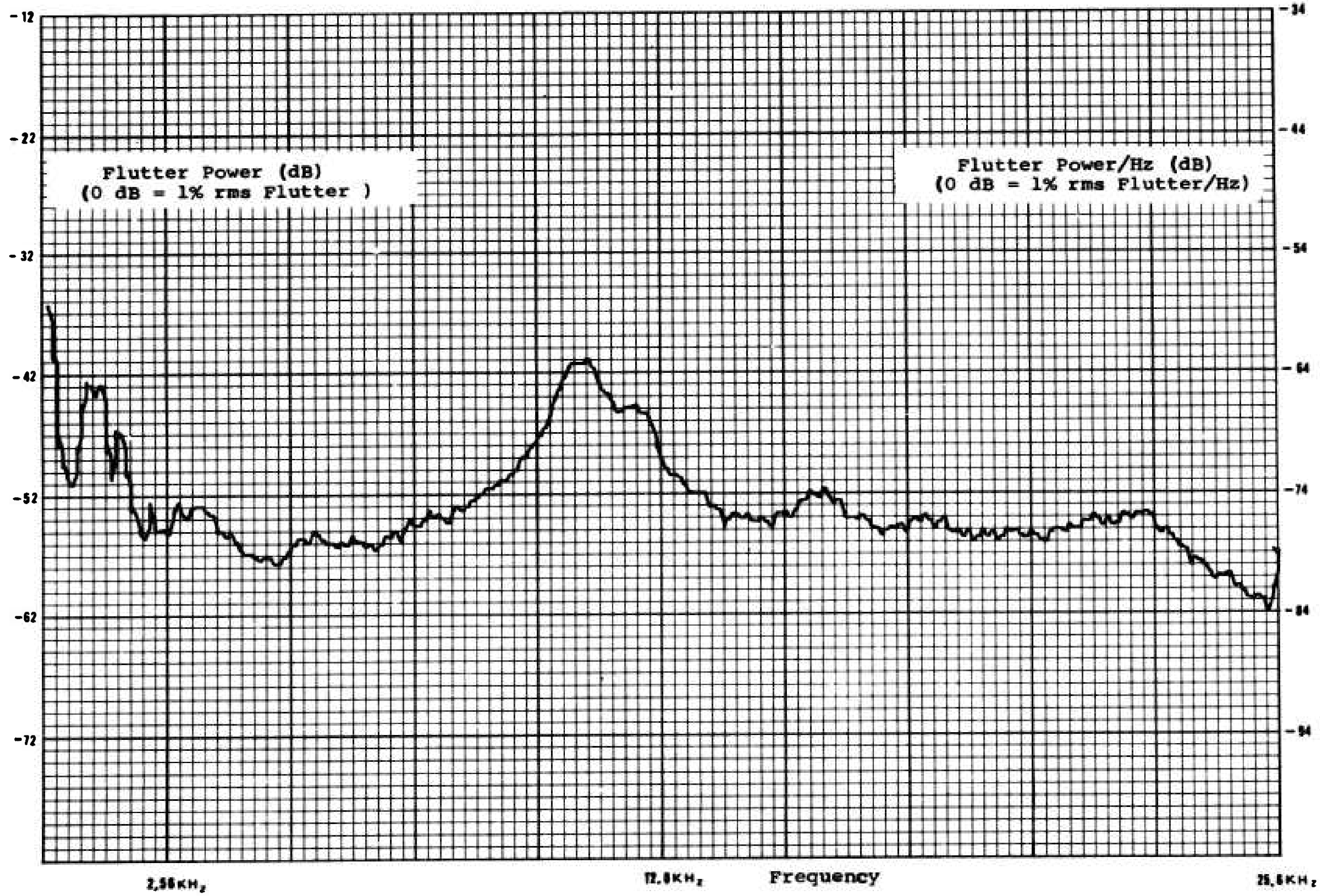

Figure F-23. Flutter Power Spectral Density, Recorder E, 25.6 kHz Bandwidth.

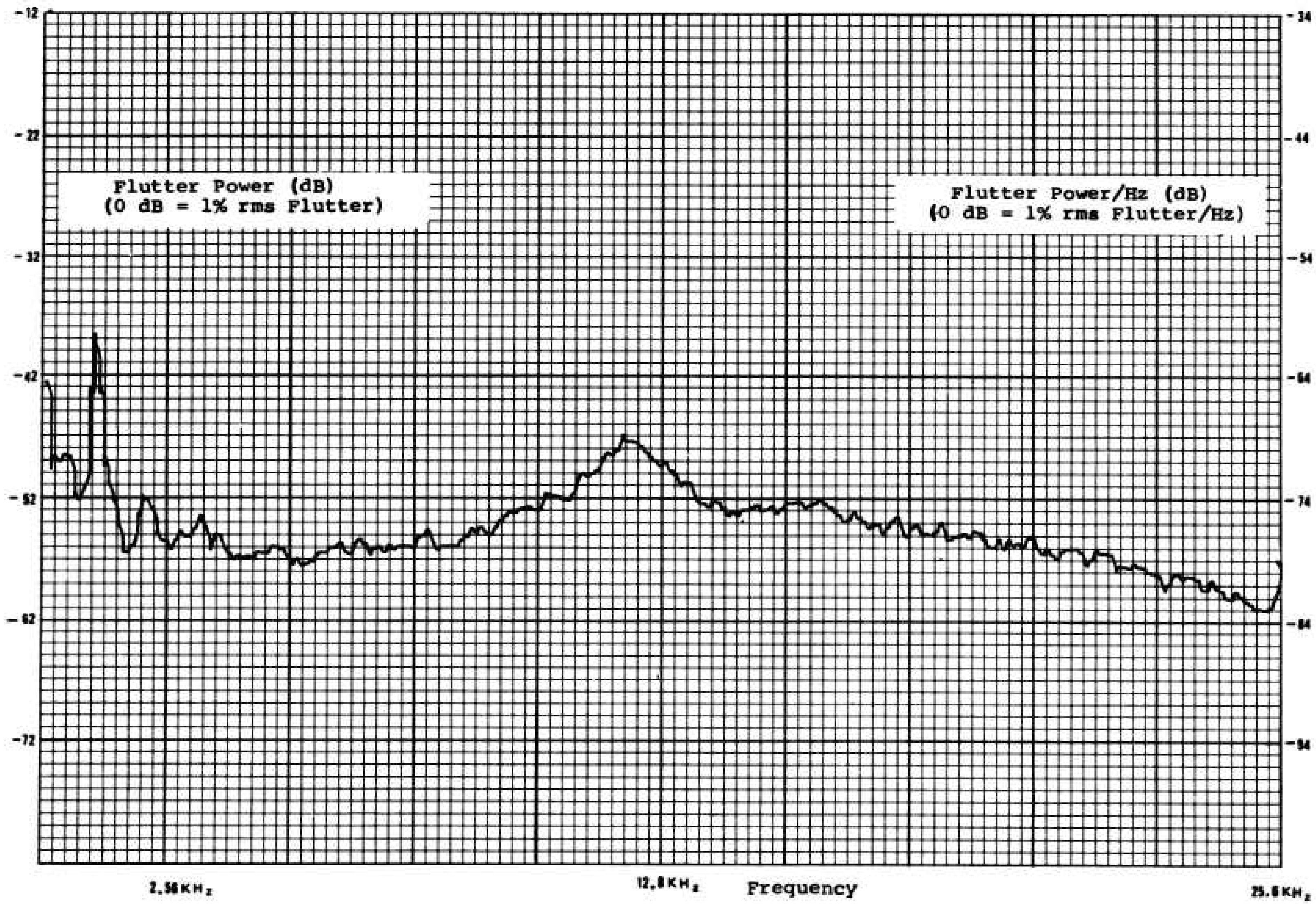

Figure F-24. Flutter Power Spectral Density, Recorder F, 25.6 kHz Bandwidth.

APPENDIX G

DITDE POWER SPECTRAL DENSITY PLOTS

Figures G-1 through G-12 present the DITDE spectra of the four tape recorders with the tape servo capability used in this study.

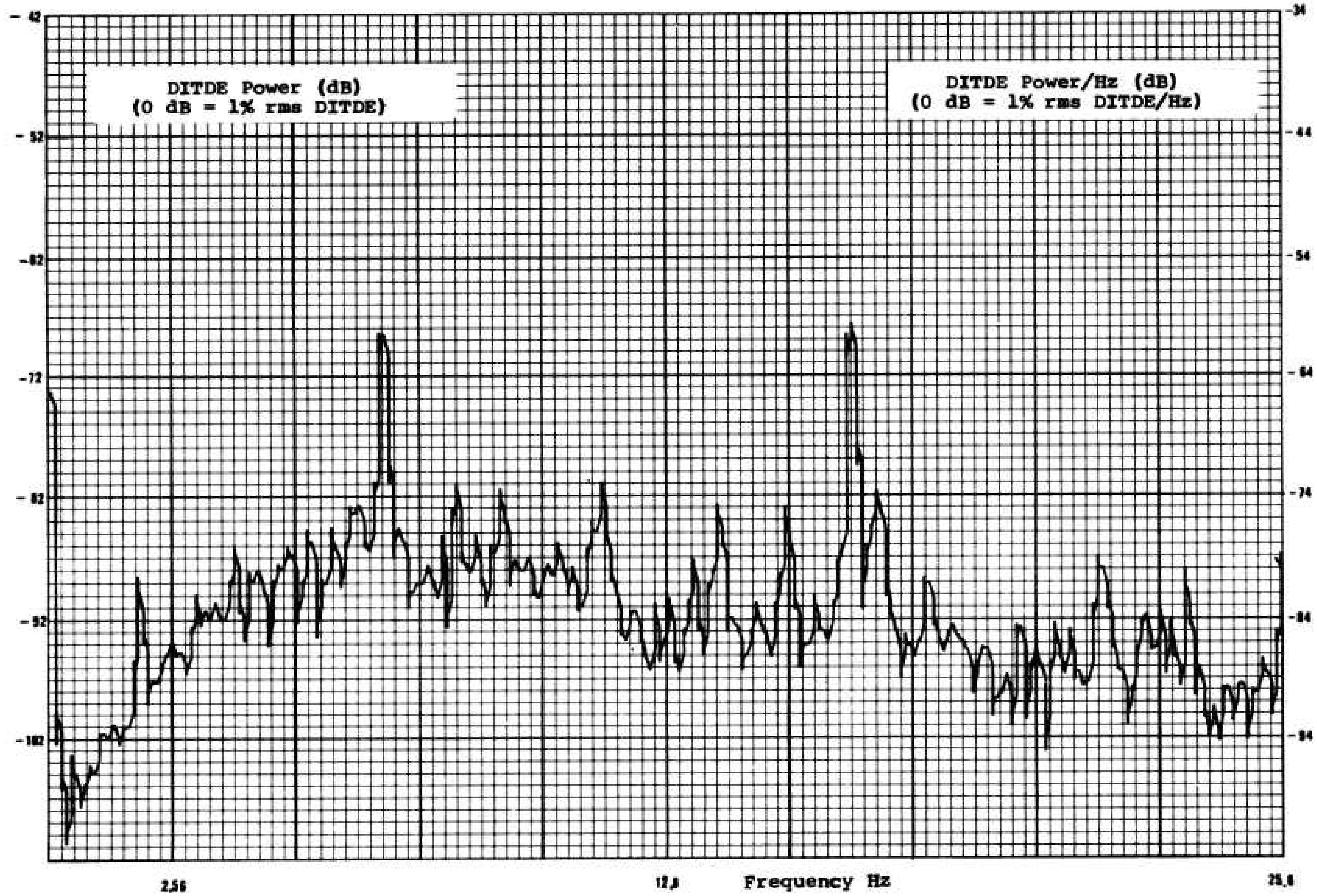

Figure G-1. DITDE Power Spectral Density, Recorder B, 25.6 Hz Bandwidth.

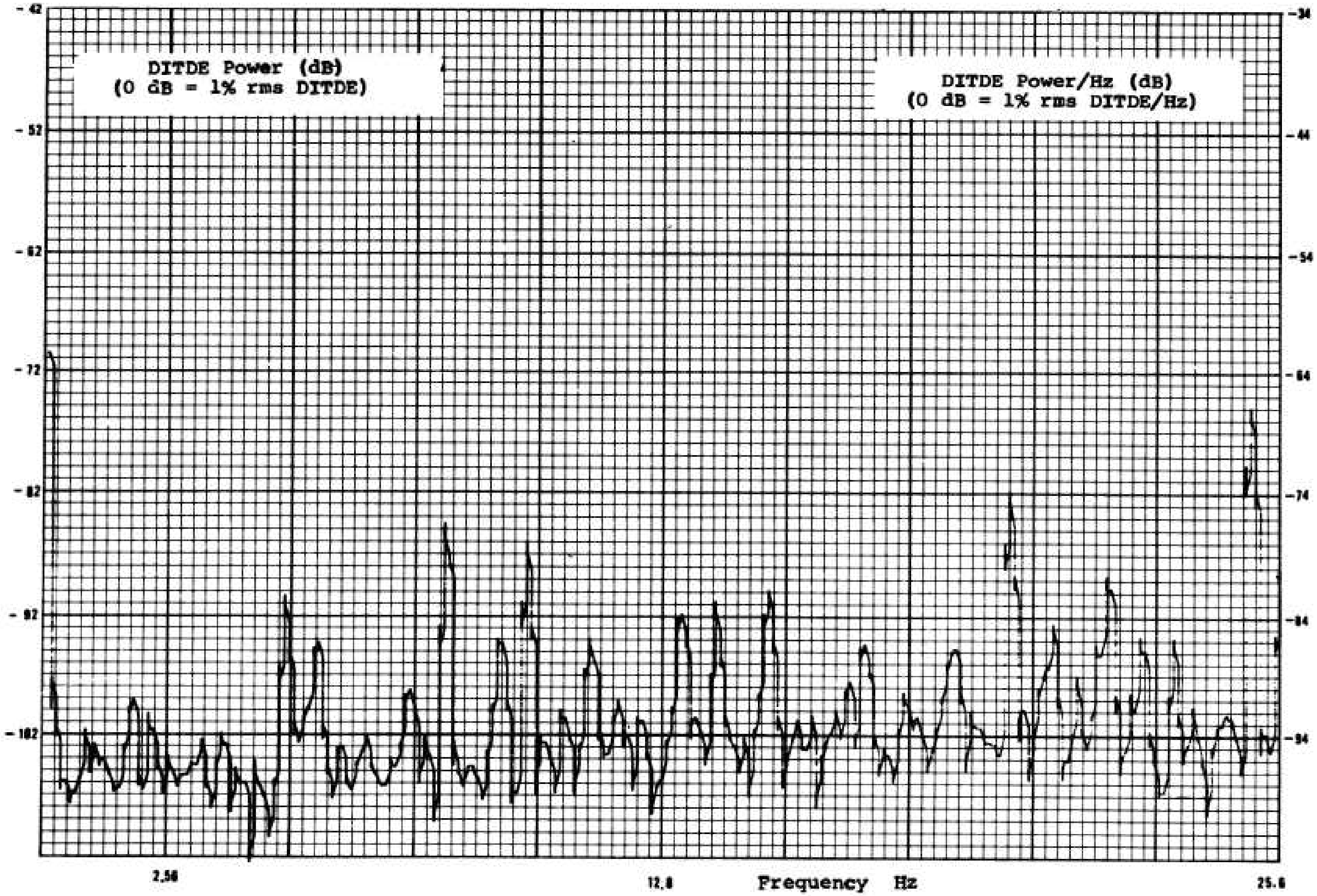

Figure G-2. DITDE Power Spectral Density, Recorder C, 25.6 Hz Bandwidth.

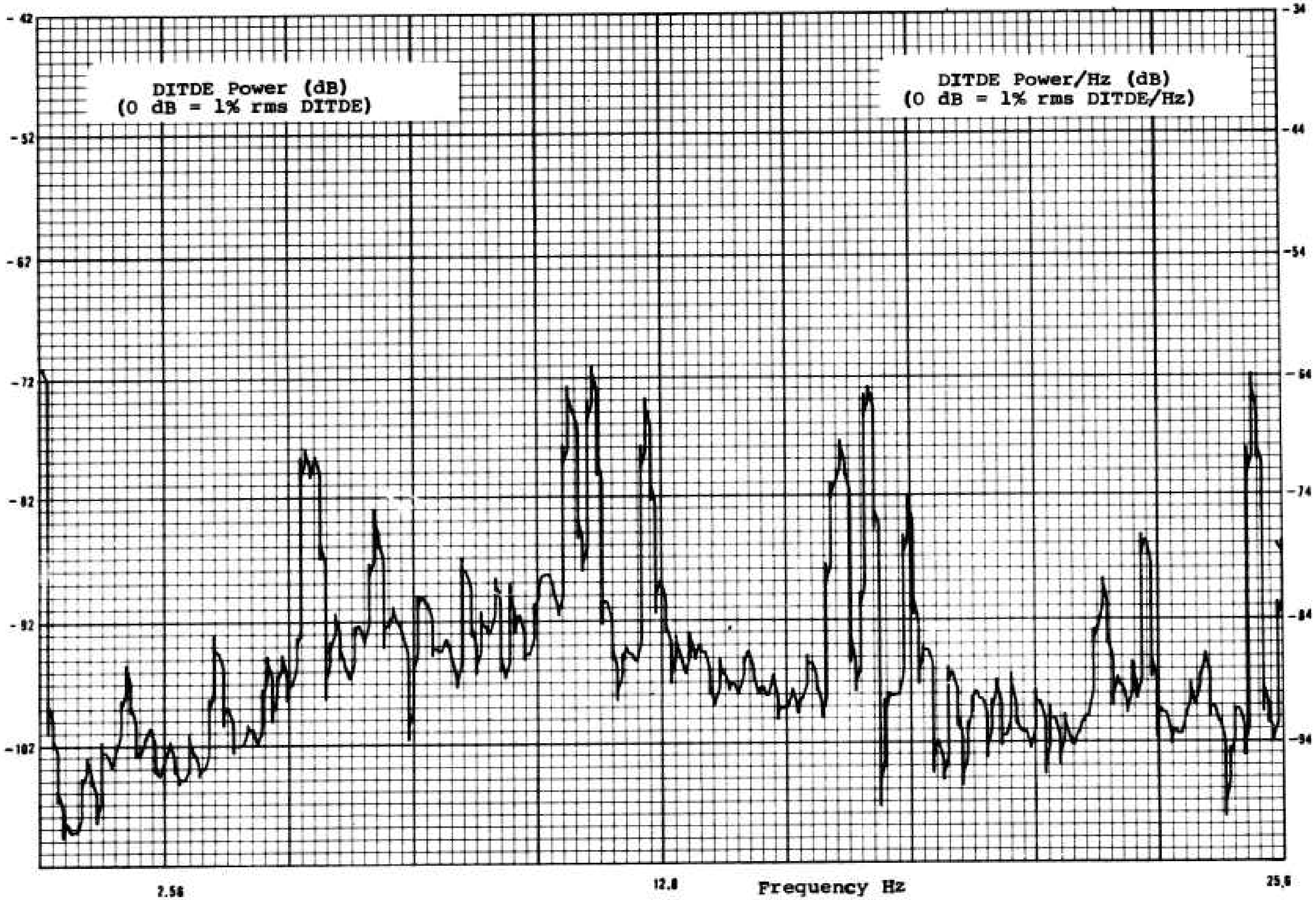

Figure G-3. DITDE Power Spectral Density, Recorder E, 25.6 Hz Bandwidth.

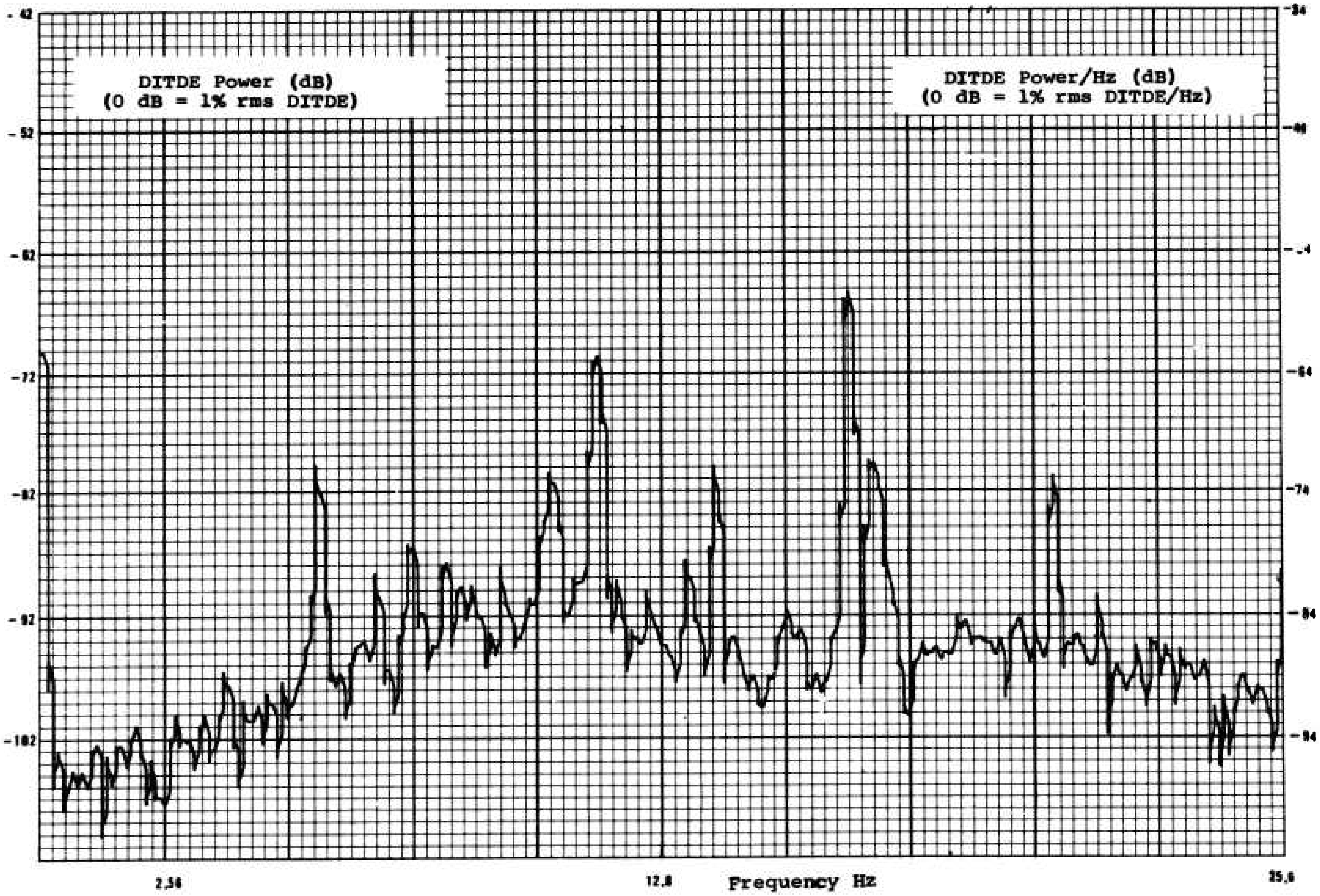

Figure G-4. DITDE Power Spectral Density, Recorder F, 25.6 Hz Bandwidth.

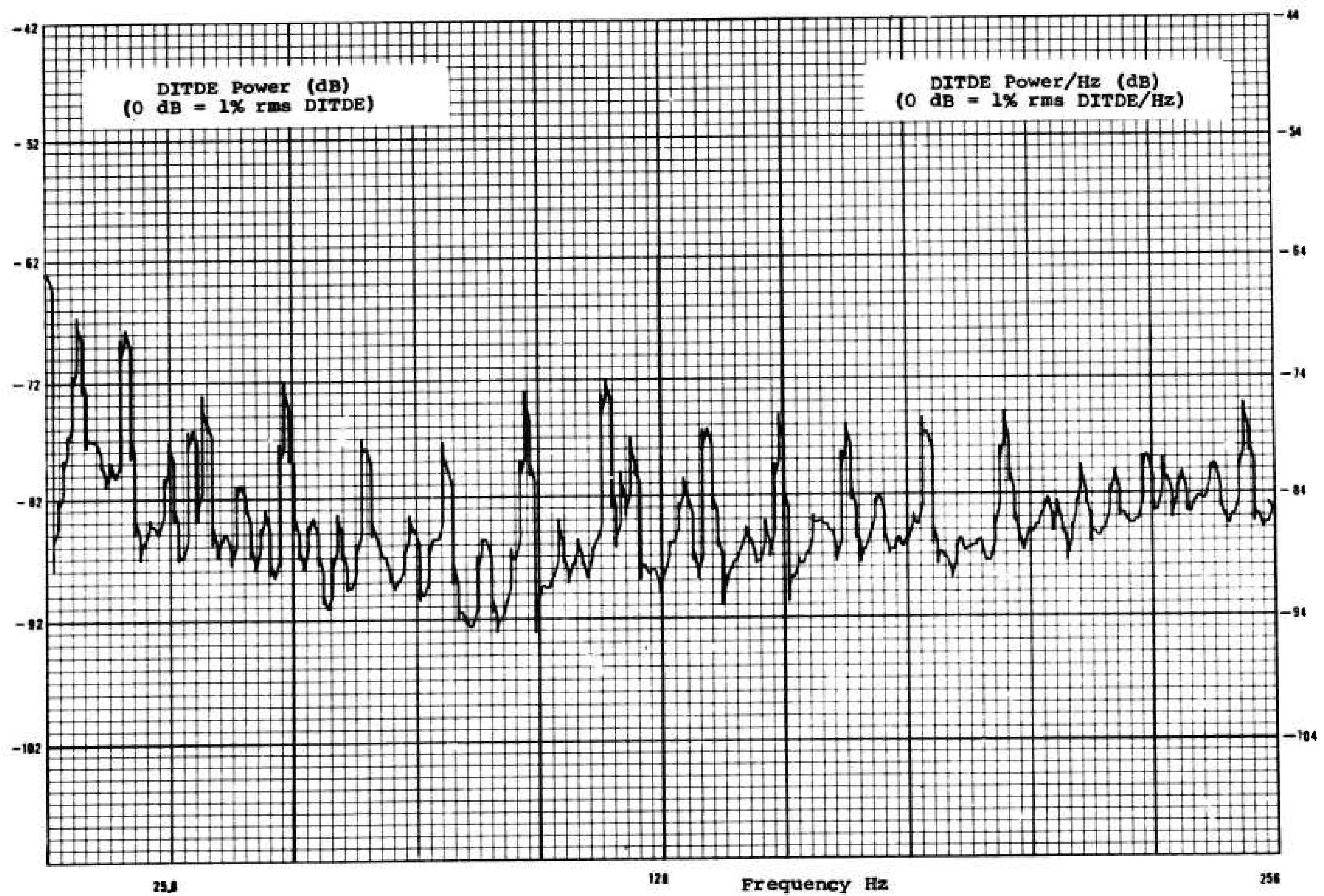

Figure G-5. DITDE Power Spectral Density, Recorder B, 256 Hz Bandwidth.

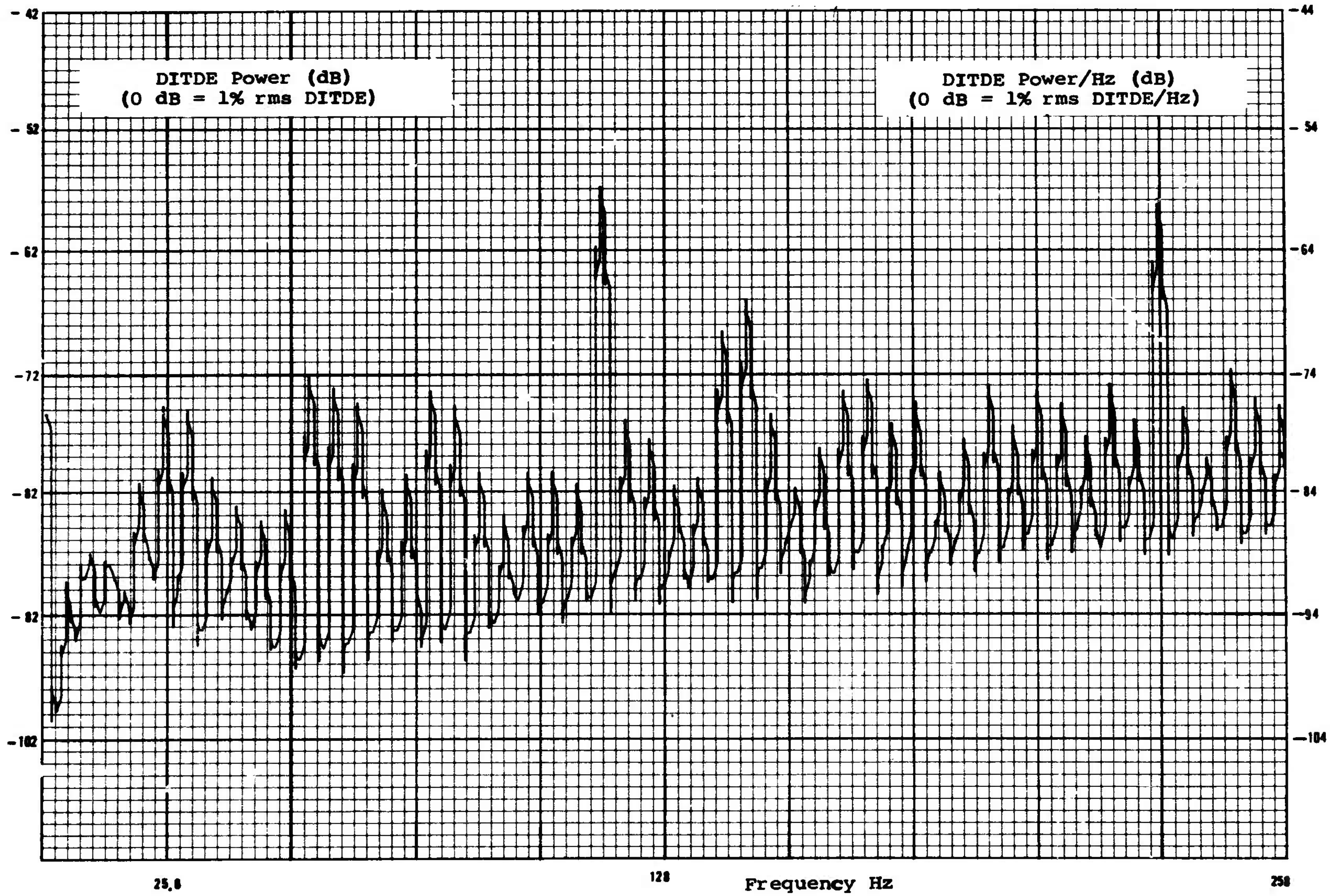

Figure G-6. DITDE Power Spectral Density, Recorder C, 256 Hz Bandwidth.

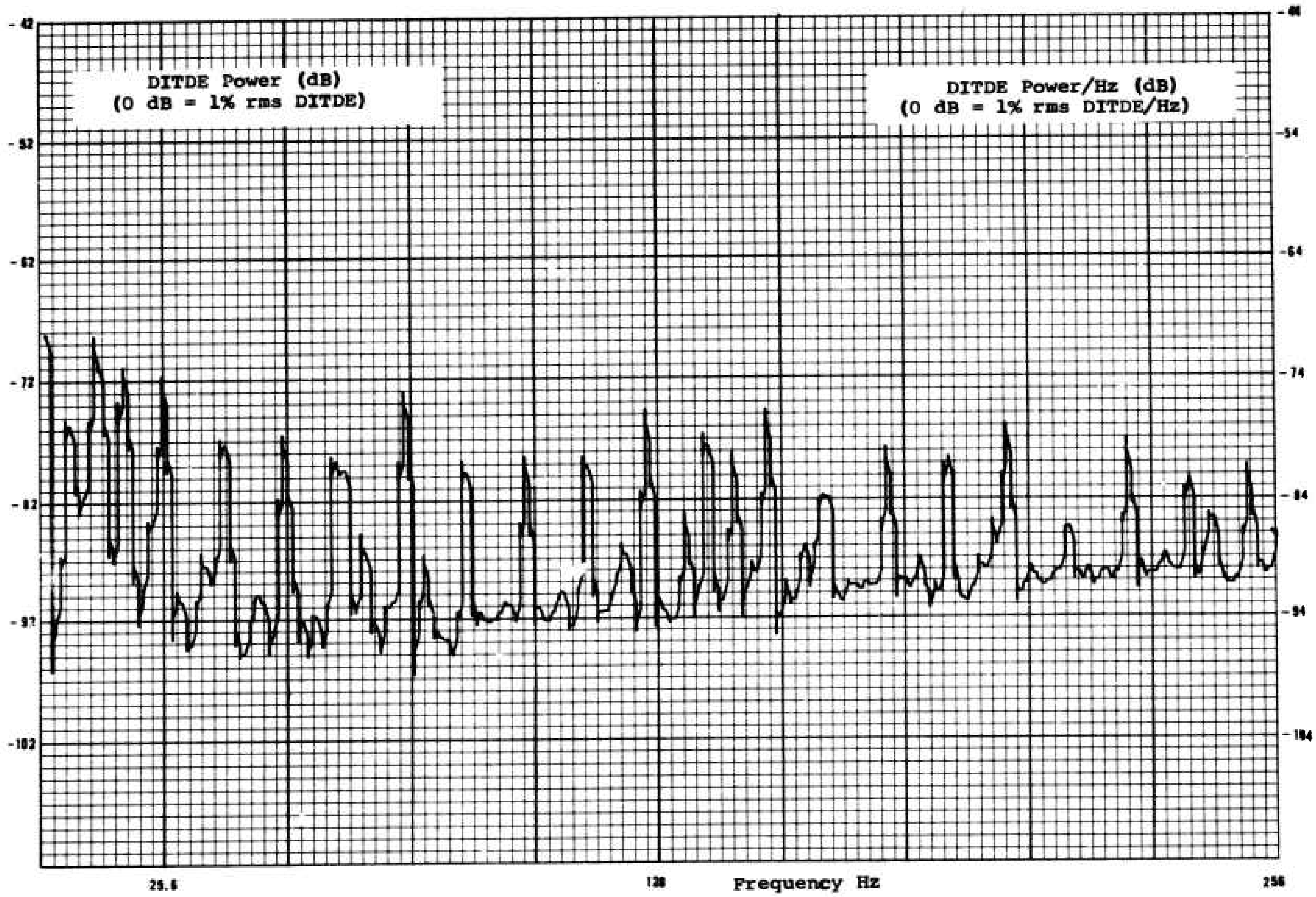

Figure G-7. DITDE Power Spectral Density, Recorder E, 256 Hz Bandwidth.

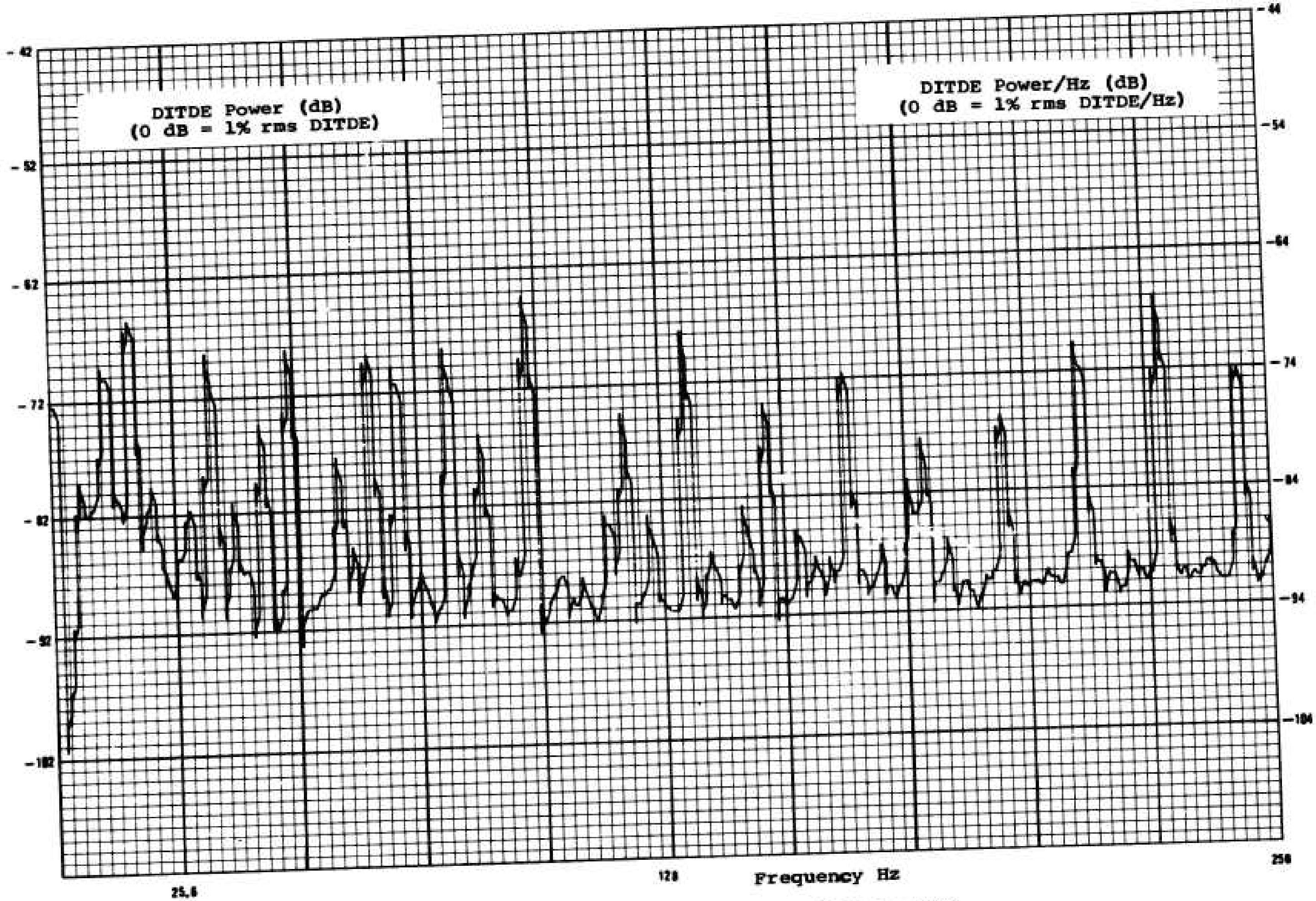

Figure G-8. DITDE Power Spectral Density, Recorder F, 256 Hz Bandwidth.

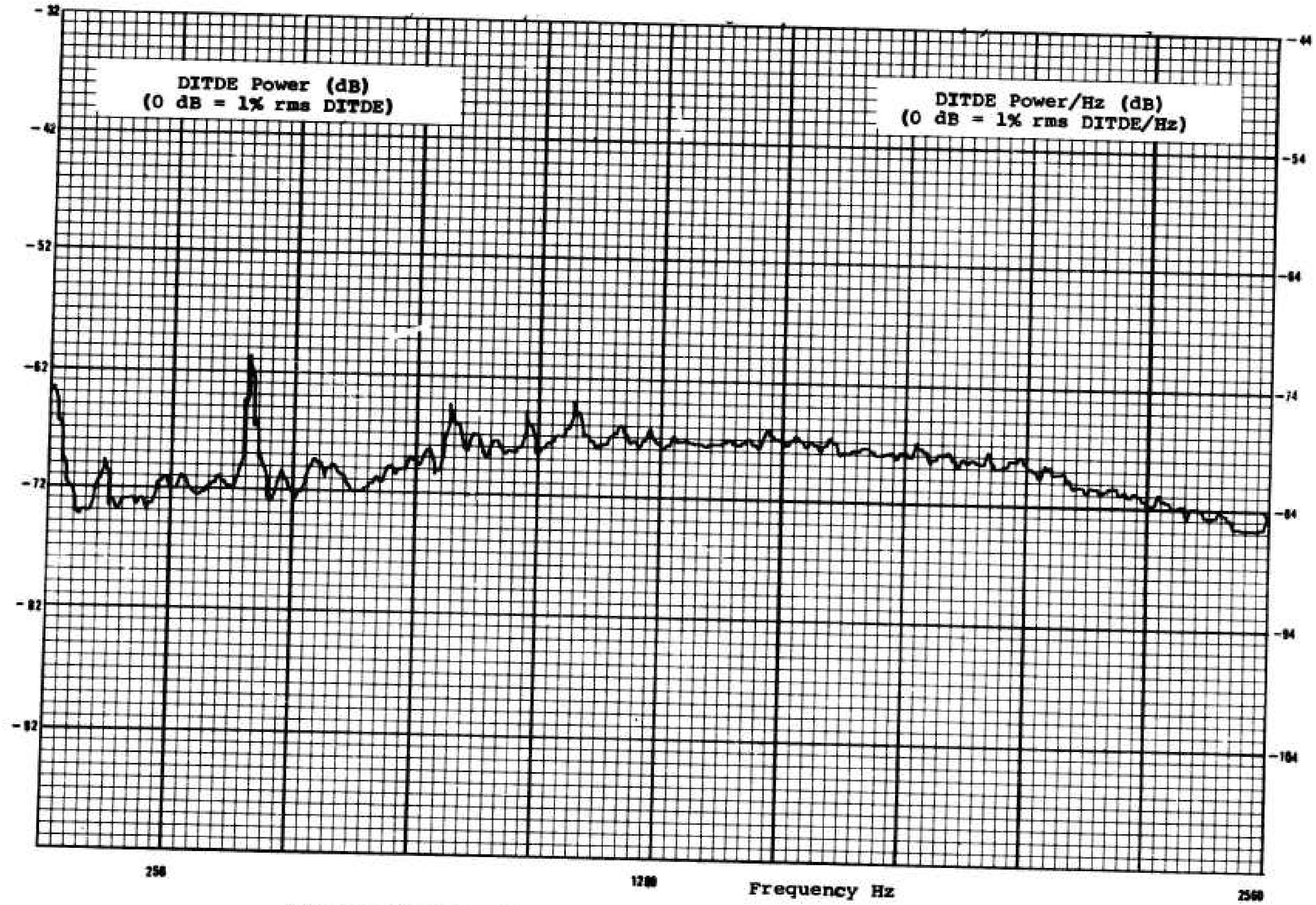

Figure G-9. DITDE Power Spectral Density, Recorder B, 2.56 kHz Bandwidth.

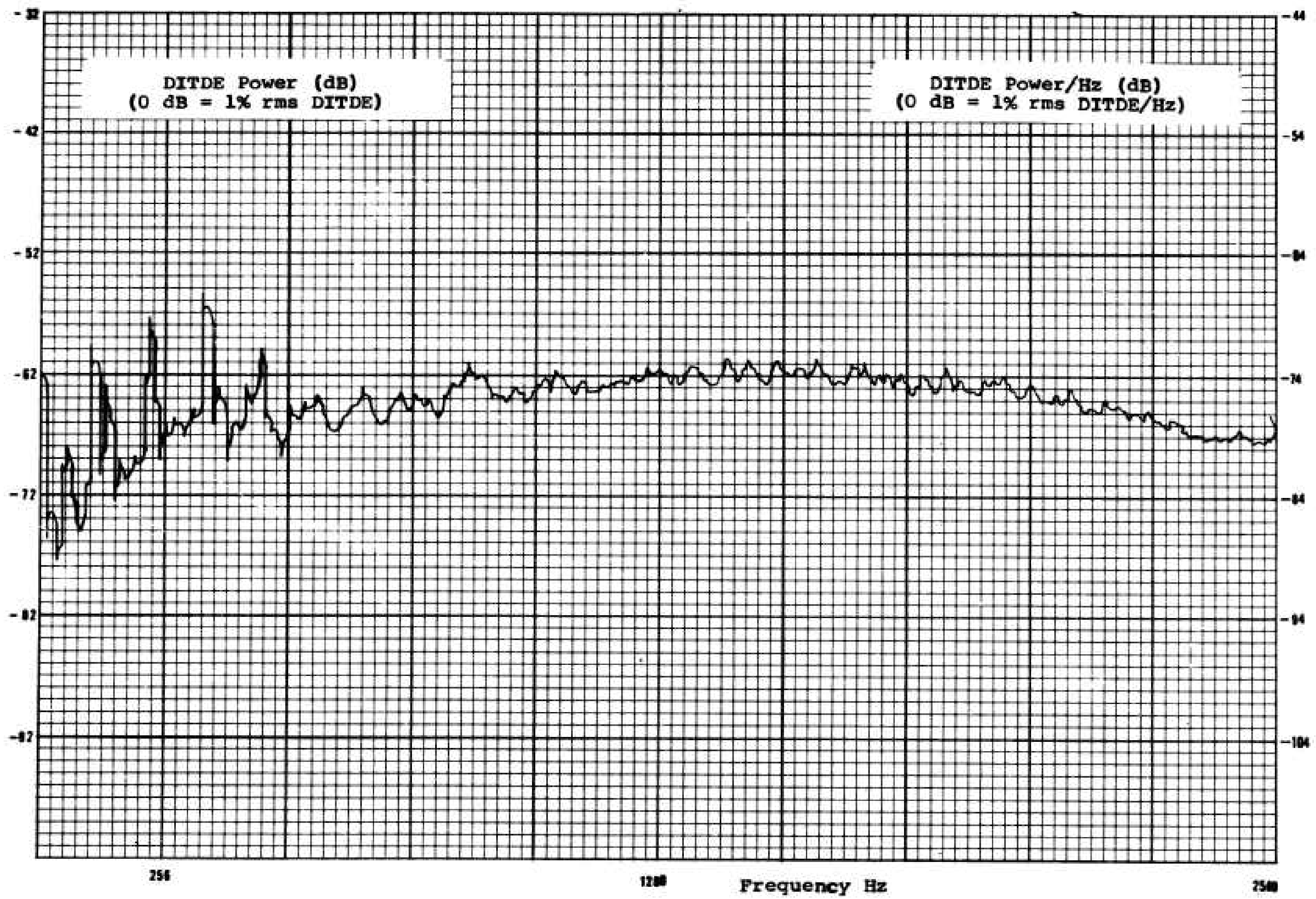

Figure G-10. DITDE Power Spectral Density, Recorder C, 2.56 kHz Bandwidth.

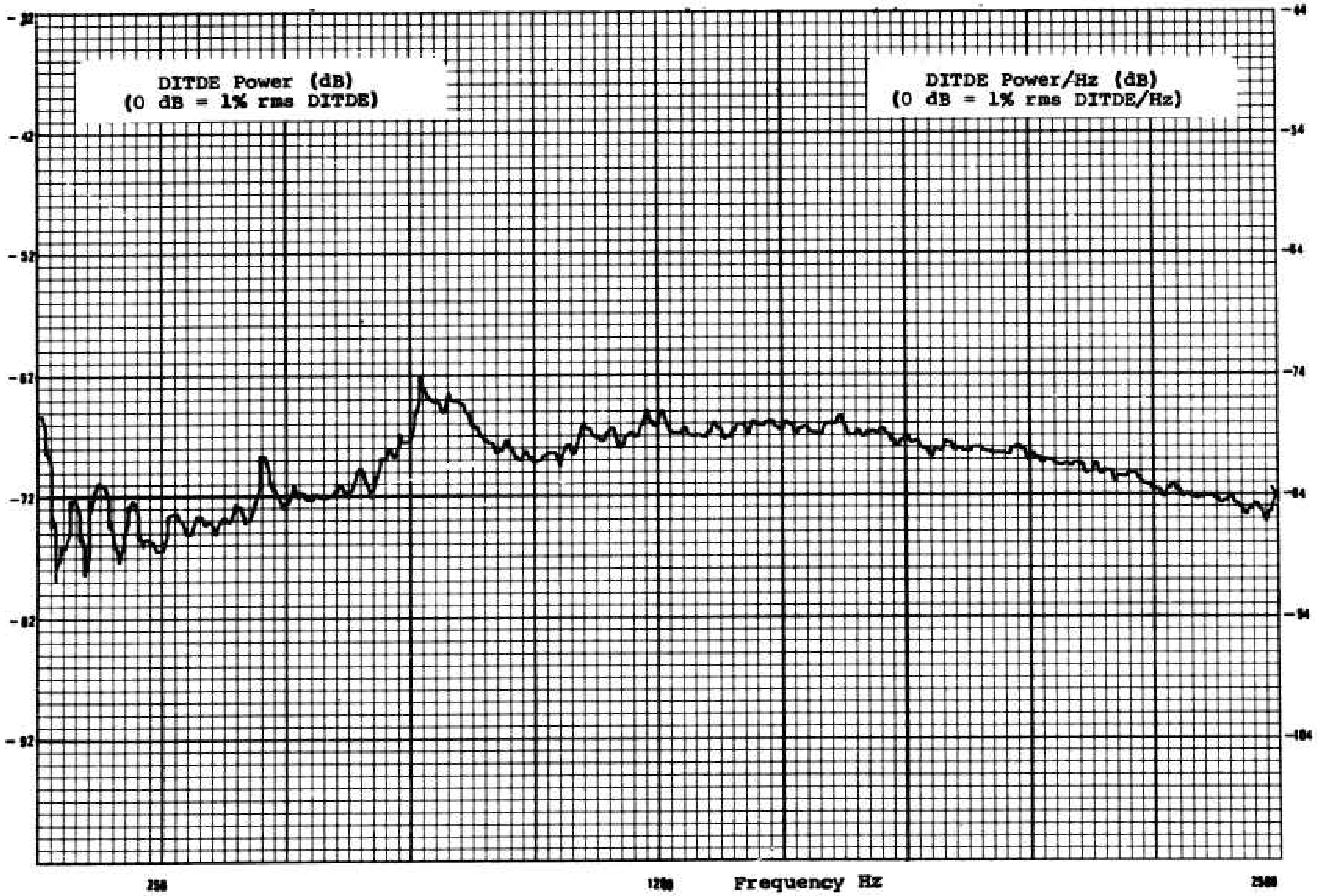

Figure G-11. DITDE Power Spectral Density, Recorder E, 2.56 kHz Bandwidth.

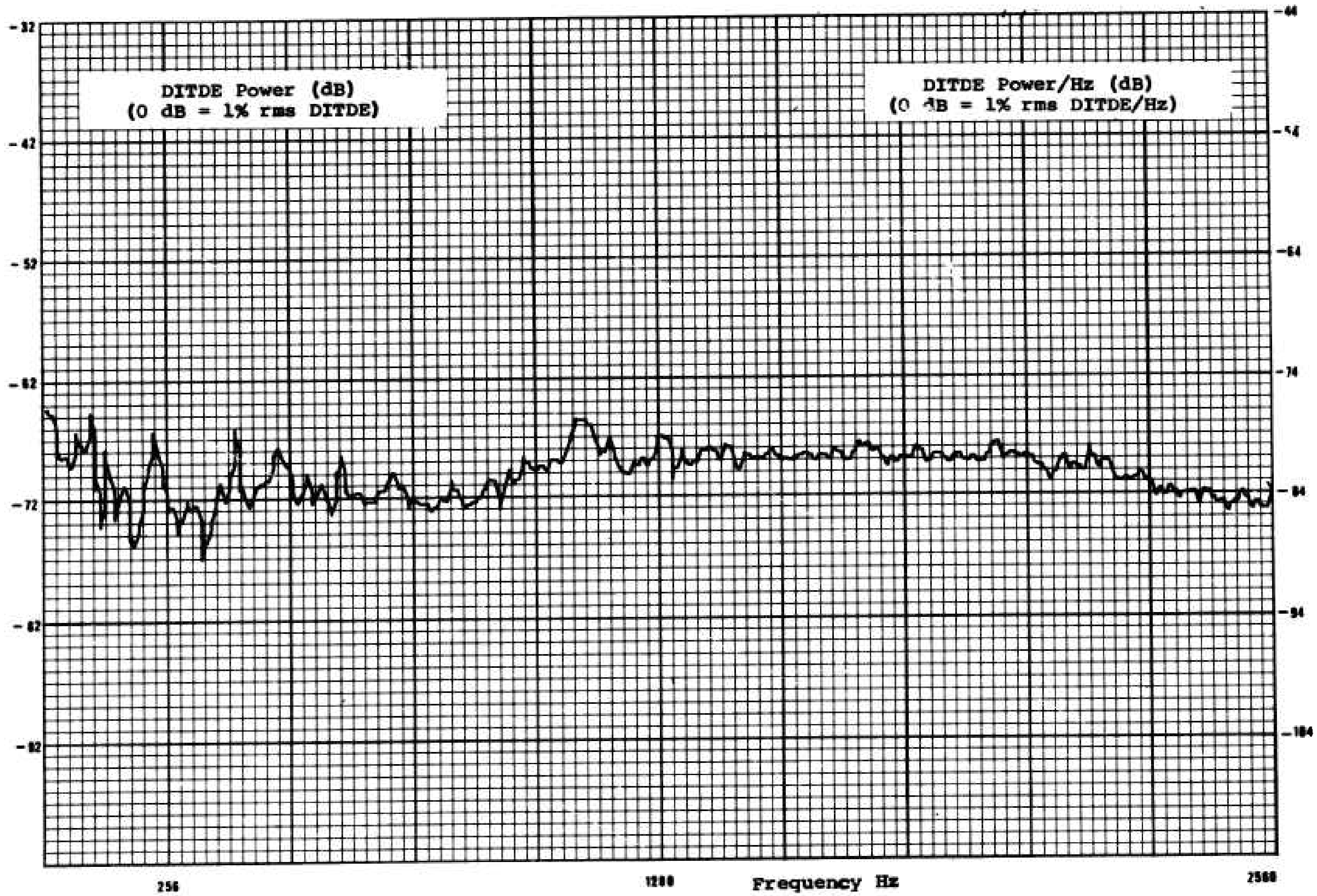

Figure G-12. DITDE Power Spectral Density, Recorder F, 2.56 kHz Bandwidth.

INITIAL DISTRIBUTION

EXTERNAL	Copies
Commander Naval Air Systems Command Headquarters Washington, DC 20361	
Attn: AIR-954	2
AIR-6502	1
Defense Documentation Center Cameron Station Alexandria, VA 22314	
Attn: TIOG	12
Commander Naval Sea Systems Command Headquarters Washington, DC 20362	
Attn: SEA-653	1
SEA-6543	1
Commanding Officer U.S. Naval Station Atlantic Fleet Weapons Range Box 545 FPO New York 09551	
Attn: H. T. Herring	1
Commanding Officer Naval Avionics Facility 21st and Arlington Avenue Indianapolis, IN 46218	
Attn: Code 906	1
Code 814	
(J. Brining)	1
(K. Burgess)	1
Officer-in-Charge Fleet Analysis Center Naval Weapons Station, Seal Beach Corona, CA 91720	
Attn: Code 851	1
Code 8513	1
Code 8522	1
Commander Naval Air Test Center Telemetry Data Center TDS/TSD Patuxent River, MD 20670	
Attn: H. O. Norfolk, Jr.	4

EXTERNAL	Copies
DDR&E AD(TR) The Pentagon Washington, DC 20301	
Attn: J. A. Webster	1
Commanding Officer Naval Ship Weapons Systems Engineering Station Port Hueneme, CA 93043	
Attn: Code 4920 (C. B. Tendick)	1
Commander Naval Weapons Center China Lake, CA 93555	
Attn: Code 373	1
Code 374	1
Code 533	1
Code 3742 (R. E. Rockwell)	1
Code 451 (K. D. Cox)	1
Commander U.S. Naval Ordnance Missile Test Facility White Sands Missile Range, NM 88002	
Attn: Code 502 (W. W. Bohn)	1
Director of Navy Ranges and Targets Point Mugu, CA 93042	
Attn: AIR-630	1
AIR-6302	1
AIR-6302D	1
Commanding Officer Yuma Proving Ground Yuma, AZ 85364	
Attn: STEYP-MDP (H. S. McElfresh)	1
Commanding Officer Ballistic Missile Defense Systems Command P.O. Box 1500 Huntsville, AL 35807	
Attn: BMDSC-RD (G. E. Wooden)	1
BMDSC-ROO (D. E. Parker)	1

EXTERNAL	Copies
PICATINNY Bldg. 65, SMUPA-RX Dover, NJ 07801 Attn: Telemetry Division, TSD (J. C. Greenfield)	1
Commanding Officer U.S. Army Missile Command Redstone Arsenal, AL 35809 Attn: AMSMI-RTA, Bldg. 7855 (R. D. Bibb)	1
Commanding Officer U.S. Army Electronic Proving Ground Fort Huachuca, AZ 85613 Attn: STEEP-MT-I (W. T. Lyon)	1
Commanding General Department of the Army White Sands Missile Range, NM 88002 Attn: STEWS-ID-IT (B. Chin)	1
(J. D. Cates)	1
STEWS-ID-S (B. E. Norman)	1
(E. Bejarno)	1
ADTC Eglin AFB, FL 32542 Attn: ADTC - TSGGS (E. J. Poschell)	1
ADTC - TSGPG (B. L. Culberson)	1
Vitro Services (R. L. Manley)	1
AFSWC Holloman AFB, NM 88330 Attn: 6585 TG/TKIA (J. A. Haden)	1
AFSWC Kirtland AFB, NM 87115 Attn: AFSWC - TED (CAPT R. J. Skelton)	1
4900 TG/FTEI (J. C. Scott)	1

EXTERNAL	Copies
AFCRL - LCS L. G. Hanscom Field Bedford, MA 01730 Attn: C. H. Reynolds	1
SAMTEC Vandenberg AFB, CA 93437 Attn: SAMTEC - ENIT (D. K. Manoa)	1
SAMTEC - ROOE (K. O. Schoeck)	1
AFETR Patrick AFB, FL 32925 Attn: AFETR - ENIB (F. Mann)	1
AFFTC Edwards AFB, CA 93523 Attn: AFFTC - DOESD (J. Ramos)	1
Sandia Laboratories Kirtland AFB East Albuquerque, NM 87115 Attn: Division 1251 (R. S. Reynolds)	1
Division 9486, Box 5800 (P. L. Walter)	1
Division 9421, Box 5800 (H. O. Jeske)	1
AFSCD Sunnyvale, CA 94086 Attn: Det 1, AFSCF - DOZR (G. V. Kreider)	1
AFSCF Aerospace Corporation P.O. Box 92957 Los Angeles, CA 90009 Attn: C. Nakamura Bldg. 115/1341	1
National Bureau of Standards Electronic Division Bldg. 225, Room A109 Gaithersburg, MD 20760 Attn: GSA-FSS (J. J. Fiori)	1

EXTERNAL	Copies
National Bureau of Standards Washington, DC 20234 Attn: Div. 425.03 (P. S. Lederer)	1
Aerospace Corporation Suite 4040 955 L'Enfant Plaza S.W. Washington, DC 20024 Attn: Dr. W. R. Hedeman	6
National Aeronautics and Space Administration Goddard Space Flight Center Greenbelt, MD 20771 Attn: Code 730.4 (W. B. Poland, Jr.)	2
Code 734 (R. M. Muller)	1
(C. Trevathan)	1
National Aeronautics and Space Administration 1520 H Street N.W. Washington, DC 20546 Attn: Code MF (W. E. Miller, Jr.)	1
Marshall Space Flight Center Huntsville, AL 35812 Attn: Code S&E-ASTR-I (W. Threlkeld)	1
Boeing Company, ASG, The Systems Instrumentation and Telemetry Seattle, WA 98124 Attn: Org. 2-5180 MH 8H-07 (V. A. Jennings)	1
Data Control Systems, Inc. Commerce Drive Danbury, CT 06810 Attn: M. Pizzuti	1
D. A. Zeller	1
Data Control Systems, Inc. East Liberty Street Danbury, CT 06810 Attn: T. Castellano	1

EXTERNAL	Copies
EMR Telemetry P.O. Box 3041 Sarasota, FL 33578 Attn: S. Bass	1
G. Tremain	1
Federal Electric Corporation Vandenberg AFB, CA 93437 Attn: R. Streich	1
Grumman Aerospace Corporation Instrumentation PLT 6 Calverton, NY 11933 Attn: R. S. McElhiney	1
E. Charland	1
Harris Electronic Systems Div. P.O. Box 37 Melbourne, FL 32935 Attn: C. Curry	1
IED 7440 Ronson Road San Diego, CA 92111 Attn: C. Brewster	1
Jet Propulsion Laboratory 4800 Oak Grove Drive (156-142) Pasadena, CA 91103 Attn: R. Piereson	1
Martin-Marietta Corporation P.O. Box 179 Denver, CO 80201 Attn: MS 8200 (C. M. Kortman)	1
(S. Hurst)	1
McDonnell-Douglas Astronautics 5301 Bolsa Avenue Huntington Beach, CA 92647 Attn: A3-833-BBSO (D. R. Andelin)	1
A3-250-AG30 (R. M. Frahm)	1
Microcom 1115 Mearns Road Warminster, PA 18974 Attn: C. Rosen	1
T. Grady	1

EXTERNAL	Copies	EXTERNAL	Copies
Monitor Systems 401 Commerce Drive Fort Washington, PA 19034 Attn: D. Mahoney	1		
Sandia Corporation Box 5800 Albuquerque, NM 87115 Attn: Division 9421 (C. S. Johnson)	1		
Teledyne Telemetry Company 1901 South Bundy Drive Los Angeles, CA 90025 Attn: H. F. Pruss	1		
University of Michigan Computer, Information and Control Engineering East Engineering, 1520 Ann Arbor, MI 48104 Attn: L. L. Rauch, PhD	1		
University of Southern California Olin Hall, University Park Los Angeles, CA 90007 Attn: Dr. W. C. Lindsey	1		
Mr. E. J. Baghdady 21 Overlook Drive Weston, MA 02193	1		
Mr. L. W. Gardenhire 906 Whitmire Drive Melbourne, FL 32935	1		
Mr. E. H. Straehley Consulting Services 1631 Platevna Road Santa Barbara, CA 93103	1		

INTERNAL	Copies
Technical Director	
Code 0002	
W. L. Miller	1
Project Management Group	
Code 0100	
LT COL C. L. Phillips	1
Code 0150	
M. H. Cain	1
Systems Evaluation Directorate	
Code 1001	
CAPT D. D. Buck	1
Code 1002	
R. S. Nelson	1
Weapons Systems Test Department	
Code 1142	
C. N. Gorevin	1
RF Weapons Systems Division	
Code 1262	
D. H. Barthuli	1
Weapons Evaluation Department	
Code 1300	
Dr. M. A. Garcia	1
Fleet Weapons Engineering Directorate	
Code 2001	
CAPT D. DeWitt	1
Range Directorate	
Code 3001	
CAPT G. M. Dempsey	1
Capabilitities Development Department	
Code 3100	
W. C. Christensen	1
Code 3101	
J. A. Means	1
Development Management Division	
Code 3120	
H. J. Crawford	1

INTERNAL	Copies
Measurement Systems Development Division	
Code 3140	
T. R. Carr	1
Code 3142	
R. W. Lytle	1
C. G. Ashley	1
J. Anderson	1
Code 3143	
M. A. Bondelid	1
Code 3145	
Z. H. Blankers	1
Control Systems Development Division	
Code 3150	
J. R. Scott	1
Code 3151	
A. H. Weishaar	1
J. L. Weblemoe	1
Code 3153	
D. E. Ogden	1
Code 3154	
P. M. Newton	1
C. E. Ohlen	1
System Development Support Division	
Code 3160	
E. F. Mutz	1
Code 3161	
R. L. Nifong	1
Code 3163	
F. L. Allard	1
Data Collection Division	
Code 3410	
R. P. Carpenter	1
Code 3411	
R. J. Roanhaus	1
R. H. Wymore	1
J. T. Dickman	1
W. T. Norton	1
Code 3412	
F. D. Leiblein	1
Data Control Division	
Code 3440	
W. F. Tolman	1

INTERNAL	Copies
Engineering Applications Directorate	
Code 4001	
N. F. Rohn	1
Code 4002	
LCDR R. P. Evans	1
Equipment Support Division	
Code 4131-1	
R. W. Kenny	1
Technical Publications Division	
Code 4250-1	
M. F. Hayes	10
Code 4251	
D. S. Walker	1
Code 4253-3	
Technical Reports Library	2
Instrumentation Department	
Code 4300	
V. E. Orris	1
Instrumentation Development Division	
Code 4320	
K. L. Berns	1
Code 4321	
F. R. Hartzler	1
D. R. Hust	1
D. H. Rilling	1
M. V. Wechsler	1
Code 4322	
E. R. Hill	1
D. R. Knight	1
D. A. King	1
D. L. Laubacher	1
Code 4323	
E. L. Law	50
B. E. Bishop	1
E. T. Kimball	1
C. M. Kaloi	1

INTERNAL	Copies
Instrumentation Engineering Division	
Code 4330	
R. P. Tegt	1
Code 4331	
M. A. Beckman	1
T. P. Waddell	1
Instrumentation Support Division	
Code 4340	
J. D. Martin	1
Code 4341	
E. R. Sandy	1
G. J. Harbold	1
N. R. Dragoo	1
D. J. DeJong	1
Office of Patent Counsel	
Code PC	
Dr. J. M. St. Amand	1